**IVAN CÉLIO ANDRADE RIBEIRO**

# SUSTAINABLE METHODS TO TRANSFORM EGGSHELLS AND VACCINE WASTES INTO VALUE-ADDED BY-PRODUCTS

**LAVRAS - MG**

**2022**

**IVAN CÉLIO ANDRADE RIBEIRO**

# SUSTAINABLE METHODS TO TRANSFORM EGGSHELLS AND VACCINE WASTES INTO VALUE-ADDED BY-PRODUCTS

Tese apresentada à Universidade Federal de Lavras, como parte das exigências do Programa de Pós-graduação em Ciência do Solo, área de concentração em Fertilidade do Solo e Nutrição de Plantas, para obtenção do título de Doutor.

Prof. Dr. Leônidas Carrijo Azevedo Melo
Orientador

Prof. Dr. Luiz Roberto Guimarães Guilherme
Coorientador

**LAVRAS - MG**

**2022**

**IVAN CÉLIO ANDRADE RIBEIRO**

# SUSTAINABLE METHODS TO TRANSFORM EGGSHELLS AND VACCINE WASTES INTO VALUE-ADDED BY-PRODUCTS

# MÉTODOS SUSTENTÁVEIS PARA TRANSFORMAR CASCAS DE OVOS E RESÍDUOS DE VACINA EM SUBPRODUTOS DE VALOR AGREGADO

Tese apresentada à Universidade Federal de Lavras, como parte das exigências do Programa de Pós-graduação em Ciência do Solo, área de concentração em Fertilidade do Solo e Nutrição de Plantas, para obtenção do título de Doutor.

APROVADA em 28 de janeiro de 2022.

| | |
|---|---|
| Dr. Hudson Wallace Pereira de Carvalho | CENA/USP |
| Dr. Ronaldo Fia | DAM/UFLA |
| Dr. Douglas Ramos Guelfi Silva | DCS/UFLA |
| Dr. Guilherme Lopes | DCS/UFLA |

Prof. Dr. Leônidas Carrijo Azevedo Melo
Orientador

Prof. Dr. Luiz Roberto Guimarães Guilherme
Coorientador

**LAVRAS - MG**

**2022**

**Ficha catalográfica elaborada pelo Sistema de Geração de Ficha Catalográfica da Biblioteca Universitária da UFLA, com dados informados pelo(a) próprio(a) autor(a).**

Ribeiro, Ivan Célio Andrade.
Sustainable methods to transform eggshells and vaccine wastes into value-added by-products / Ivan Célio Andrade Ribeiro. - 2022.
127 p. : il.

Orientador(a): Leônidas Carrijo Azevedo Melo.
Coorientador(a): Luiz Roberto Guimarães Guilherme.
Tese (doutorado) - Universidade Federal de Lavras, 2022.
Bibliografia.

1. Circular economy. 2. Waste valorization. 3. Hydroxyl-Eggshell. I. Melo, Leônidas Carrijo Azevedo. II. Guilherme, Luiz Roberto Guimarães. III. Título.

*Ao meu pai, Geraldo, à minha noiva, Jéssica, aos meus tios, Eunice, Raimundo e Emília*

*Dedico*

## AGRADECIMENTOS

Em primeiro lugar agradeço a Deus, por me conduzir e fortalecer sempre, tornando essa conquista possível.

Ao meu Pai Geraldo, um exemplo em minha vida e meu grande incentivador. Esse título de doutor torna-se realidade graças a todo o apoio de meu pai para comigo desde o início de minha vida escolar.

À minha noiva Jéssica, por todo apoio, compreensão, amor e carinho! Minha grande incentivadora e parceira, uma bênção na minha vida. Juntos somos mais!

Aos professores Dr. Luiz R. G. Guilherme (Bebeto) e Dr. Leônidas C. A. Melo, pelos ensinamentos e participação na execução deste trabalho. Agradeço o acolhimento, confiança, incentivo e motivação do professor Bebeto, que me fizeram crescer profissionalmente e pessoalmente, superando cada vez mais as dificuldades para alcançar tantas vitórias.

Aos membros da banca pela cordialidade e aceite do convite.

Aos amigos do Programa de Pós-graduação em Ciência do Solo (PPGCS) e aos demais amigos conquistados na UFLA e em Lavras, por todos os momentos agradáveis compartilhados.

À Universidade Federal de Lavras pela oportunidade, em especial ao Programa de Pós-graduação em Ciência do Solo, vinculado ao Departamento de Ciência do Solo (DCS).

Aos funcionários do DCS e do Laboratório de Microscopia Eletrônica e Análise Ultraestrutural (LME/UFLA), pela atenção e profissionalismo.

Aos alunos de iniciação científica, pelo auxílio e convivência na execução das atividades laboratoriais.

Ao professor Johannes Lehmann, da Cornell University, pela oportunidade, convívio e ensinamentos durante o doutorado sanduíche.

Aos órgãos de fomento Capes, Fapemig e CNPq, pelo apoio financeiro. O presente trabalho foi realizado com apoio da Coordenação de Aperfeiçoamento de Pessoal de Nível Superior – Brasil (CAPES) – Código de Financiamento 001.

A todos que contribuíram, direta e indiretamente, para a realização deste trabalho: MUITO OBRIGADO!

*“Na natureza nada se cria, nada se perde, tudo se transforma”.*

*(Antoine-Laurent Lavoisier)*

## RESUMO GERAL

Atualmente, a população mundial está consumindo mais recursos naturais do que o planeta Terra pode se regenerar de forma sustentável. Recursos não renováveis, como rochas, têm sido usados para produzir fertilizantes para aumentar a produtividade das culturas e garantir a segurança alimentar. Estas rochas também são usadas na fabricação de produtos químicos de grau analítico para tratar águas residuais. A substituição parcial de rochas por resíduos sólidos gerados em processos industriais é uma forma sustentável e inovadora de reciclar esses materiais e minimizar o uso de recursos não renováveis. Este trabalho apresenta metodologias simples para transformar resíduos sólidos gerados por empresas de ovos e indústrias de vacinas em subprodutos que podem substituir parcialmente compostos de grau analítico e fertilizantes comerciais. Primeiramente, propusemos a transformação de cascas de ovos em um sólido branco denominado "Hidroxicasca" (ES-OH). Experimentos em batelada provaram que a ES-OH tem um alto potencial para remoção de arsênio (As) e fósforo (P). A capacidade máxima de remoção de As e P de ES-OH foi de 529 e 329 mg $g^{-1}$, respectivamente. Espectroscopia no infravermelho por transformada de Fourier (FTIR), microscopia eletrônica de varredura com espectroscopia por energia dispersiva de raios X (MEV/EDS) e difração de raios X (DRX) foram utilizadas para caracterizar o material antes e após a reação de As e P. FTIR, SEM-EDS e XRD confirmaram que o processo primário de recuperação de P por ES-OH foi via precipitação de hidroxiapatita, enquanto a remoção de As aconteceu pela precipitação de cristais de vladimirita. Além disso, um experimento em vaso confirmou que o ES-OH enriquecido com P foi eficaz tanto quanto o superfosfato triplo (TSP, um fertilizante comercial) no rendimento da grama com a vantagem de manter quase quatro vezes mais P disponível e o pH do solo mais alto do que TSP após o cultivo. Para os resíduos das indústrias de vacinas (VW), propusemos a transformação química e térmica deste material em um fertilizante organomineral. O processo aqui proposto possibilita a esterilização desse resíduo biologicamente contaminado e permite a produção de um fertilizante verde com maior teor de fósforo e menor acidez do que os fertilizantes comerciais convencionais. Os métodos descritos nesta tese estão prontos para serem implementados em escala industrial. Além de ser uma nova e econômica fonte de renda, empresas produtoras de ovos e indústrias de vacinas podem implementar os processos de produção propostos como uma forma ambientalmente correta local de reciclagem de seus resíduos sólidos, criando subprodutos com grande potencial para serem usados na agricultura como fertilizante alternativo ou em estações de tratamento de efluentes.



**Palavras-chave:** Economia Circular. Valorização de resíduos. Hidroxicasca. Fertilizante alternativo. Dia da Sobrecarga da Terra

## GENERAL ABSTRACT

Today the world population is already consuming more natural resources than the planet Earth can sustainably regenerate itself. Nonrenewable resources such as rocks have been used to synthesize fertilizers to increase crop productivity and ensure food security. These rocks are also used in the synthesis of analytical-grade chemicals to clean wastewaters. The partial substitution of rocks by solid wastes generated in industrial processes is a sustainable and innovative way to recycle these materials and minimize the use of nonrenewable resources. This work presents straightforward methodologies to transform solid waste generates from egg companies and vaccine industries into byproducts that can partially replace analytical grade compounds and commercial fertilizers. First, we proposed the transformation of eggshells into a white solid named as "Hydroxyl-Eggshell" (ES-OH). Batch experiments proved that ES-OH has a high potential for arsenic (As) and phosphorus (P) removal. The maximum As and P removal capacity of ES-OH was 529 and 329 mg $g^{-1}$, respectively. Fourier transform infrared spectroscopy (FTIR), scanning electron microscopy with energy dispersive X-ray spectrometry (SEM-EDS), and X-ray diffraction (XRD) were used to characterize the material before and after As and P reaction. FTIR, SEM-EDS, and XRD confirmed that the primary process of P recovered by ES-OH was via precipitation of hydroxyapatite, while As removal happened by the precipitation of vladimirite crystals. Also, a pot experiment confirmed that the P-loaded ES-OH was as effective as triple superphosphate (TSP, a commercial fertilizer) on grass yield with the advantage of maintaining nearly four-fold more available P and higher soil pH than TSP after cultivation. For the vaccine industries waste (VW), we proposed this material's chemical and thermal transformation into an organomineral fertilizer. The process proposed here enables the sterilization of this biologically contaminated waste and allows for the production of a green fertilizer with higher phosphorus content and smaller acidity than conventional commercial fertilizers. The methods described in this thesis are ready to be implemented on an industrial scale. Besides being a novel and economical income source, egg-producing companies and vaccine industries might implement the proposed production processes as a local environmentally-friendly way of recycling their solid wastes, creating byproducts with great potential to be used in agriculture as an alternative fertilizer or in wastewaters treatment plants.



**Keywords:** Circular economy. Waste valorization. Hydroxyl-Eggshell. Alternative fertilizer. Earth Overshoot Day

## TABLE OF CONTENTS

# FIRST PART

## 1. GENERAL INTRODUCTION

Ensuring food security using natural resources in a sustainable form is one of the most significant challenges humankind and the agricultural sector must solve for the next century. On the one side, it is clear that today's world population is already consuming more natural resources than the planet Earth can sustainably regenerate itself. Indeed, in 1970, the date when humanity's demand for ecological resources and services exceeded what Earth could regenerate in that year - the so-called **Earth Overshoot Day** - happened on December 30, whereas in 2021, it fell on July 29. On another side, the human population will reach up to 9.8 billion by 2050, demanding a considerable increase in food production (KOPITTTKE et al., 2019; RAHMAN; HAQUE; KHAN, 2021).

Modern agriculture uses a high amount of fertilizer to provide nutrient needs to increase crop production and meet the current food demand. However, most commercial fertilizers are obtained from natural rocks, non-renewable resources. The partial replacement of rocks by wastes generated in several activities - industrial processes included - is one way to minimize the use of these natural resources and perfectly fits the Circular Economic concept. In fact, in recent years, the circular economy has gained increasing prominence as a tool that presents solutions to some of the world's most pressing crosscutting sustainable development challenges. The circular economy is an integral part of the sustainability agenda and can contribute to several different Sustainable Development Goals (SDGs) (UN, 2021). It is evident that SDG 12 - Responsible consumption and production -, is at the heart of the circular economy. However, this concept holds particular potential for achieving multiple SDGs, including SDGs 6 on energy, 8 on economic growth, 11 on sustainable cities, 12 on sustainable consumption and production, 13 on climate change, 14 on oceans, and 15 on life on land.

Some solid wastes have high nutrient content and most of the time they are directly disposed of into water or soil, causing environmental issues. Among them, stand out residues discarded by egg-processing and vaccine industries. Each one has a different physical, chemical, and biological composition. In order to increase their agricultural potential and minimize environmental contamination risks, each one of these wastes has to be chemically transformed.

The egg-processing industries generate eggshells (ES) as final waste. It is estimated that around seven million tons of ES are discarded in the world per year (OLIVEIRA; BENELLI; AMANTE, 2013). Due to its natural porosity and high concentration (~95%) of calcium carbonate,

ES has been used as a natural bioadsorbent for heavy metals in contaminated areas (ASHRAFI et al., 2015) and industrial effluents (WANG; WEI; HUANG, 2013). There is also the possibility of using ES as a soil amendment, but the amount generated is not enough to meet the demand of large agricultural areas. Thus, the ES must be transformed into a material with greater added value and for local use, if possible, within the company itself.

The waste generated by vaccine industries has a different chemical composition and also presents a high risk of environmental contamination. In short, this waste is generated whenever a virus sample is inoculated into the egg for replication to take place. After the incubation period, the liquid where the virus has multiplied is extracted, leaving most of the egg in the shell. The remaining material is crushed and dried, forming a powder residue. According to the Brazilian legislation, due to its high potential of microbial contamination, solid waste from vaccine industries has to be disposed of into Class 1 landfills, which are specialized places that receive only hazardous solids (BRASIL, 2004, 2005). The Brazilian legislation also requires that contaminated solids must pass thru a microbial inactivation treatment inside the industry previously to sending them to landfills. Hence, there are two major expenses: biological inactivation and corrected landfill disposal.

In this work, we propose easy methods to transform either eggshell or vaccine wastes into value-added byproducts. The eggshells were transformed into a white solid labeled as “Hydroxy-Eggshell” (ES-OH). ES-OH has the potential to be used in the final treatment of effluents generated by the processing industry itself for the precipitation of hydroxyapatite aiming at phosphate removal. We also proved in this work that ES-OH can be used to treat effluents rich in arsenic (As) by the precipitation of vladimirite crystals. The vaccine waste was thermally converted into a fully sterilized phosphorus-rich biochar with agronomic efficiency similar to that of highly concentrated soluble phosphate fertilizers.

The methodologies proposed here are simple, do not require specialized labor, and can be implemented on an industrial scale. The processes are innovative and have as main objective the production of byproducts with greater value. The use of these residues for these purposes is especially interesting, since in addition to the growing production in Brazil and worldwide, the literature available so far is unprecedented on the subject, mainly concerning vaccine residues that have been disposed of in landfills at a high cost, compromising the environment and missing a great opportunity for recycling nutrients in agriculture.

## REFERENCES


ASHRAFI, M. et al. Immobilization of Pb, Cd, and Zn in a contaminated soil using eggshell and banana stem amendments: metal leachability and a sequential extraction study. **Environmental Science and Pollution Research**, v. 22, n. 1, p. 223–230, 2015.

BRASIL. **Resolução Rdc Nº 306, De 7 De Dezembro De 2004**. Disponível em: <https://bvsms.saude.gov.br/bvs/saudelegis/anvisa/2004/res0306_07_12_2004.html>. Acesso em: 23 mar. 2021.

BRASIL. **RESOLUÇÃO CONAMA nº 358, de 29 de abril de 2005**. Disponível em: <http://www2.mma.gov.br/port/conama/legiabre.cfm?codlegi=462>. Acesso em: 23 mar. 2021.

OLIVEIRA, D. A. et al. A literature review on adding value to solid residues: Egg shells. **Journal of Cleaner Production**, v. 46, p. 42–47, 2013.

RAHMAN, M. H.; HAQUE, K. M. S.; KHAN, M. Z. H. A review on application of controlled released fertilizers influencing the sustainable agricultural production: A Cleaner production process. **Environmental Technology & Innovation**, v. 23, p. 101697, 2021.

WANG, S.; WEI, M. H.; HUANG, Y. M. Biosorption of Multifold Toxic Heavy Metal Ions from Aqueous Water onto Food Residue Eggshell Membrane Functionalized with Ammonium Thioglycolate. **J Agric Food Chem**, v. 61, n. 21, p. 4988–4996, 2013.

United Nations. 2021. Circular Economy for the SDGs: From Concept to Practice General Assembly and ECOSOC Joint MeetingDraft Concept and Programme for the joint meeting of the Economic and Financial (Second Committee) of the 73rd UN General Assembly and the UN Economic and Social Council. Available at: https://www.un.org/en/ga/second/73/jm_conceptnote.pdf. Accessed on January 15, 2021

## SECOND PART - ARTICLES

Article 1 - HYDROXYL-EGGSHELL: A NOVEL EGGSHELL BYPRODUCT HIGHLY EFFECTIVE TO RECOVER PHOSPHORUS FROM AQUEOUS SOLUTIONS

(Article published in Journal of Cleaner Production)
DOI: https://doi.org/10.1016/j.jclepro.2020.123042

**Hydroxyl-eggshell: a novel eggshell byproduct highly effective to recover phosphorus from aqueous solutions**

Ivan Célio Andrade Ribeiro[a], Jéssica Cristina Teodoro[b], Luiz Roberto Guimarães Guilherme[a], Leônidas Carrijo Azevedo Melo[a]

[a] Department of Soil Science, Federal University of Lavras, Lavras – Minas Gerais, Postal code 37200-000, Brazil

[b] Department of Biology, Federal University of Lavras, Lavras – Minas Gerais, Postal code 37200-000, Brazil

**Corresponding author:**
Leônidas Carrijo Azevedo Melo,
Department of Soil Science,
Federal University of Lavras,
Lavras - Minas Gerais,
Brazil, Postal code 37200-000.
Phone: +55 35 3829-1541
Fax: +55 35 3829-1256
E-mail: leonidas.melo@ufla.br

## Graphical Abstract

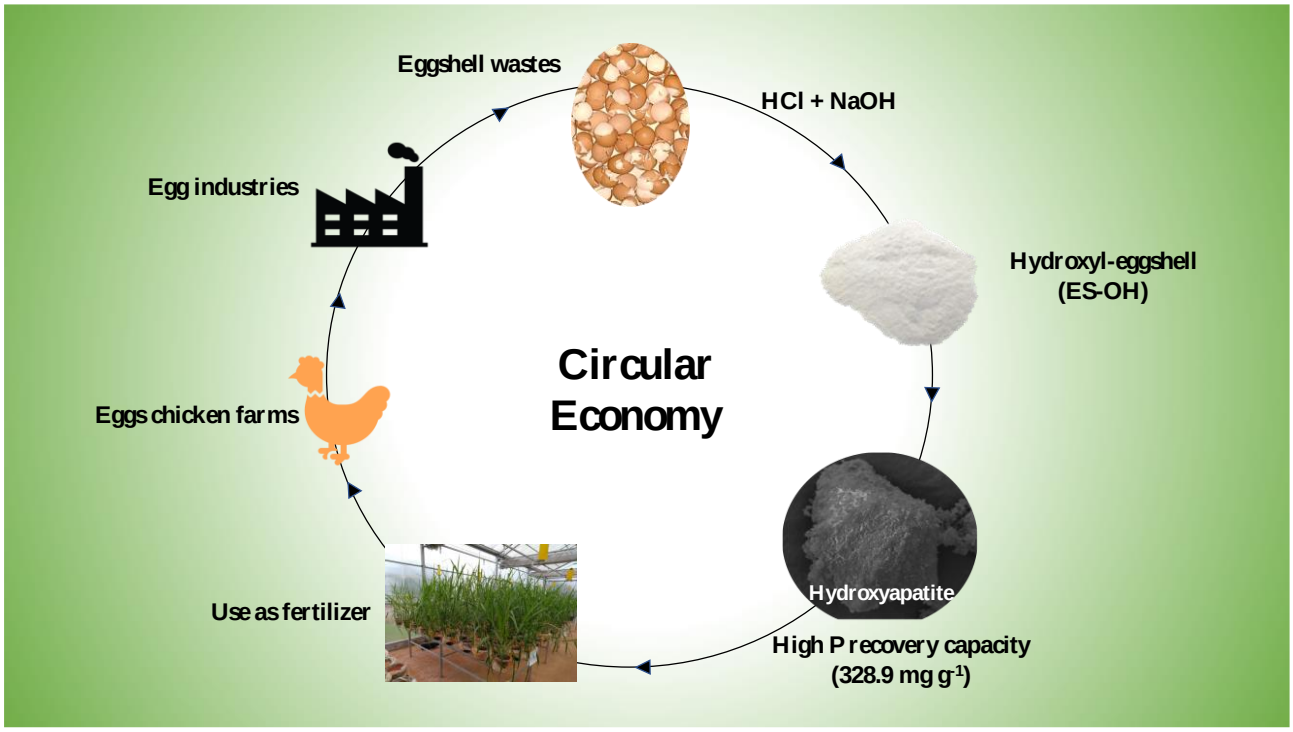

## Highlights

- A novel eggshell byproduct named Hydroxyl-Eggshell (ES-OH) was synthesized.
- ES-OH shows P recovery capacity as high as 327 mg $g^{-1}$.
- Precipitation as hydroxyapatite was the predominant P recovery mechanism.
- Soil available P from P-loaded ES-OH was higher than triple superphosphate.

**Abstract**

Efficient recovery and reuse systems are an ever-increasing challenge for global phosphorus security. This work presents a standard and straightforward methodology to produce a novel eggshell byproduct with a high P-recovery capacity. The material was obtained from chicken eggshells after reaction with hydrochloric acid and sodium hydroxide solutions and named as Hydroxyl-Eggshell (ES-OH). Batch experiments were conducted to investigate the effects of ES-OH doses, contact time, and initial P concentration on the recovery process. Fourier transform infrared spectroscopy (FTIR), scanning electron microscopy with energy dispersive X-ray spectrometry (SEM-EDS), and X-ray diffraction (XRD) were used to characterize the material before and after P reaction. The kinetics study showed that the pseudo-second-order model described well the process. The maximum P recovery capacity was 328.9 mg $g^{-1}$, which is higher than that found for other materials derived from eggshells. FTIR, SEM-EDS, and XRD confirmed that the primary process of P recovered by ES-OH is via precipitation as hydroxyapatite. Finally, a pot experiment confirmed that the P-loaded ES-OH was as effective as triple superphosphate (TSP) on grass yield with the advantage of maintaining nearly four-fold more available P and higher soil pH than TSP after cultivation. The results presented in this work showed that ES-OH is a promising material for P recovery from aqueous solution, forming a material with great potential to be used in agriculture as an alternative phosphate fertilizer.

**Keywords**: hydroxyapatite; waste valorization; precipitates; circular economy

## 1. Introduction

Phosphorus (P) is an essential element for all living organisms. Although P levels in freshwaters are often low, wastewaters, such as sewage and agro-industrial effluents may contain significant amounts of this nutrient (Cieślik; Konieczka, 2017). The disposal of P-containing wastewater triggers the eutrophication process, which is the uncontrolled multiplication of algae and other aquatic microorganisms in the water (Karunanithi et al., 2015). Some algae release toxins that cause severe human health problems and are difficult to remove even after water treatment (Hill et al., 2013).

Most P present in wastewaters is in the soluble form of orthophosphates (Metcalf; Eddy, 2014). Therefore, its recovery is performed by techniques that transfer the dissolved P to a solid fraction with subsequent removal in separation systems. Phosphorus recovery techniques include biological (Yadav; Pruthi; Kumar, 2016), physical-chemical (Park et al., 2016), or the combination of both of these processes (Pratt et al., 2012). Precipitation is the most efficient process to reduce total P concentrations to stringent levels (<0.05 mg/L) but is also expensive and can cost nearly $100 to remove each kg of P (Bashar et al., 2018).

A viable alternative to minimize P recovery costs is the replacement of standard reagents by solid wastes discarded in the environment. Among these wastes, eggshells - a final waste in egg industries - is of great interest, mainly due to their increasing generation by the breaking operations for processing eggs. This process of industrialization provides economic advantages, extending the product lifetime, besides facilitating transportation and conservation. Yet, it generates considerable amounts of eggshells in a concentrated form, which are undervalued for application as a liming material in soil or simply discarded. Annually, around 7 million tons of this waste are generated worldwide (Oliveira et al., 2013).

More than 90% of the eggshell chemical composition is calcium carbonate ($CaCO_3$), a chemical compound that gives this waste the potential to remove heavy metals such as Pb, Cd, and Cu (Ahmad et al., 2012; Zheng et al., 2007), as well as Ni (De Angelis et al., 2017) from aqueous solution. Moreover, eggshell has the potential for soil remediation by minimizing the mobility of Pb and Zn from mining areas (Soares et al., 2015).

Despite its suitability for metal mobilization, few studies have focused on the application of eggshells to recover P from wastewaters. Eggshell has a naturally low capacity to recover P, and some methodologies have been proposed to increase its potential, such as calcination (Köse; Kivanç, 2011; Torit; Phihusut, 2018), iron-enrichment (Mezenner; Bensmaili, 2009), and its incorporation into carbon-rich materials followed by pyrolysis, for biochar production (Liu; Shen; Qi, 2019). Nonetheless, the proposed methodologies are costly due to energy demand and still generate materials with low P retention capacity.

To overcome these limitations, this work aimed to propose an inexpensive and straightforward methodology to produce a novel byproduct from eggshells with high P recovery potential. The mechanisms of P recovery by this material from synthetic aqueous solutions are investigated through batch experiments and spectroscopic characterization (XRD, FTIR, and SEM-EDS). Moreover, this study aimed to evaluate the capacity of this P-loaded byproduct to act as a potential fertilizer. The new byproduct fits well into the concept of a circular economy, as the final material obtained after P recovery is adequate and safe to be used in agriculture as an alternative phosphate fertilizer (Longhurst et al., 2019), which showed excellent performance in a P-fixing soil.

## 2. Material and methods

Waste eggshells were donated by Aviário Santo Antônio, one of the biggest egg industries in Brazil, located in Nepomuceno, State of Minas Gerais. All reagents used were of analytical grade and all aqueous solutions were prepared using deionized water.

## 2.1. Hydroxyl-eggshell (ES-OH) production

The production process of ES-OH is unique and has a patent deposit in the National Institute of Industrial Property (INPI), Brazil (Ribeiro et al., 2019). Briefly, the eggshells waste, including the membranes, were washed with deionized water, dried in an oven at 100 °C for 24 h and crushed to pass a 0.5 mm sieve. Small portions of that material (100 g) were added in a glass beaker containing 500 mL of concentrated hydrochloric acid solution (1.0 mol $L^{-1}$), under constant stirring until stopping the formation of bubbles in the system. The bubbles come from the release of carbon dioxide ($CO_2$) during the reaction of HCl with the $CaCO_3$ present in the eggshell, as shown in Eq. 1.

$$CaCO_3 + 2HCl \rightarrow CaCl_2 + CO_2 + H_2O \qquad \text{Eq. 1}$$

When the system reached equilibrium, 500 mL of a 1.0 mol $L^{-1}$ sodium hydroxide solution was added to the beaker, which instantly converted all the previous calcium chloride ($CaCl_2$) formed into calcium hydroxide [$Ca(OH)_2$], as shown in Eq. 2:

$$CaCl_2 + 2\,NaOH \rightarrow Ca(OH)_2 + 2\,NaCl \qquad \text{Eq. 2}$$

After two hours of stirring, the solid was left to settle down in the beaker, and the supernatant was removed and replaced with 1000 mL of deionized water. The system was again placed under constant stirring for 5 min, followed by an additional two hours of resting as well as another

replacement of the supernatant with deionized water (1000 mL). This procedure was repeated three times to remove the excess of sodium chloride (NaCl) formed in the process. Finally, the remaining solid material was transferred to porcelain capsules and oven-dried at 100 °C for 24 h and cooled to room temperature. Subsequently, the material was removed from the recipient, crushed with a pestle and homogenized using a 0.5 mm sieve. Finally, with the initial mass of eggshells (100 g), it was possible to obtain 67 g of the new product. This new product was named as "Hydroxyl-Eggshell" (ES-OH), i.e., calcium hydroxide obtained from the eggshell. Based on this bench top production process, an estimate of the capital cost to produce one kilogram of this new material is presented on Table 1. Labor costs were not contemplated in this assessment, which considered only the costs of chemical reagents used and the energy consumption for 2-hours use of a magnetic stirrer (Fanem, model 258, and P = 320 W).

**Table 1.** Estimation of capital cost needs to produce 1 kg of ES-OH.

| Material | Market cost (A) (US$/kg or /kWh) | Consumption (B) (kg or kWh) | Cost (AxB) (US$) |
|---|---|---|---|
| HCl | 10.0* | 0.27 | 2.72 |
| NaOH | 1.78* | 0.31 | 0.56 |
| Energy | 0.14** | 9.55 | 1.20 |
| | | Total | 4.48 |

*Average of three values found on the Brazilian online market **Based on energy price applied for the industrial category in Minas Gerais state, Brazil. Links in Table S1.

To prove its similarity to $Ca(OH)_2$, a suspension with 5.0 g $L^{-1}$ of ES-OH was prepared in deionized water, stirred at 120 rpm for 2 h, filtered using a 0.45 μm membrane filter and the soluble Ca was measured by inductively coupled plasma optical emission spectrometry (ICP-OES). Calcium

concentration at equilibrium was predicted for a solution containing 5.0 g $L^{-1}$ of portlandite [$Ca(OH)_2$] at 760 ppm [$CO_2$] atmosphere using Visual MINTEQ 3.0 (Gustafsson, 2010). ES-OH showed a very similar Ca concentration (0.876 g $L^{-1}$) at equilibrium when compared with that of portlandite (0.885 g $L^{-1}$).

## 2.2. Phosphorus recovery experiments

Phosphorus recovery experiments were carried out at room temperature (25±3 °C), and a synthetic P-stock solution was prepared by dilution of monobasic potassium phosphate ($KH_2PO_4$) in deionized water. The effect of different ES-OH doses, 0.5, 1.0, 2.0, 5.0, and 10.0 g $L^{-1}$, on P recovery efficiency was evaluated in solutions containing 500 mg $L^{-1}$ P at pH 5.5 (natural pH of the solution). Each suspension was kept under stirring at 120 rpm for 24 h of reaction time. Next, the equilibrium solution was filtered using a 0.45 μm membrane filter, and the remaining P was quantified by inductively coupled plasma optical emission spectrometry (ICP-OES - P determination range = 0.01-80 mg $L^{-1}$).

A kinetics study experiment was performed in centrifuge tubes containing 40 mL of a 500 mg $L^{-1}$ P solution and 5.0 g $L^{-1}$ of ES-OH. The suspension was stirred at 120 rpm in different time intervals (15, 30, 40, 60, 90, 180, 240, 480, 960, and 1440 min) with triplicates for each time. Then, the suspensions were filtered through 0.45-μm membrane filters, and the P concentrations at different equilibrium times were measured by ICP-OES. Pseudo-first order and pseudo-second-order models, as expressed in Eq. 3 and 4, were used to fit the experimental data for better understanding P recovery kinetics.

$$\ln(Q_e - Q_t) = \ln Q_e - k_1 t \quad \text{Eq. 3}$$

$$\frac{t}{Q_t} = \frac{1}{Q_e^2} + \frac{t}{k2Q_e} \quad \text{Eq. 4}$$

where $Q_e$ and $Q_t$ represent the amount of P recovered at equilibrium and at a given time interval (t), respectively; $k_1$ and $k_2$ are pseudo-first, and second-order constants of P recovery kinetics, respectively.

The influence of initial P concentration was evaluated in the range of 0 to 10,000 mg $L^{-1}$ P. For that, 40 mL of each solution at natural pH were reacted with 0.2 g of ES-OH (dose of 5.0 g $L^{-1}$), followed by 24 h of shaking. This high range was chosen based on previous tests aiming to reach the maximum P recovery capacity of ES-OH. After the shaking time, the suspensions were filtered, and the P at equilibrium was analyzed by the same procedure previously described. To further investigate the mechanism of P recovery, the original data were fitted to the original non-linear Langmuir (LANGMUIR, 1918) and Freundlich (Freundlich, 1907) isotherms as shown in equations 5 and 6, respectively:

$$q = \frac{q_{max}\, k_l\, C_e}{(1 + KC_e)} \quad \text{Eq. 5}$$

$$q = k_f C e^{1/n} \quad \text{Eq. 6}$$

where q represents equilibrium recovery capacity; Ce is the P concentration at equilibrium; $q_{max}$ is the maximum recovery capacity of the material; n is the recovery intensity of the adsorbent; and $K_l$ and $K_f$ are the Langmuir and Freundlich adsorption constants, respectively.

All P recovery tests in this work were performed in triplicate. The mean values and standard errors were calculated and reported in the corresponding table or figure. Additional replicates were performed whenever the variation among replicate results was higher than 5%. Also, all of the equations presented in this work were fitted using the generalized reduced gradient algorithm, an Excel 2016 solver method, aiming to produce the highest corresponding coefficient of determination ($R^2$).

## 2.3. Hydroxyl-eggshell (ES-OH) characterization

Material characterization analyses were performed in ES-OH before and after P recovery tests. Surface morphology and the main composition of the materials were evaluated in a Quanta 650FEG Scanning Electron Microscope (SEM) with an X-ray microanalysis system by dispersive energy spectroscopy (EDS). Fourier transform infrared (FTIR) spectra were also collected to evaluate the modification of the functional groups of the materials using a Digilab Excalibur spectrometer with a spectral range 4000-400 $cm^{-1}$ under 4 $cm^{-1}$ resolution with 16 scans.

Lastly, X-ray diffraction (XRD) analyses were carried out to identify the minerals formed in ES-OH before and after P recovery tests. The analyses were performed using a Rigaku Miniflex II equipment with CuKα radiation and a graphite monochromatic beam, in the range of 3 - 60° 2θ, step size of 0.02 2θ degree and counting time of 5 s/step. The diffractograms were interpreted using the Match® program and compared with the database available at "mindat.org".

## 2.4. Greenhouse experiment

A pot experiment was carried out under greenhouse conditions aiming to investigate the capacity of ES-OH precipitated after the recovery test as a P source to grow grass. Initially, each pot was filled up with a plastic bag containing 1.0 kg of a soil sample from the top 20 cm of a highly

weathered soil classified as Ultisol (STAFF, 1999), with the following physical and chemical characteristics: clay = 670 g $kg^{-1}$; pH in water = 4.8; organic matter = 20.0 g $kg^{-1}$; P (Mehlich-1) = 0.35 mg $kg^{-1}$; K = 0.06 $cmol_c$ $kg^{-1}$; Ca = 0.30 $cmol_c$ $kg^{-1}$; Mg = 0.11 $cmol_c$ $kg^{-1}$; Al = 0.3 $cmol_c$ $kg^{-1}$; H + Al = 4.99 $cmol_c$ $kg^{-1}$. Based on these characteristics, liming was performed, aiming to increase the base saturation to 70% using $CaCO_3$ and $MgCO_3$ in a Ca/Mg molar ratio of 3:1, and then incubated with humidity close to 70% of soil water holding capacity during 30 days. After this time, the soil was air-dried and thoroughly mixed with 200 mg of P soluble in neutral ammonium citrate from P-loaded ES-OH and triple superphosphate (positive control). A control treatment without the addition of P was also evaluated. Subsequently, the following nutrients were applied as a solution (in mg $kg^{-1}$): N (50), K (100), S (40), B (0.8), Cu (1.5), Fe (3.0), Mn (3.5), Mo (0.1), and Zn (5.0), which are the recommended amounts for pot experiments in nutrient-deficient soils (Oliveira et al., 1991). The experiment was carried out in a completely randomized design with four replicates.

Ten seeds of grass (*Urochloa Brizantha*) were sown in each pot and thinned to four seedlings after ten days of emergence. During cultivation, after 15, 30, 60, 75, 90, 105, and 120 days, additional doses of 50 mg $kg^{-1}$ of N as ammonium nitrate ($NH_4NO_3$) were applied. Soil moisture was maintained close to field capacity by daily weighing, and the volume was refilled with deionized water whenever needed. After 60 and 120 days, the plants were harvested at 10 cm from the soil, placed in paper bags and oven-dried (65-70 °C) to constant weight. The final weight of the two harvests was recorded for each sample as shoot biomass (SB). After the second harvest, a representative soil sample was collected in each pot to measure soil pH and the remaining plant-available P by the anion-exchange resin method (Van Raij; Quaggio; Da Silva, 1986). Finally, the amount of P uptake by the grass was estimated multiplying the P content in shoot biomass with the respective dry mass in each harvest.

## 3. Results and discussion

In this section, findings obtained from batch phosphorus recovery experiments using ES-OH and the material characterization before and after these tests are presented and discussed. Additionally, a greenhouse experiment with P-loaded ES-OH applied to soil as an alternative fertilizer, as well as the economic and environmental significance of this novel byproduct, are discussed.

### 3.1 Phosphorus recovery experiments

The effect of ES-OH doses on P recovery efficiency and the final pH of the solution is shown in Fig. 1. Both P recovery rate and final pH increased with increasing the ES-OH dose, reaching the maximum recovery rate (~100%) at 5.0 g $L^{-1}$. This first step was essential to define the optimum ES-OH dosage for the succeeding experiments. The composition of the ES-OH, which is mainly $Ca(OH)_2$, allows the formation of hydroxyapatite via solution precipitation at pH > 10 (Cichy; Ku; Krzto, 2019). In fact, a simulation using Visual MINTEQ for 5.0 g $L^{-1}$ of ES-OH, with the same pH and P concentration shown in Fig. 1, also confirmed the hypothesis that the main mineral precipitated was hydroxyapatite, with a saturation index equal to 26.4. The Eq. 7 shows the reaction of hydroxyapatite formation.

$$5\,Ca^{2+} + 3\,PO_4^{3-} + OH^- \leftrightarrow Ca_5(PO_4)_3OH \qquad \text{Eq. 7}$$

Samples of the precipitate formed after the P recovery test at 5.0 g $L^{-1}$ dose were used for further mineralogical, morphological analyzes, and pot experiments.

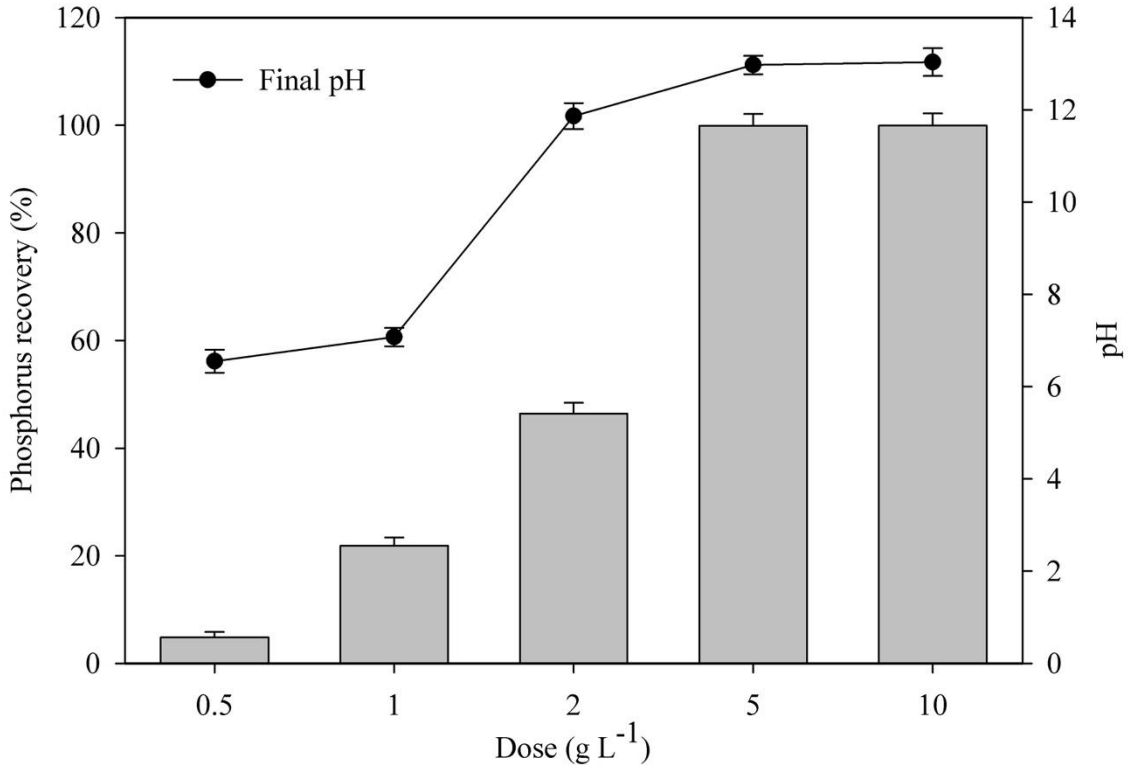


**Fig. 1.** Effect of ES-OH dosage on P recovery and final pH of the solution. Experimental conditions: Initial P concentration = 500 mg $L^{-1}$; Initial solution pH = 5.5.

The kinetics of P recovery from a solution with 500 mg $L^{-1}$ of P and 5.0 g $L^{-1}$ of ES-OH is shown in Fig. 2. There was a rapid phase over the first 20 min, followed by a slow P recovery phase, reaching the equilibrium after 60 min. This fast removal reaction is one additional evidence suggesting that P recovery by ES-OH is via precipitation of calcium phosphates (Torit; Phihusut, 2018). A similar result, using biochar enriched with calcium hydroxide is proposed by Wang et al. (2018), who reported precipitation of calcium phosphate as a fast mechanism of P removal from synthetic solutions.

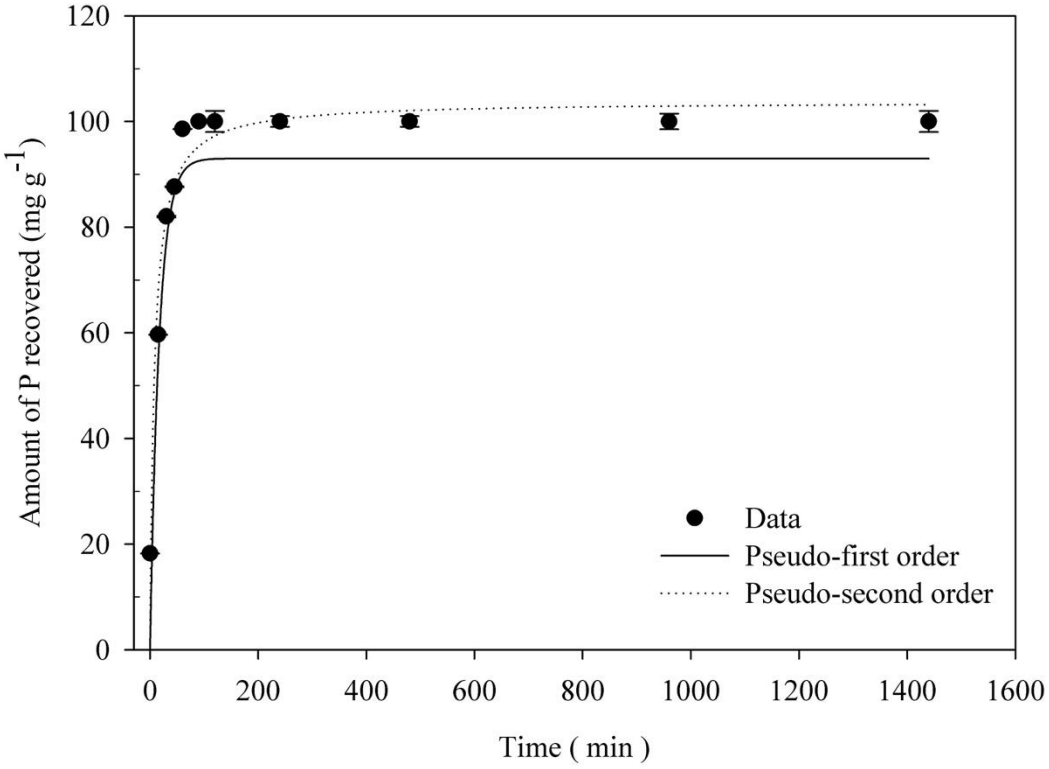


**Fig. 2.** Kinetics of P recovery efficiency by ES-OH. Experimental conditions: ES-OH dose = 5.0 g $L^{-1}$; Initial P concentration = 500 mg $L^{-1}$; Initial solution pH = 5.5.

The pseudo-second-order equation fitted the experimental data better than the pseudo-first-order model, presenting a higher coefficient of determination (Table 2). A better adjustment of the kinetics with the pseudo-second-order model might infer that the mechanism of P recovery is based on reactions involving the sharing of electrons (Mitrogiannis et al., 2017). This electron sharing may occur through the ionic bonds between the ions $Ca^{2+}$ presented in ES-OH with the orthophosphates ($PO_4^{3-}$/$HPO_4^{2-}$/$HPO_4^{2-}$) ions in solution (Dai et al., 2017). For the conditions previously described, i.e., ES-OH dose of 5.0 g $L^{-1}$ and final pH higher than 12.3, the main orthophosphate form present in the solution is $PO_4^{-3,}$ which represents the ideal conditions and is another evidence to confirm the hypothesis of hydroxyapatite formation, as shown on Eq. 5.

**Table 2**: Adsorption kinetics and isotherms models' parameters for P recovered using ES-OH.

| Model | Parameter 1 | Parameter 2 | $R^2$ |
|---|---|---|---|
| Pseudo-first order | Qe = 93 mg $g^{-1}$ | $k_1$ = 0.06 $min^{-1}$ | 0.92 |
| Pseudo-second order | Qe = 103.7 mg $g^{-1}$ | $k_2$ = 0.001 g $mg^{-1}$ $min^{-1}$ | 0.95 |
| Langmuir | $Q_{max}$ = 328.9 mg $g^{-1}$ | K = 0.004 L $mg^{-1}$ | 0.98 |
| Freundlich | $K_f$ = 41.7 mg $g^{-1}$ | n = 4.41 | 0.83 |

$Q_e$ = amount of P recovery at equilibrium; $k_1$ = pseudo-first order rate constant; $k_2$ = pseudo-second order rate constant; $Q_{max}$ = maximum recovery capacity; $K_f$ and n Freundlich affinity and linearity constants respectively.

Finally, to better understand the P recovery mechanism, the P concentration at equilibrium was measured after 24h shaking of suspensions containing 5.0 g $L^{-1}$ of ES-OH and increasing P concentrations. The observed data were fitted to Langmuir and Freundlich isotherms which can be visualized in Fig. 3, and the corresponding fitting parameters in Table 2.

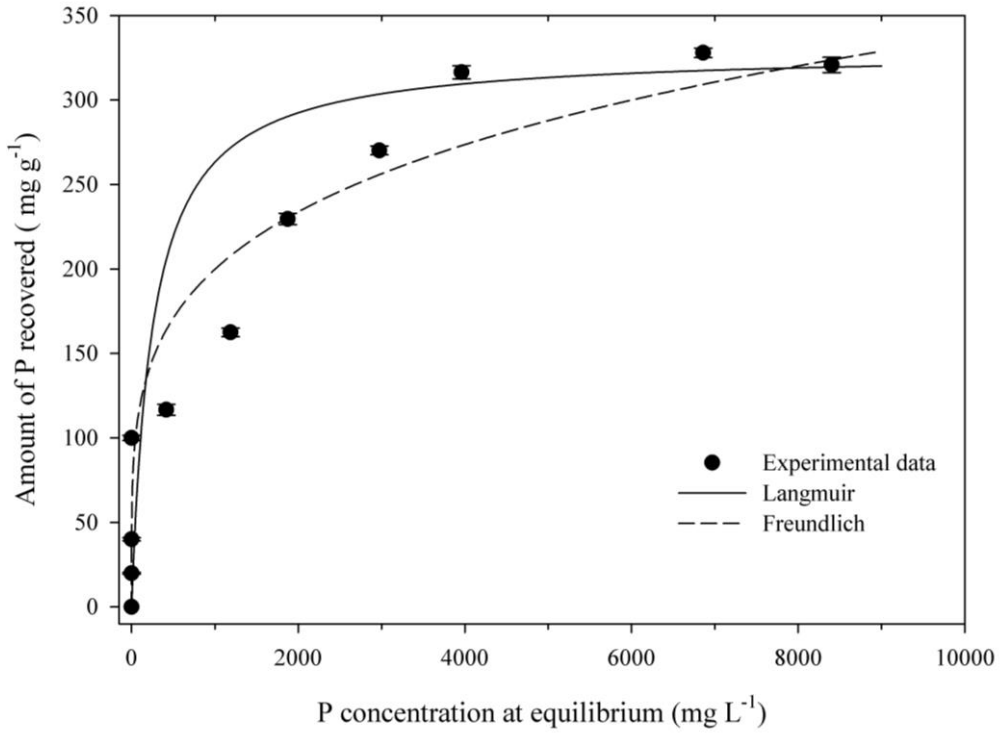


**Fig. 3.** Fitted Langmuir and Freundlich isotherm models for P sorption onto ES-OH

The Langmuir model had a better fitting ($R^2$ = 0.98) to P sorption data when compared with the Freundlich model ($R^2$ = 0.83). The maximum recovery capacity for ES-OH was 328.9 mg $g^{-1}$ or 32.8% of P. Such a high P recovery capacity makes this material a potential adsorbent for recovering phosphorus from wastewaters with a very wide range of P concentrations (Peng et al., 2018). However, assuming that ES-OH is mainly composed of calcium hydroxide, there is no calcium phosphate mineral with such a high P concentration (Ralph, 2004). Thus, the assumption of a completely homogeneous sorption surface proposed by the Langmuir model is not valid for this material. A better explanation for the mechanism of P recovery is the formation of double layers on ES-OH, as shown in Fig. 4. The hypothesis is that the second layer form to neutralize the excess of positive charge remaining on ES-OH particle by a weak interaction bond with the negative charge of orthophosphates ions.

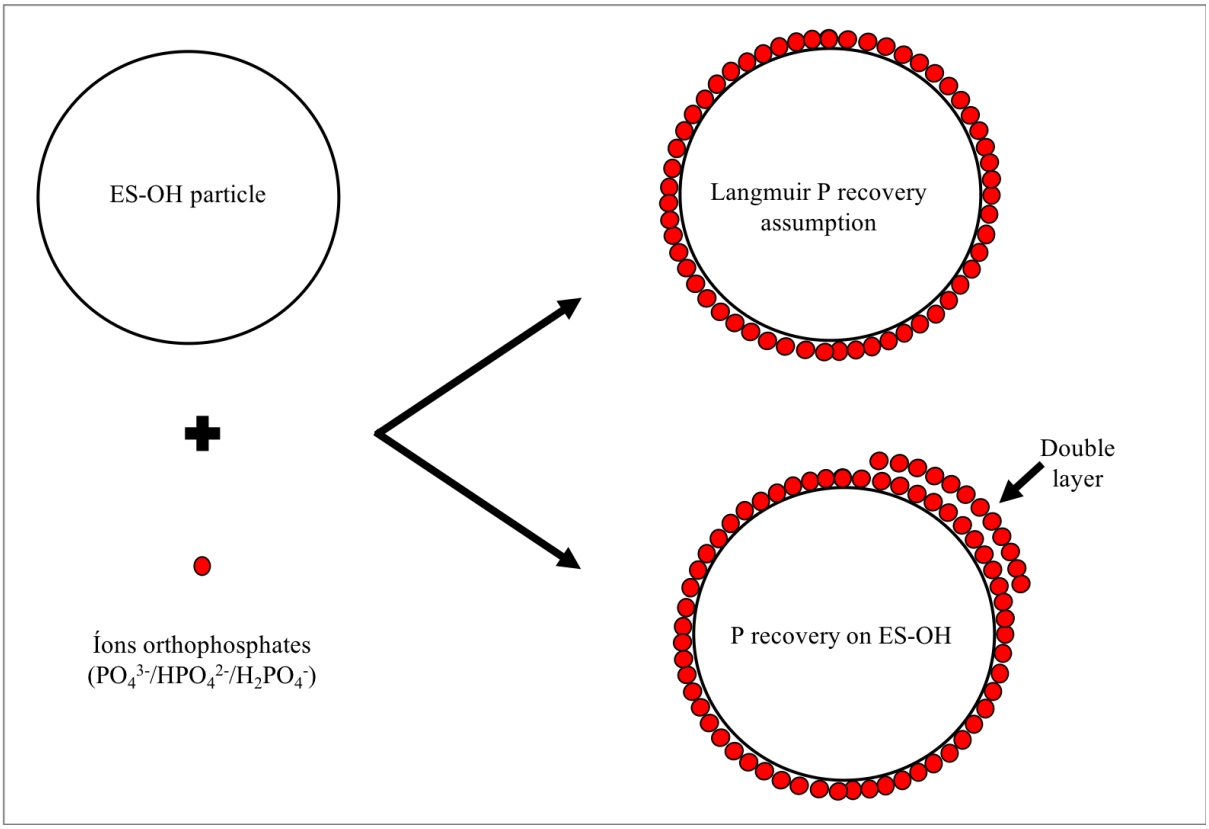


**Fig. 4**. Proposed mechanism of phosphorus recovery into ES-OH

The P recovery capacity of the ES-OH estimated by the Langmuir model in this study was greater than any previous values reported for other eggshell-derived materials designed for the same purpose (Table 3). Another advantage is the low energy cost and simplicity of the process to obtain the ES-OH when compared with other materials obtained by the processes presented in Table 3, which require more sophisticated equipment and are high energy-consuming due to the need of calcination or pyrolysis.

**Table 3.** Maximum P recovery capacity of different eggshell-derived materials from literature.

| Material | P range ($mg\ L^{-1}$) | Dose ($g\ L^{-1}$)* | Recovery capacity ($mg\ g^{-1}$)** | Reference |
|---|---|---|---|---|
| Iron enriched eggshells | 4 - 140 | 7.50 | 14.49 | (MEZENNER; BENSMAILI, 2009) |
| Calcined eggshell 800°C | 0 – 200 | 10.0 | 23.02 | (KÖSE; KIVANÇ, 2011) |
| Eggshell ash | 0.5 – 3 | 20.0 | 121.0 | (TORIT; PHIHUSUT, 2018) |
| Calcined eggshell 900°C | 1 - 250 | 0.44 | 31.74 | (PANAGIOTOU et al., 2018) |
| Eggshell enriched biochar | 0 – 200 | 0.25 | 231.0 | (LIU; SHEN; QI, 2019) |
| Hydroxyl-eggshell | 0 – 10.000 | 5.0 | 328.9 | This study |

*Amount of raw material divided by the volume of synthetic P solution; ** Parameter estimated from Langmuir isotherm.

At saturation, the P concentration found in the ES-OH is higher than that reported for conventional soluble P fertilizers. Therefore, the material formed could be used as an alternative fertilizer to grow plants, especially because it acts as a slow-release fertilizer avoiding fast adsorption in weathered tropical soils and reducing eutrophication of receiving water streams.

3.2 Hydroxyl-eggshell (ES-OH) characterization

The FTIR spectra of ES-OH before and after P recovery are presented in Fig. 5. The peak observed near 3500 $cm^{-1}$ is characteristic of the stretching vibration of hydrogen-bonded hydroxyl (-OH) (Mirghiasi et al., 2014). After reaction with P, this peak almost disappeared, indicating an interaction between –OH groups and active acidity ($H^+$) increasing the solution pH as shown in Fig. 5. The peak observed at 1423 $cm^{-1}$ was attributed to carbonate groups ($CO^{-3}$) (Bekiaris et al., 2016), which can be due to atmospheric carbon dioxide ($CO_2$) reacting with ions hydrogen ($H^+$) dissociated from the salt ($KH_2PO_4$) used to prepare the P solutions. The great peak at 1020 $cm^{-1}$ and the two smaller peaks at 961 and 876 $cm^{-1}$ were observed only after the reaction with P and are attributed to the bending vibration of phosphate groups (Siow et al., 2014). A likely explanation is that calcium ($Ca^{2+}$) ions dissociated from ES-OH reacted with phosphate groups in solution and precipitated as calcium phosphates.

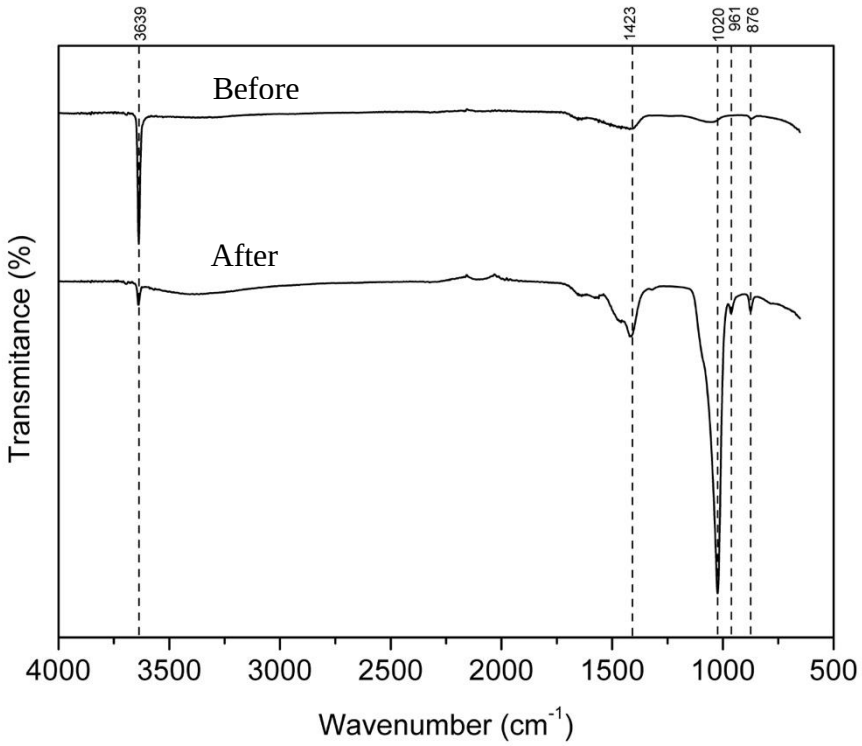


**Fig. 5.** FT-IR spectra of ES-OH before and after reaction with P.

The surface of pristine ES-OH has a regular structure composed of the union of little circular spots (Fig. 6a). In contrast, after the reaction with P, more prominent structures were formed (Fig. 6b), which suggests that precipitation took place and played an essential role in P recovery by ES-OH. Calcium was the main component in pristine ES-OH by EDS, while a considerable peak of P was observed after the reaction with P, confirming the precipitation of calcium phosphates, which will be further endorsed by XRD. Sodium and Cl were also observed in both materials, whereas K appeared only after P reaction. Potassium comes from the salt used in the preparation of the P solution, while Na and Cl remained as impurities from the ES-OH production process, even after the washing procedure.

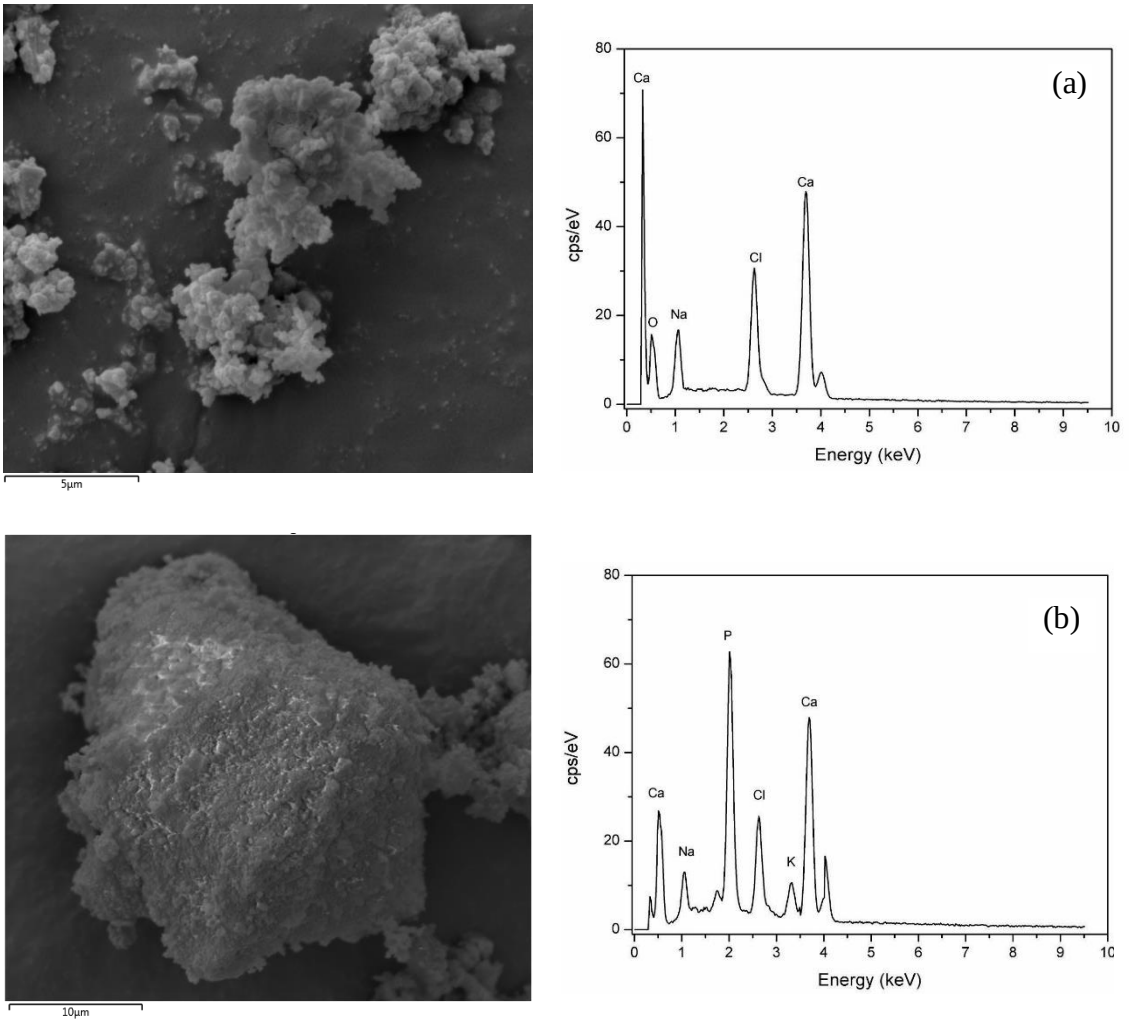


**Fig. 6.** Images of scanning electron microscopy with energy dispersive X-ray (SEM-EDS) of hydroxyl-eggshell (ES-OH) before (a) and after reaction with P (b).

The XRD analysis of the materials is shown in Fig. 7. Calcium hydroxide [$Ca(OH)_2$] were identified only in ES-OH by the peaks at 18.1°, 34.2°, 47.1°, and 50.7° 2θ. The XRD analysis in pristine ES-OH also revealed the presence of sodium chloride (NaCl) at 33.1° and 46.5° 2θ. These results are consistent with Eq. 3 presented for ES-OH production. The diffractogram after the P reaction (Fig. 7) showed patterns at 22.64°, 25.8°, 31.7°, 46.8°, and 49.6° 2θ compatible with the presence of hydroxyapatite. This mineral generally precipitates after the reaction of calcium hydroxide enriched with a concentrated P solution (Antunes et al., 2018; Wang et al., 2018). This

newly-formed hydroxyapatite can be considered a product with much higher market value than eggshells and has the potential to be used as a phosphate fertilizer.

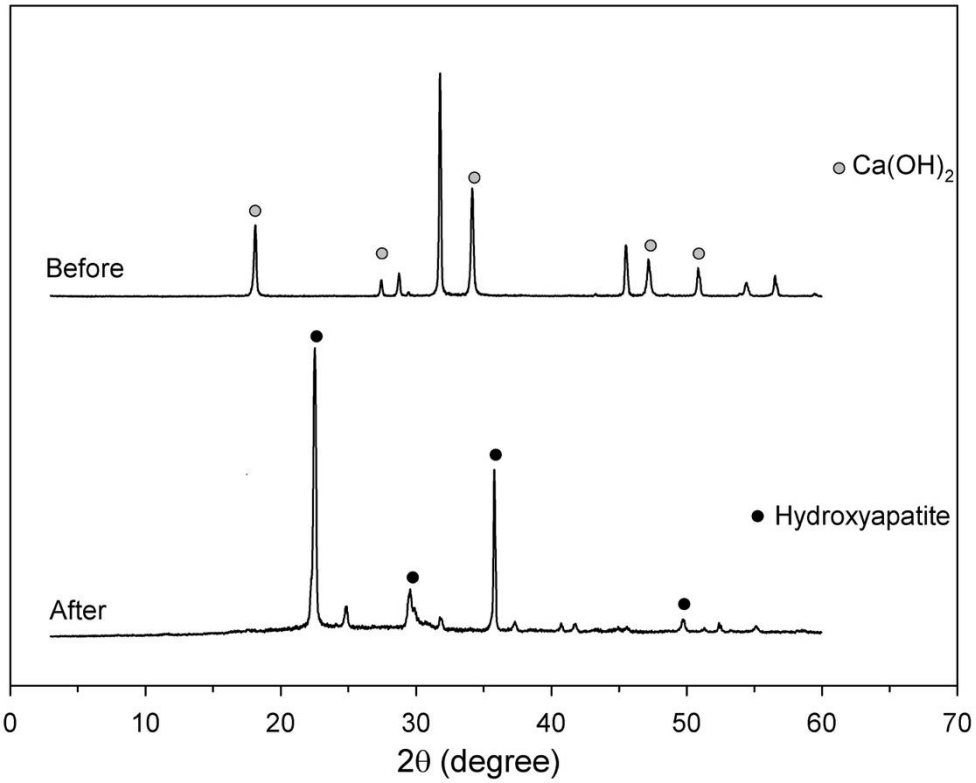


**Fig. 7.** X-ray diffraction analysis of hydroxy-eggshell (ES-OH) before (a) and after reaction with P (b).

3.3. P-loaded ES-OH as phosphate fertilizer

Plant growth, as measured by shoot biomass, was significantly improved by the application of P-loaded ES-OH and triple superphosphate (Fig. 8a). The control without P showed a negligible shoot biomass yield due to the very low P availability, which confirms that the biomass production of this grass was caused by adding P as a fertilizer. The application of ES-OH also increased soil pH (Fig. 8b), which could be explained by the dissolution of hydroxyapatite (Eq. 5) as it was shown to be the main mineral phase precipitated on ES-OH after P recovery. Phosphorus uptake in the treatment with P-loaded ES-OH was comparable to that of the TSP (Fig. 8c), indicating P availability from this alternative P fertilizer.

An outstanding result was the four-fold higher resin P soil available in P-loaded ES-OH after cultivation when compared with TSP (Fig. 8d), which is a reference of soluble P fertilizer (Novais, 2007). This result can be due to the low water-soluble P content from ES-OH (Table 3), which released P more slowly and steadily than TSP and also due to its alkaline reaction that buffered the soil pH to the optimum level for P availability (Penn; Camberato, 2019), even after grass cultivation (Fig. 8b). Since the P extracted by the resin represents the amount of P available to plants (Van Raij; Quaggio; Da Silva, 1986), the outperform of the P-loaded ES-OH in this short-term experiment shows the potential of this source as an enhanced efficient P fertilizer with a higher residual effect of the fertilization.

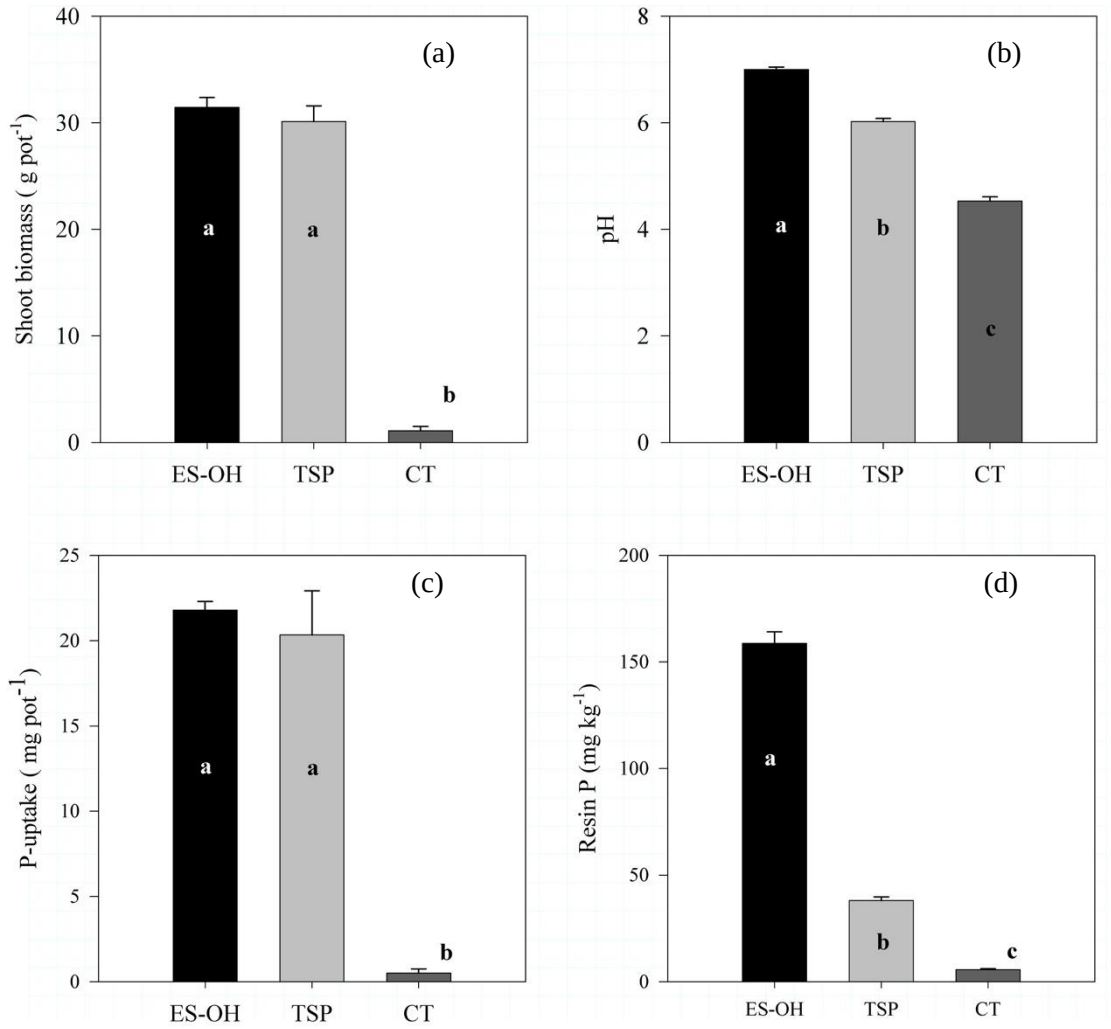


**Fig. 8.** Values of shoot biomass (a), pH (b), P uptake (c), and soil resin P (d) after grass cultivation. Different letters inside the bars indicate significant differences according to the Tukey test ($p < 0.05$).

As shown in Table 4, triple superphosphate is a highly water-soluble phosphate fertilizer, then once applied to the soil, most of its P is immediately released to the medium and is sorbed by soil particles, mainly in acidic and highly weathered soils such as the one used in this study. This process is a major problem faced by Brazilian farmers during P fertilization (Rodrigues et al., 2016). Conversely, P present in P-loaded ES-OH is practically insoluble in water showing 0.5% of the total P (Table 4). Therefore, the P content in this material is released in small proportions over time,

limiting the fast adsorption by the soil. Based on these results, use the ES-OH load with P should be considered a potential alternative to partially substitute conventional phosphate fertilizers.

**Table 4**

Phosphorus contents of TSP and P-loaded ES-OH

| Material | Total P | NCA*-soluble P | Water-soluble P |
|---|---|---|---|
| | g $kg^{-1}$ | | |
| TSP | 226 ± 0.9 | 192 ± 0.5 (85%) | 148 ± 1.1 (65%) |
| P-loaded ES-OH | 122 ± 1.0 | 83.8 ± 2.3 (69%) | 0.62 ± 0.01 (0.5%) |

*NCA – Neutral ammonium citrate; Total P, NCA-soluble P, and Water-soluble P were determined according to (BRASIL, 2014). Values in brackets are the percentage of total P.

3.4 Economic and Environmental Significance

All results previously reported were consistent with the formation of hydroxyapatite and confirmed that the process for obtaining ES-OH from eggshell wastes resulted in a material with high P recovery potential from aqueous solutions. Hence, this novel material has a high potential for P recovery in waters with a wide concentration range of this element. The P-loaded material can be an alternative and efficient slow-release phosphate fertilizer. Although cost analyses for a direct comparison of technologies involving different scales (i.e. bench top *vs* pilot *vs* full-scale treatments) might be misleading, based on the production cost ($4.48) and the P recovery capacity (328.9 mg $g^{-1}$) of ES-OH, the investment to remove each kg of P from water solutions is estimated as $13.62, which is low when compared with the market price of other existing techniques to remove P (Bashar et al., 2018).

According to these findings, there is no technical barrier towards optimizing the transformation of eggshells into ES-OH and its subsequent use to obtain high purity hydroxyapatite.

Research still needs to be carried out to confirm the performance of ES-OH for P recovery in real wastewaters. Also, the conversion of eggshell wastes into ES-OH at an industrial scale could result in economic benefits when compared with conventional disposal methods (Oliveira; Benelli; Amante, 2013). Besides commercialization, ES-OH can be used in effluent treatment systems from industries, minimizing costs and providing an environmentally friendly solution. Ultimately, the process fits well into the concept of a circular economy, as it relies on demonstrating the quality and environmental safety of a waste that can be recovered and reused as a beneficial product for agriculture.

## 4. Conclusion

In this work, a standard and straightforward methodology to produce ES-OH, a new eggshell waste byproduct, with a high P recovery capacity was proposed. Langmuir sorption showed that the maximum P recovery capacity of ES-OH was 328.9 mg $g^{-1}$. Spectroscopies analyses, such as SEM-EDS, FTIR, and XRD, consistently indicate that the main mechanism of P recovery by ES-OH was due to precipitation of newly-formed hydroxyapatites. The P-loaded byproduct demonstrates excellent potential as an alternative P fertilizer, which could ultimately be commercialized in specialized markets, enabling a new source of income for the egg-processing industries and reducing the liability with wastes generated. Future studies should focus on P recovery using different types of wastewaters aiming to investigate the mechanisms of P removal as well if the P-loaded material formed has the potential to be used as a fertilizer. Finally, this study provides a new environmentally friendly process for eggshells waste treatment producing an excellent P-recovery byproduct and a potential phosphate fertilizer substitute.

## Acknowledgments

The authors are grateful to the eggshell samples provided by Aviário Santo Antônio Company in Nepomuceno-MG, Brazil. The SEM-EDS analyzes were performed at the Brazilian Nanotechnology National Laboratory – LNNano (Proposal Nº SEM 24432). This work was funded by the National Council for Scientific and Technological Development - CNPq (Grant Nº 404076/2016-5). Scholarship to the first author was provided by the Coordination for the Improvement of Higher Education Personnel – CAPES (Proex 590-2014). LRGG and LCAM are Research Fellows of CNPq.

## References

Ahmad, M., Usman, A.R.A., Lee, S.S., Kim, S.C., Joo, J.H., Yang, J.E., Ok, Y.S., 2012. Eggshell and coral wastes as low cost sorbents for the removal of $Pb^{2+}$, $Cd^{2+}$ and $Cu^{2+}$ from aqueous solutions. J. Ind. Eng. Chem. 18, 198-204. https://doi.org/10.1016/j.jiec.2011.11.013.

Antunes, E., Jacob, M.V., Brodie, G., Schneider, P.A., 2018. Isotherms, kinetics and mechanism analysis of phosphorus recovery from aqueous solution by calcium rich biochar produced from biosolids via microwave pyrolysis. J. Environ. Chem. Eng. 6, 395-403. https://doi.org/10.1016/j.jece.2017.12.011.

Bashar, R., Gungor, K., Karthikeyan, K.G., Barak, P., 2018. Cost effectiveness of phosphorus removal processes in municipal wastewater treatment. Chemosphere 197, 280-290. https://doi.org/10.1016/j.chemosphere.2017.12.169.

Brasil, 2014. Ministerio da Agricultura, Pecuaria e Abastecimento. Manual of Official Analytical Methods for Mineral, Organic, Organomineral Fertilizers and Correctives (Manual de Metodos Analíticos Oficiais para Fertilizantes Minerais, Orgânicos, Organominerais e Corretivos, in Portuguese). MAPA/SDA/CGAL, Brasília, p. 220.

Bekiaris, G., Peltre, C., Jensen, L.S., Bruun, S., 2016. Using FTIR-photoacoustic spectroscopy for phosphorus speciation analysis of biochars. Spectrochim. Acta Part A Mol. Biomol. Spectrosc. 168, 29-36. https://doi.org/10.1016/j.saa.2016.05.049.

Cichy, B., Ku, E., Krzto, H., 2019. Phosphorus recovery from acidic wastewater by hydroxyapatite precipitation. J. Environ. Manag. 232, 421-427. https://doi.org/10.1016/j.jenvman.2018.11.072.

Cieslik, B., Konieczka, P., 2017. A review of phosphorus recovery methods at various steps of wastewater treatment and sewage sludge management. The concept of “no solid waste generation” and analytical methods. J. Clean. Prod. 142, 1728-1740. https://doi.org/10.1016/j.jclepro.2016.11.116.

Dai, L., Tan, F., Li, H., Zhu, N., He, M., Zhu, Q., Hu, G.,Wang, L., Zhao, J., 2017. Calcium rich biochar from the pyrolysis of crab shell for phosphorus removal. J. Environ. Manag. 198, 707-4. https://doi.org/10.1016/j.jenvman.2017.04.057.

De Angelis, G., Medeghini, L., Conte, A.M., Mignardi, S., 2017. Recycling of eggshell waste into low-cost adsorbent for Ni removal from wastewater. J. Clean. Prod. 164, 1497-1506. https://doi.org/10.1016/j.jclepro.2017.07.085.

Freundlich, H., 1907. Adsorption in solutions (Über die adsorption in lösungen, in German). Z. Phys. Chem. 57, 385-470.

Gustafsson, J.P., 2010. Visual MINTEQ Version 3.0. KTH, Dept. L. Water Resour. Eng. Stock. Sweden.

Hill, L.M., Bowerman,W.W., Roos, J.C., Bridges,W.C., Anderson, M.D., 2013. Effects of water quality changes on phytoplankton and lesser flamingo Phoeniconaias minor populations at Kamfers Dam, a saline wetland near Kimberley, South Africa. Afr. J. Aquat. Sci. 38, 287-294.

Karunanithi, R., Szogi, A.A., Bolan, N., Naidu, R., Loganathan, P., Hunt, P.G., Vanotti, M.B., Saint, C.P., Ok, Y.S., Krishnamoorthy, S., 2015. Phosphorus Recovery and Reuse from Waste Streams, Advances in Agronomy. Elsevier Ltd. https://doi.org/10.1016/bs.agron.2014.12.005.

Köse, T.E., Kıvanç, B., 2011. Adsorption of phosphate from aqueous solutions using calcined waste eggshell. Chem. Eng. J. 178, 34-39. https://doi.org/10.1016/ j.cej.2011.09.129.

Langmuir, I., 1918. The adsorption of gases on plane surfaces of glass, mica and platinum. J. Am. Chem. Soc. 40, 1361-1403. https://doi.org/10.1021/ ja02242a004.

Liu, X., Shen, F., Qi, X., 2019. Adsorption recovery of phosphate from aqueous solution by CaO-biochar composites prepared from eggshell and rice straw. Sci. Total Environ. 666, 694-702. https://doi.org/10.1016/j.scitotenv.2019.02.227.

Longhurst, P.J., Tompkins, D., Pollard, S.J.T., Hough, R.L., Chambers, B., Gale, P.,Tyrrel, S., Villa, R., Taylor, M., Wu, S., Sakrabani, R., Litterick, A., Snary, E., Leinster, P., Sweet, N., 2019. Risk assessments for quality-assured, sourcesegregated composts and anaerobic digestates for a circular bioeconomy in the UK. Environ. Int. 127, 253-266. https://doi.org/10.1016/j.envint.2019.03.044.

Metcalf, Eddy, 2014. Wastewater Engineering: Treatment and Resource Recovery, fifth ed. McGraw-Hill Education.

Mezenner, N.Y., Bensmaili, A., 2009. Kinetics and thermodynamic study of phosphate adsorption on iron hydroxide-eggshell waste. Chem. Eng. J. 147, 87-96. https://doi.org/10.1016/j.cej.2008.06.024.

Mirghiasi, Z., Bakhtiari, F., Darezereshki, E., Esmaeilzadeh, E., 2014. Preparation and characterization of CaO nanoparticles from Ca(OH)2 by direct thermal decomposition method. J. Ind. Eng. Chem. 20, 113-117. https://doi.org/10.1016/j.jiec.2013.04.018.

Mitrogiannis, D., Psychoyou, M., Baziotis, I., Inglezakis, V.J., Koukouzas, N., Tsoukalas, N., Palles, D., Kamitsos, E., Oikonomou, G., Markou, G., 2017. Removal of phosphate from aqueous solutions by adsorption onto Ca(OH)2 treated natural clinoptilolite. Chem. Eng. J. 320, 510-522. https://doi.org/10.1016/ j.cej.2017.03.063.

Novais, R.F., Smyth, T.J., Nunes, F.N., 2007. Phosphorus (f_osforo, in Portuguese). In: Novais, R.F., Alvarez, V.H., De Barros, N.F., Fontes, R.L., Cantarutti, R.B., Neves, J.C.L. (Eds.), Soil Fertility (Fertilidade do solo, in Portuguese), Sociedade Brasileira de Ciência do Solo), pp. 471-550.

Novais, R.F., Neves, J.C.L., Barros, N.F., 1991. Essay in controlled environment (ensaio em ambiente controlado, in Portuguese). In: Oliveira, A.J., Garrido, W.E., Araújo, J.D., Lourenço, S. (Eds.), Research Methods in Soil Fertility (Métodos de Pesquisa em Fertilidade do Solo, in Portuguese). Embrapa-SEA, Brasília, pp. 189-254.

Oliveira, D.A., Benelli, P., Amante, E.R., 2013. A literature review on adding value to solid residues: egg shells. J. Clean. Prod. 46, 42-47. https://doi.org/10.1016/j.jclepro.2012.09.045.

Oliveira, D.A., Benelli, P., Amante, E.R., Guru, P.S., Dash, S., 2013. A literature review on adding value to solid residues: egg shells. J. Clean. Prod. 46, 42-47. https://doi.org/10.1016/j.jclepro.2012.09.045.

Panagiotou, E., Kafa, N., Koutsokeras, L., Kouis, P., Nikolaou, P., Constantinides, G., Vyrides, I., 2018. Turning calcined waste egg shells and wastewater to Brushite: phosphorus adsorption from aqua media and anaerobic sludge leach water. J. Clean. Prod. https://doi.org/10.1016/j.jclepro.2018.01.014.

Park, J.-H., Kim, S.-H., Delaune, R.D., Kang, B.-H., Kang, S.-W., Cho, J.-S., Ok, Y.S., Seo, D.-C., 2016. Enhancement of phosphorus removal with near-neutral pH utilizing steel and ferronickel slags for application of constructed wetlands. Ecol. Eng. 95, 612-621.

Peng, L., Dai, H., Wu, Y., Peng, Y., Lu, X., 2018. A comprehensive review of phosphorus recovery from wastewater by crystallization processes. Chemosphere 197, 768-781. https://doi.org/10.1016/j.chemosphere.2018.01.098.

Penn, C.J., Camberato, J.J., 2019. A critical review on soil chemical processes that control how soil ph affects phosphorus availability to plants. Agric. For. 9, 1-18. https://doi.org/10.3390/agriculture9060120.

Pratt, C., Parsons, S.A., Soares, A., Martin, B.D., 2012. Biologically and chemically mediated adsorption and precipitation of phosphorus from wastewater. Curr. Opin. Biotechnol. 23, 890-896.

Ralph, J., 2004. Mindat. orgethe mineral database [WWW Document]. Mindat, Surrey, Engl. URL. https://www.mindat.org/chemsearch.php. accessed 2.4.20.

Ribeiro, I.C.A., Melo, L.C.A., Guilherme, L.R.G., Teodoro, J.C., 2019. Calcium Hydroxide production process using eggshell (Processo de Produção de Hidróxido de Cálcio a Partir da Casca de Ovo, in Portuguese). BR 10 2019 018675 5.

Rodrigues, M., Pavinato, P.S., Withers, P.J.A., Teles, A.P.B., Herrera, W.F.B., 2016. Legacy phosphorus and no tillage agriculture in tropical oxisols of the Brazilian savanna. Sci. Total Environ. 542, 1050e1061. https://doi.org/10.1016/j.scitotenv.2015.08.118.

Siow, K.S., Britcher, L., Kumar, S., Griesser, H.J., 2014. Deposition and XPS and FTIR analysis of plasma polymer coatings containing phosphorus. Plasma Process. Polym. 11, 133-141. https://doi.org/10.1002/ppap.201300115.

Soares, M.A.R., Quina, M.J., Quinta-Ferreira, R.M., Soares Margarida, J., Quinta-Ferreira, Rosa, M., M.A.R.Q., 2015. Immobilisation of lead and zinc in contaminated soil using compost derived from industrial eggshell. J. Environ. Manag. 164, 137-145. https://doi.org/10.1016/j.jenvman.2015.08.042.

Staff, S.S., 1999. Soil Taxonomy: A Basic System of Soil Classification for Making and Interpreting Soil Surveys, second ed. Natural Resources Conservation Service. U.S.

Torit, J., Phihusut, D., 2018. Phosphorus removal from wastewater using eggshell ash. Environ. Sci. Pollut. Res. https://doi.org/10.1007/s11356-018-3305-3.

Van Raij, B., Quaggio, J.A., Da Silva, N.M., 1986. Extraction of phosphorus, potassium, calcium, and magnesium from soils by an ion-exchange resin procedure.
Commun. Soil Sci. Plant Anal. 17, 547-566.

Wang, S., Kong, L., Long, J., Su, M., Diao, Z., Chang, X., Chen, D., Song, G., Shih, K., 2018. Adsorption of phosphorus by calcium-flour biochar: isotherm, kinetic and transformation studies. Chemosphere 195, 666-672. https://doi.org/10.1016/j.chemosphere.2017.12.101.

Yadav, D., Pruthi, V., Kumar, P., 2016. Enhanced biological phosphorus removal in aerated stirred tank reactor using aerobic bacterial consortium. J.Water Process Eng. 13, 61-69.

Zheng, W., Li, X. ming, Yang, Q., Zeng, G. ming, Shen, X. xin, Zhang, Y., Liu, J. jin, 2007. Adsorption of Cd(II) and Cu(II) from aqueous solution by carbonate hydroxylapatite derived from eggshell waste. J. Hazard Mater. 147, 534-539. https://doi.org/10.1016/j.jhazmat.2007.01.048.

**Supplementary material**

Table S1. Value of each material needy to prepare ES-OH.

| Material | Market price (US$/kg or US$/kWh)* | Source link verified on 03-26-2020 |
|---|---|---|
| HCl | 9.05 | https://www.didaticasp.com.br/acido-cloridrico-pa-37-5l-pfssp |
| | 8.90 | https://www.metaquimica.com/acido-cloridrico-pa-acs-37-1000ml-quimica-moderna-controlado-policia-federal-formula-hcl.html |
| | 12.06 | https://www.didaticasp.com.br/acido-cloridrico-pa-37-1l-pfssp |
| NaOH | 2.30 | https://www.lojaquimica.com.br/materia-prima/hidroxidos/soda-caustica-99-5-kg-escama |
| | 1.34 | https://www.casadosquimicos.com.br/materias-primas/hidroxidos/soda-caustica-escamas-99-10-kgs |
| | 1.68 | https://www.lojaopqquimica.com.br/materia-prima/soda-caustica-escamas-25-kg-20-kg-15-kg-10-kg-05-kg-e-01-kg |
| Energy | 0.14 | https://www.cemig.com.br/pt-br/atendimento/Paginas/valores_de_tarifa_e_servicos.aspx |

* Market price for the Brazilian conditions considering 1 US$ = R$ 5.01 (verified on 03/26/2020);
HCl – density = 1.49 g $cm^{-3}$, purity = 37%;
NaOH – purity = 95%

Article 2 - FAST AND EFFECTIVE ARSENIC REMOVAL FROM AQUEOUS SOLUTIONS BY A NOVEL LOW-COST EGGSHELL BYPRODUCT

(Article published in Science of the Total Environment)
DOI: https://doi.org/10.1016/j.scitotenv.2021.147022

**Fast and effective arsenic removal from aqueous solutions by a novel low-cost eggshell byproduct**

Ivan Célio Andrade Ribeiro[a], Isabela Cristina Filardi Vasques[b], Jéssica Cristina Teodoro[c], Marcelo Braga Bueno Guerra[d], Jefferson Santana da Silva Carneiro[a], Leônidas Carrijo Azevedo Melo[a], Luiz Roberto Guimarães Guilherme[a*]

[a] Department of Soil Science, Federal University of Lavras, Lavras – Minas Gerais, Postal code 37200-900, Brazil

[b] Department of Soil Science, Federal University of Viçosa, Viçosa – Minas Gerais, Postal code 36570-900, Brazil

[c] Department of Biology, Federal University of Lavras, Lavras – Minas Gerais, Postal code 37200-900, Brazil

[d] Department of Chemistry, Federal University of Lavras, Lavras – Minas Gerais, Postal code 37200-900, Brazil

[*] Corresponding author:
Luiz Roberto Guimarães Guilherme,
Department of Soil Science,
Federal University of Lavras,
Lavras, Minas Gerais, Brazil
Postal code 37200-900.
Phone: +55 35 38291259
E-mail: guilherm@ufla.br

**Graphical Abstract**

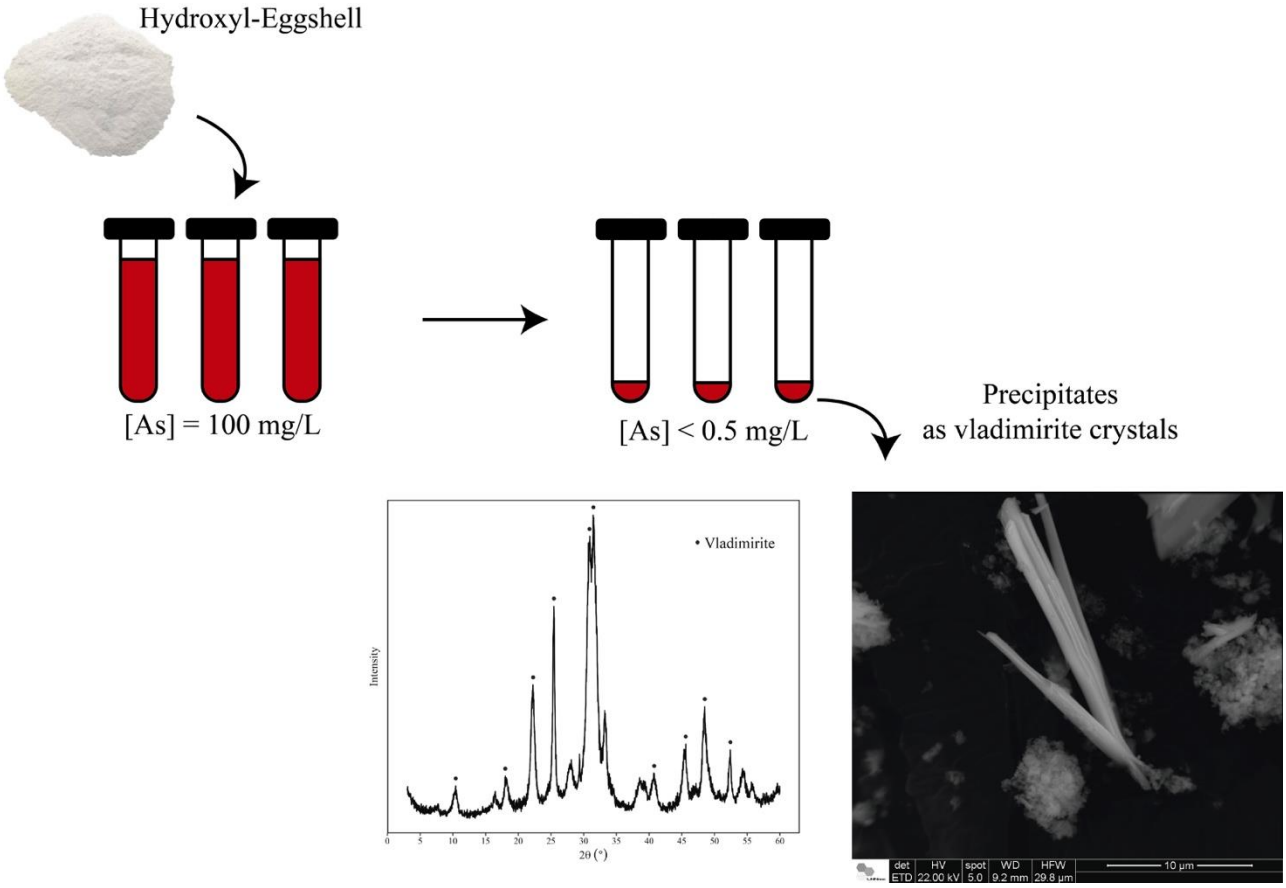

## Highlights

- In less than 15 minutes, ES-OH removes 99% of the As from an aqueous solution
- As concentration at equilibrium solution attends Brazilian discharge legislation
- Arsenic removal capacity of ES-OH is 529 mg $g^{-1}$
- Precipitation of vladimirite is the predominant As removal mechanism.

**Abstract**

Developing alternative green solutions for local and correct recycling of eggshells waste (ES) are needed by the egg-processing industries. In this study, we proposed transforming ES into a novel low-cost chemical compound named hydroxyl-eggshell (ES-OH) and investigated its capacity for arsenic (As) removal from aqueous solutions. Laboratory experiments were conducted to investigate the effects of ES-OH doses, pH, kinetics, and isotherms on As removal efficiency. The kinetics study showed that ES-OH removed nearly all As from solution in less than 15 min. The pseudo-second-order model described the process, and the maximum As removal capacity predicted by the Langmuir isotherm model was 529 mg $g^{-1}$. Using Fourier transform infrared spectroscopy (FTIR), scanning electron microscopy with energy dispersive X-ray detector (SEM-EDS), and X-ray diffraction (XRD), we found that the As removal mechanism by ES-OH was due to vladimirite precipitation, followed by weak electrostatic interactions between the precipitate and arsenate ions. Finally, after an economic analysis, we conclude that besides being a novel and economical income source, egg-producing companies might implement the ES-OH production process as a local environmentally-friendly way of recycling eggshells and reducing water As contamination.

**Keywords**: waste valorization; circular economy; vladimirite; calcium arsenate

## 1. Introduction

Arsenic contamination in drinking water reservoirs is recognized as a global environmental issue (Bundschuh et al., 2012; 2013). Although many strategies have been used to mitigate the impacts of elevated As levels in the environment in recent decades, several studies recently reported toxic amounts of this chemical element in freshwater resources of different places around the world, for instance: Bangladesh, India, USA, China, Japan (Lin et al., 2019a; Zhang et al., 2019), and twenty Latin American countries (Bundschuh et al., 2020; 2021). High As levels in potable water might be related to either natural or anthropogenic processes, *i.e.*, when As is released by weathering arsenic-enriched rocks or mining activities (Bundschuh et a., 2013). It is well-documented that ingestion of As-contaminated water can cause severe health effects, such as skin lesions, cancer, and nerve tissue injuries (Chiban et al., 2012; Lazaridis et al., 2002; Bundschuh et al., 2021). Given these recognized toxic effects, the World Health Organization (WHO) set at 10 μg $L^{-1}$ the maximum allowed concentration of As in drinking water (World Health Organization, 2017). Therefore, when present at high levels, As must be appropriately removed from aqueous media in order to decrease human health risks.

There are several techniques currently available for As removal from aqueous solutions, such as the use of filtration membranes, photocatalysis, ion exchange, chemical precipitation, electrochemical treatment, and adsorption (Liu et al., 2020). However, these technologies demand sophisticated equipment, expensive analytical grade chemicals, and highly skilled laborers, making them challenging to implement in industrial wastewater treatment plants (Litter et al., 2019).

The development of alternative materials aiming to reduce both the complexity and treatment costs of As removal from aqueous solutions has received considerable attention in recent years (Amen et al., 2020; Liu et al., 2020). Generally, solid wastes from different industrial and agroindustry activities, such as red mud (Lopes et al., 2013, Costa et al., 2020), rice straw (Seyfferth et al., 2019; Wu et al., 2018), corn stem (Lin et al., 2019b), *Citrus limmeta* (peel and pulp) waste (Verma et al., 2019), iron sludge from water treatment plants (Litter et al., 2019), among others, are used in nature as As adsorbents. The use of locally-produced solid wastes in this process can reduce As treatment costs and create an extra income source for the companies, with the additional advantage of proposing an environmentally-friendly method of solid waste disposal (Lin et al., 2019a).

However, due to their chemical composition, some solid wastes need to be transformed prior to their beneficial use in the environment. Several physicochemical processes can transform useless

solid wastes into valuable byproducts with high As removal capacity. Eggshell (ES) is an example of unvalued solid waste that, after chemical transformation, becomes a valuable material (Ahmad et al., 2017; Quina; Soares; Quinta-Ferreira, 2017; Ribeiro et al., 2020). According to Nassar and Alotaibi (2021), around 250,000 tons of ES are generated annually worldwide by the food processing industries. A minor portion of this is used as an amendment in agriculture for soil pH correction or in animal feed formulations, generally by using the eggshell membrane. However, the most significant fraction is landfilled or improperly discarded (Oliveira et al., 2013). According to Cree and Rutter (2015), each egg-processing industry in the USA expends annually around US$100,000 for ES disposal in landfills.

The ES has been used to remove dyes (Tsai et al., 2008), $Pb^{2+}$ and $Cd^{2+}$ (Lee et al., 2013), $Cu^{2+,}$ $Zn^{2+}$, $Ni^{2+}$, and $Co^{2+}$ (Sankaran et al., 2020), and hazardous organic contaminants (Kalsi et al., 2021) from aqueous solutions. However, to the best of our knowledge, there is a lack of information about using ES as an alternative sorbent for As removal from aqueous solutions or effluents. ES is composed of 95% of calcium carbonate ($CaCO_3$), which is ineffective in removing As from the solution (Zhang et al., 2019). Therefore, before being used as an alternative material for As removal, ES has to be previously chemically transformed.

Recently, our research group proposed an inexpensive and straightforward approach to transform the eggshells into a novel compound named hydroxy-eggshells (ES-OH), which showed higher phosphorus (P) removal capacity than the pristine powdered eggshell (Ribeiro et al., 2020). In this study, P was removed mainly by precipitation as hydroxyapatite, resulting in a P-enriched fertilizer well adapted to the concept of a circular economy. Arsenic and phosphorus are from group 15, sharing similar chemical properties. Due to this fact, we hypothesize that ES-OH might also remove arsenate from an aqueous solution by precipitation, similarly to what we have reported for phosphate. Indeed, in wastewater treatment plants that use coagulants to remove P by precipitation, studies have also reported As removal via co-precipitation (Metcalf and Eddy, 2007).

Considering the extensive scientific, regulatory policy, and public interest regarding water contamination by As, this study aimed to evaluate the As removal capacity of ES-OH from aqueous solutions. We performed several batch experiments testing ES-OH doses, the effect of initial pH, kinetics experiments, and sorption isotherms to evaluate the As removal capacity of ES-OH. Also, we characterized ES-OH before and after As removal according to their surface morphology and chemical composition, chemical functional groups, and crystalline structures by using the following

analytical methods: SEM-EDS, FTIR, and XRD. Finally, by combining batch experiments with spectroscopic analyses, we were able to unravel the mechanism of As removal by ES-OH.

## 2. Materials and methods

### 2.1 Synthesis of eggshell byproduct

Aviário Santo Antônio, located in Nepomuceno, state of Minas Gerais, Brazil, donated the eggshells waste. The solid waste was washed with deionized water, dried in an oven at 100 °C for 24 h, ground, and sieved (< 0.5 mm). After that, a portion of powdered ES (100 g) was dissolved by 200 mL of 1.0 mol $L^{-1}$ HCl solution in a glass beaker under constant stirring. 200 mL of 1 mol $L^{-1}$ NaOH solution was then added to the beaker, precipitating a white solid. The solid was left to settle down in the beaker, and the supernatant was removed and replaced with 1000 mL of deionized water. Again, the system was placed under constant stirring for 5 min, followed by an additional settling time of 2 h and another replacement of the supernatant with deionized water (1000 mL). This procedure was repeated ten times to remove the excess of sodium chloride (NaCl). Subsequently, the white solid was transferred to a round porcelain evaporating pan and oven-dried at 100 °C until constant weight. Lastly, a white precipitate was removed from the recipient, finely ground in an agate mortar, homogenized, and sieved (< 0.5 mm). The novel material is from now on named "Hydroxyl-Eggshell" (ES-OH). There are additional details about this synthesis process in our previous study (Ribeiro et al., 2020).

### 2.2 Material characterization

First, the point of zero charge (PZC) was determined in the ES-OH according to described in Feizi and Jalali (2016) with modifications. The PZC was measured by adding 10 g $L^{-1}$ of ES-OH in 0.1 mol $L^{-1}$ NaCl at initial pH values of 2.0, 5.0, 7.0, 9.0, and 13.0. The samples were placed on an orbital shaker for 24 h, and the equilibrium pH was measured ( pH-meter model Digimed). A linear model was calculated using the difference between the final and initial pH (ΔpH) and initial pH as response and explanatory variables. The intersection point of the model (ΔpH = 0) was assumed as the material's PZC value.

The specific surface area of the ES-OH was measured using the BET-$N_2$ method on a Quantachrome, Quantasorb Surface Area Analyzer before As removal experiments. Fourier transform infrared (FTIR) spectra were collected to evaluate the functional groups' modification of each material using a Digilab Excalibur spectrometer with a spectral range 4000-400 $cm^{-1}$ under 4 $cm^{-1}$ resolution with 16 consecutive scans. X-ray diffraction (XRD) analyzes were carried out to identify the minerals formed in ES-OH before and after As removal tests. The analyzes were performed using a Rigaku Miniflex II equipment with CuKα radiation and a graphite monochromatic beam, ranging from 3 to 60 2θ degrees, a step size of 0.02 2θ degree, and counting time of 5 $step^{-1}$. The diffractograms were interpreted using the database available at "RRUFF$^{TM}$" (Ralph, 2004).

Lastly, the surface morphology and the size distribution of each material were evaluated in a Quanta 650FEG Scanning Electron Microscope (SEM). Simultaneously, at the same surface locations, elemental distribution analyzes were also conducted using energy-dispersive X-ray spectroscopy (EDS) model Oxford. Previous to SEM-EDS, ES-OH samples were adhered to an aluminum stub with conductive carbon tape and covered with a 16 nm carbon layer by sputtering. FTIR, XRD, and SEM-EDS analyzes were performed in ES-OH previous and after the As removal tests to elucidate the removal mechanism.

## 2.3 Batch arsenic removal experiments

Arsenic removal experiments were carried out at room temperature (25 ± 3 ºC), and synthetic As-stock solution was prepared by diluting sodium arsenate dibasic heptahydrate ($Na_2HAsO_4 \cdot 7H_2O$) in deionized water. The optimum dose used in all other experiments in this study was determined by varying the ES-OH doses (0.5, 1.0, 2.0, 5.0, and 10.0 g $L^{-1}$) into plastic polyethylene centrifuge tubes with 40 mL of solution at the concentrations of 150 and 1200 mg $L^{-1}$ of As. Each treatment flask was shaken for 24 h, and then the supernatant was filtered through a 0.45 μm pore size membrane filter. The remaining As in the solution was quantified by inductively coupled plasma optical emission spectrometry (SPECTROBLUE, SPECTRO Analytical Instruments Inc., Germany) using the following measurement conditions: RF applied power (1400 kW); argon flow rate: plasma (12 L $min^{-1}$), auxiliary (0.80 L $min^{-1}$) and nebulizer (0.85 L $min^{-1}$). The monitored arsenic emission line was 189.042 nm. The efficiency of As removal was calculated by Eq. 1:

$$E = \frac{C_0 - C_e}{C_0} \times 100 \qquad \text{Eq. 1}$$

Where E is the efficiency of As removal (%), $C_0$, and $C_e$ are the initial and the equilibrium As concentration (mg $L^{-1}$).

Once the best ES-OH dose and As concentration was chosen, the next step was to evaluate the pH influence on As removal by the ES-OH. The initial pH values assessed were 3.0, 5.0, 7.0, 9.0, and 12.0 in plastic tubes containing 2.0 g $L^{-1}$ of ES-OH and 40 mL of a solution with 100.0 mg $L^{-1}$ of As. The flasks were shaken for 24 h, and then the supernatant was filtered using a 0.45 µm membrane filter. The remaining As was quantified by ICP OES, and Eq.1 was used to calculate the As removal efficiency.

Finally, the kinetics of As removal was evaluated at the optimal dose of ES-OH (2 g $L^{-1}$) with an initial As concentration of 100 mg $L^{-1}$. For that, plastic tubes containing the suspension were shaken for 15, 30, 40, 60, 90, and 120 min, then filtered through 0.45-µm pore size membrane filters, and the As concentrations measured by ICP OES. The data were fitted to nonlinear forms of pseudo-first-order and pseudo-second-order, as expressed in Eq. 2 and , respectively (Tran et al., 2017):

$$q_t = q_e(1 - e^{k_1 t}) \qquad \text{Eq. 2}$$

$$q_t = \frac{q_e^2 k_2 t}{1 + k_2 q_e t} \qquad \text{Eq. 3}$$

Where $q_e$ (mg $g^{-1}$) and qt (mg $g^{-1}$) are the amounts of As removed at equilibrium and at time t (min), respectively; $k_1$ (1 $min^{-1}$) and $k_2$ (g $mg^{-1}$ $min^{-1}$) are the constant rates of the pseudo-first and second-order equations.

The influence of initial As concentration was evaluated in the range of 100 to 5,000 mg $L^{-1}$ at the optimal dose of ES-OH, aiming to reach its maximum As removal capacity. For that, 40 mL of each solution, at pH 7.60, was left to react with 0.08 g of ES-OH during a 24h-shaking period. Supernatants were filtered through 0.45-µm pore size membranes, and As concentration at equilibrium was determined as previously described. The As removal capacity (q) was assessed by

the ratio of the difference between initial and equilibrium As concentration and the optimal adsorbent dose (d), Eq. 5.

$$q = \frac{(C_0 - C_e)}{d} \quad \text{Eq. 4}$$

The original data were fitted to the original nonlinear forms of Langmuir, Freundlich, Redlich-Peterson, and Temkin isotherm models, as shown from Eq. 3 to 8, respectively (Al-Ghouti and Da'ana, 2020):

$$q = \frac{q_{max} k_L C_e}{1 + bC_e} \quad \text{Eq. 5}$$

$$q = k_F C_e^{1/n} \quad \text{Eq. 6}$$

$$q = \frac{K_R C_e}{1 + a_R C_e^g} \quad \text{Eq. 7}$$

$$q = \frac{RT}{b_T} k_T C_e \quad \text{Eq. 8}$$

where *Ce* is the equilibrium As concentration; *q* is the As removal capacity of ES-OH at equilibrium (mg $g^{-1}$); $q_{max}$ is the maximum removal capacity of ES-OH (mg $g^{-1}$), and *KL* (L $g^{-1}$) is the Langmuir constant; *n* and $k_F$ (mg $g^{-1}$) are the Freundlich constants; *KR* (L $mg^{-1}$) and $a_R$ are the Redlich-Peterson constants; $k_T$ (L $g^{-1}$) and $b_T$ are the Temkin (J $mol^{-1}$) constants; *T* is the temperature (K); *R* is the universal gas constant 0.082 L atm $mol^{-1}$ $K^{-1}$.

All batch experiments were run in triplicate, and the mean values were used to analyze the results. Additional tests were performed whenever the relative difference between replicates was higher than 5%. Nonlinear kinetics and isotherm models were fitted to the experimental data using the "nlstools" package from R (Baty et al., 2015; TEAM, 2016). The coefficient of determination ($R^2$), along with the Akaike information criterion (AIC), was used to assess the best model in each case (Al-Ghouti; Da'Ana, 2020; Dávila-Jiménez et al., 2014).

## 3. Results and discussion

### 3.1. Characterization of ES-OH

The specific surface area of the ES-OH was 11.3 $m^2$ $g^{-1}$, which is approximately five times greater than the specific surface area of a composite of $MnO_2$ impregnated with alginate beads used efficiently to remove As from wastewaters (Shim et al., 2019) and is similar to the specific surface area of Fe-Mn-La-impregnated biochar composites (12.23 $m^2$ $g^{-1}$), which was stated to be a useful As adsorbent (Lin et al., 2019b). This result suggests that ES-OH might be a promising alternative for As removal.

Fig. 1 illustrates some selected properties of ES-OH. The external surface of ES-OH is mainly composed of sphere-like structures exhibiting diameters from 0.05 to 0.5 mm (Fig. 1a). Calcium (Ca) and oxygen (O) are the major constituents of these structures (Fig. 1b, EDS spectra) as confirmed by Kα (0.525 keV and 3.692 keV) from O and Ca X-ray characteristic emission lines, respectively, according to X-Ray data Booklet (Thompson, 2009). Different from a previous study (Ribeiro et al., 2020), sodium was not detected by EDS. Therefore, the cleaning procedure with deionized water was successfully achieved, producing a byproduct with higher purity, hence, higher added value. It is important to point out that the Kα signal at 0.277 keV is related to carbon (C) from the material used to cover the test sample submitted to SEM analysis.

Fig. 1c shows the FTIR spectra of ES-OH. The intense signal at 3642 $cm^{-1}$ corresponds to the hydroxide stretching vibration of hydroxyl groups (-OH) (Montes-Hernandez et al., 2009). The presence of Ca and '-OH' might be attributed to the transformation of eggshells into calcium hydroxide. This feature was further confirmed by the XRD spectra of ES-OH (Fig. 1d). The peaks at 18.1, 34.2, 47.1, and 50.7 2θ (º) were attributed to the presence of portlandite [$Ca(OH)_2$] ( Bouargane et al., 2020) of high crystallinity, as shown by the clean spectrum with low background and sharp diffraction peaks, similar to a pure chemical compound. For better visualization, the X-ray diffraction patterns of ES-OH, along with a standard sample of portlandite, are provided in Fig. 1S (supplementary material).

Finally, the PZC of ES-OH was 12.6 (Fig.1e). The PZC represents the pH value of the neutral colloid surface, and this result indicates that the surface of ES-OH has positive charge in a wide pH range (Markou et al., 2016). Consequently, the byproduct might exhibit a strong affinity for the negatively charged arsenate ions ($AsO_4^{3-}$) found in most contaminated sites.

3.2 Arsenic removal tests

The influence of the ES-OH dose on As removal in two As concentrations is presented in Fig. 2. Even for the lowest ES-OH dose (0.5 g $L^{-1}$), the As removal efficiency was higher than 90% for the lowest As concentration evaluated (150 mg $L^{-1}$). The maximum As removal for the higher tested As concentration was achieved for ES-OH doses higher than 5.0 g $L^{-1}$.

The characterization of the ES-OH showed that the manufacturing process was successful, and $Ca(OH)_2$ is the main product (Fig. 1), which explains the high As removal capacity due to the formation of calcium arsenate [$Ca_3(AsO_4)_2$] (Hao et al., 2018). Zhang et al. (2019) also reported high removal of soluble As by precipitation with Ca at pH 12. According to the reaction stoichiometry, 3 moles of calcium ($Ca^{2+}$) are necessary for the quantitative removal of 1 mol of arsenate ($AsO_4^{3-}$) (Eq. 1). In line with these first results, we chose the dose of 2 g $L^{-1}$ of ES-OH and 100 mg $L^{-1}$ of As for the following removal tests.

$$3Ca^{2+}_{(aq)} + 2AsO^{3-}_{4\,(aq)} \rightarrow Ca_3(AsO_4)_{2(S)} \qquad \text{Eq. 1}$$

The influence of pH on As removal using 2 g $L^{-1}$ of ES-OH, at an initial concentration of 100 mg $L^{-1}$, is illustrated in Fig. 3. In general, arsenic removal by ES-OH was not affected by the initial solution pH, which means that the efficiency of As removal using ES-OH is not affected in a wide pH range. No pH affected is a considerable advantage of ES-OH since many other adsorbents have their efficiency strongly affected by the solution pH (Markovski et al., 2014).

The equilibrium pH in each solution was increased to 12.3 ± 0.2, indicating that the ES-OH has a high alkaline capacity. This behavior might be attributed to the fast release of hydroxyl ions (-OH) from ES-OH to the solution, which decreased the concentration of hydronium ions ($H_3O^+$) by forming water ($H_2O$), and thus increasing solution pH. Besides, at such high pH, the predominant chemical species of As in the solution is arsenate (Eq. 4), reinforcing that the primary mechanism of As removal was by the formation of calcium arsenate (Bothe; Brown, 1999; Moon; Dermatas; Menounou, 2004; Zhang; Sun, 2013).

$$H_3AsO_4 + H_2O \leftrightarrow H_2AsO_4^- + H_3O^+ \qquad pK_1 = 2.19 \qquad \text{Eq. 2}$$

$$H_2AsO_4^- + H_2O \leftrightarrow HAsO_4^{-2} + H_3O^+ \qquad pK_2 = 6.94 \qquad \text{Eq. 3}$$

$$HAsO_4^{2-} + H_2O \leftrightarrow AsO_4^{-3} + H_3O^+ \qquad pK_3 = 11.5 \qquad \text{Eq. 4}$$

Another reasonable explanation for the high removal capacity showed by ES-OH is related to its high PZC (Fig. 1e). Even after the precipitation reactions have occurred, the solution pH at equilibrium was lower than the PZC of the ES-OH (Fig. 3), which indicates that the material's surface remained positively charged, favoring the removal of arsenate from the aqueous solution by electrostatic attraction. Further, the final soluble As concentration in the effluent was lower than the threshold of 0.5 mg $L^{-1}$ established by the Brazilian regulatory standards for wastewater discharge (BRASIL, 2011). Such results suggest that activities with highly-contaminated effluents, such as gold mining industries (Toujaguez et al., 2013), can count on As precipitation with the proposed byproduct to attain the legal, environmental threshold.

A kinetic study was performed to evaluate how fast ES-OH removes As from aqueous solutions and to obtain insights on the mechanism of arsenic removal by this material (Fig. 4a). The parameters of the pseudo-first-order and pseudo-second-order kinetic models, as well as the determination coefficient ($R^2$) and the Akaike information criterion (AIC) calculated from the fitting process, are reported in Table 1.

The pseudo-second-order equation fitted better to the raw dataset of this study, as indicated by the lower AIC (Table 1). Several authors argue that better adjustments using the pseudo-second-order kinetic model indicate As removal by the chemisorption process, involving valence forces by sharing or exchanging electrons between the adsorbent and adsorbate (Simonin, 2016). The sharing of electrons between $Ca^{2+}$ and $AsO_4^{3-}$ ions might have occurred in this study, resulting in calcium arsenate precipitation. However, only the fitting in the kinetic model does not allow one to conclude the real mechanism of As removal (Tran et al., 2017). The mechanisms will be further discussed in spectroscopy techniques (FTIR, SEM, and XRD) characterization.

Finally, the novel eggshell byproduct's removal capacity, at the optimal dose, was evaluated from different solutions with initial As concentration varying from 250 to 5,000 mg $L^{-1}$. Fig. 4b shows the Langmuir, Freundlich, Temkin, and Peterson isotherms fitted models, and the parameters of these models are reported in Table 1. With $R^2 > 0.80$, all of the models might be considered satisfactory to predict As removal by ES-OH. For this study, the Freundlich isotherm was the best model to represent the As removal due to the lower AIC and higher $R^2$ than other models.

The Freundlich modeling is not restricted to the monolayer formation, *i.e.*, the multi-layered process is also taken into account (Al-Ghouti and Da'ana, 2020).

The solid highlighted in red (Fig. 4b) contains *ca*. 36.6% m $m^{-1}$ of As, *i.e*., approximately the same As mass fraction found in calcium arsenate $Ca_3(AsO_4)_2$, (37.6% m $m^{-1}$ of As). After this highlighted point, instead of reaching the equilibrium, the ES-OH removal capacity slightly increased at a constant rate. The multi-layers formation of arsenate ($AsO_4^{3-}$) around the precipitate of calcium arsenate by weak electrostatic interactions might explain this improvement in arsenic removal capacity (Al-Ghouti and Da'ana, 2020). These multi-layers of arsenate proposed in the removal mechanism corroborate the previously fitted Freundlich model in our present study.

The maximum arsenic removal capacity predicted by the Langmuir model was 529 mg $g^{-1}$ of ES-OH, which was significantly higher than most of the byproducts listed in Table 2. Besides this outstanding value, ES-OH was obtained from a simple procedure using priceless solid waste and chemical compounds easy to purchase. Besides, the arsenate removal capacity of ES-OH was greater than 31 out of 32 low-cost materials reported in a review by (Chiban et al., 2012). Last of all, it is important to point out that, since there is a lack of standardized experimental conditions protocol for As removal, it is difficult to compare studies. Therefore, the comparison done here is only qualitative, and a systematic experimental design should be performed to prove which material has the higher As removal capacity per unit cost.

### 3.3 Characterization after arsenic removal

All spectroscopic analyzes were performed in the As-loaded solid formed at the point highlighted in red in the isotherm study (Fig. 4b), named hereafter as ES-OH-As.

Initially, the FTIR spectra were recorded to obtain information about the functional groups on the surface of ES-OH-As, as illustrated in Fig. 5a. The intense peak observed in this solid around 821 $cm^{-1}$ corresponds to the stretching vibration of As–O, which can be related to calcium arsenate groups (As–O–Ca) (MYNENI et al., 1998). Comparing with the spectra of ES-OH (Fig.1c), we observed that the peak near 3500 $cm^{-1}$ related to the hydrogen-bonded hydroxyl (-OH) disappeared in the ES-OH-As spectra. These profound changes in functional groups before and after As removal is because calcium ($Ca^{2+}$) was initially present as $Ca(OH)_2$ and reacted with arsenate ($AsO_4^{3-}$), forming calcium arsenate by precipitation.

Fig. 5b illustrates the X-ray diffraction patterns of ES-OH-As. The diffraction peaks at 10.4º, 18.0º, 21.0º, 25.0º, 30.9º, 31.5º, 40.8º, 45.3º, 48.5º, and 52.4º 2θ were consistent with the presence of the mineral vladimirite in the precipitate. For better visualization, the X-ray diffraction patterns of ES-OH-As along with a standard sample of vladimirite are provided in Fig. 2S (supplementary material). The crystallinity might be promoting the difference in the relative intensity between the ES-OH-As and the standard vladimirite spectra.

SEM shows the external morphology and particle size distribution of ES-OH-As (Fig. 6a). We observed that the circular spots of ES-OH shown in Fig. 1a transformed into a solid resembling a mineral phase after As reaction. The spatial distribution of Ca and As revealed by SEM-EDS analysis suggests that the crystal was mainly formed by Ca and As (Fig. 6b and c).

That external morphology of ES-OH-As revealed by SEM is similar to the outer shape of a natural vladimirite crystal (Fig. S3). All minerals are known to grow in a distinctive way, known as crystal habit, and it is one of the properties used to identify them. Based on this information, one might infer that part of the As removal capacity of ES-OH-As is due to the mineral vladimirite precipitation. Arsenic removal as a mineral such as a vladimirite implies high stability of the chemical process and a small chance of mobilizing As to the medium. However, it is essential to mention that many factors can influence calcium arsenates' stability, even the crystalline ones, such as atmospheric $CO_2$ and aging (Zhang et al., 2019).

### 3.4 Arsenic removal mechanism

Gathering the results from the batch removal experiments and spectroscopic analysis, we proposed the following As removal mechanism by ES-OH (Fig. 7). Initially, As is rapidly removed from the solution by precipitation of calcium arsenate compounds, and vladimirite was the main mineral formed in this phase. The precipitated crystals increased until the As concentration at equilibrium was around 1200 mg $L^{-1}$. After that point, weak electrostatic interactions take place on the As removal mechanism (Fig. 7). Then, layers of arsenate ions ($AsO_4^{3-}$) were formed around the precipitate by weak electrostatic interactions and increased the removal capacity up to 529 mg $g^{-1}$.

### 3.5 Environmental and Economic attributes

On average, one egg company expends about US$100,000 annually with the correct landfill disposal of eggshells in the USA (Cree and Rutter 2015). There is a possibility to transform this cost into income by using the easy chemical conversion of ES into ES-OH we proposed in this study. The novel eggshells byproduct exhibited high As removal capacity under small-scale laboratory experiments. The experiment's escalation might enable ES-OH to use in a real scenario, such as As removal from wastewater impacted by acid mine drainage (AMD) or immobilizing As in mine tailings and As-contaminated soils (Moon; Dermatas; Menounou, 2004; Zhang et al., 2020).

Precipitation with alkaline compounds, such as $Ca(OH)_2$, is a remediation technique that decreases As soluble concentration and acidity in AMD. Although $Ca(OH)_2$ is highly effective for this purpose, the cost of using a pure chemical compound is a significant issue (Migaszewski; Gałuszka; Dołęgowska, 2018). The overall cost for AMD wastewater treatment for the four highest mining countries worldwide is around US$ 32-72 billion (Cozzolino et al., 2018). The price of analytical grade $Ca(OH)_2$ from different laboratories in Brazil varies between US$ 5.54 to US$ 8.99 per kg of reagent (Table S1), while the cost of the ES-OH was US$ 4.48 on a pilot-scale basis (Ribeiro et al., 2020), which should significantly reduce with the escalation process.

Furthermore, based on the production cost of ES-OH - US$ 4.48 per kg - and considering a profit of 20% to the companies that generate the eggshell wastes, the final price will be US$ 5.38. This price is still lower than that of most chemical products available in the market, and some byproducts reported in the literature. Additionally, transportation costs towards mine sites must be added to ensure an excellent alternative for treating AMD. Transportation price depends on many factors, such as distance to mines and geographic localization. Considering the transportation cost of fertilizers in Brazil, the cost for ES-OH in ton per km is around $1.29, according to Freight Information System (SIFRECA, 2020).

Thus, the local conversion of eggshell waste into ES-OH is an alternative to avoid the landfill cost and a straightforward approach to implement the concept of circular economy inside the company.

After all, considering the excellent As removal capacity and low-cost production, ES-OH would be a useful and feasible alternative for mine industries that have to treat their effluents regarding As concentrations and acidity to cope with the legislation before discharging them into the environment. The protocol showed in this study provides, at the same time, an eco-friendly solution to eggshells disposal and a new financial resource to the chicken egg-processing companies into the

concept of "circular economy," where the focus is to reuse, repair, refurbish and recycle existing materials and products.

## 4. Conclusion

In the present study, we transformed eggshell waste into a material that enables fast As removal capacity from synthetic solutions. The isotherms showed a maximum removal capacity of 529 mg of As $g^{-1}$ of material. All spectroscopic analyzes consistently indicate that the As removal was due to precipitation of calcium arsenate compounds, and the primary mineral formed was vladimirite. Also, ES-OH can be commercialized in specialized wastewater markets, enabling an extra income source for the egg companies. Future work should focus on As removal using real wastewaters from mining industries and on the evaluation of precipitates stability.

## Acknowledgments

We are grateful to the eggshell samples provided by Aviário Santo Antônio Company, which provide us the eggshells. The Brazilian Nanotechnology National Laboratory – LNNano (Proposal Nº SEM 24432) allowed the SEM-EDS analyzes. National Council for Scientific and Technological Development CNPq (Grant Nº 420513/2018-3) for funding this work. The Coordination for the Improvement of Higher Education Personnel – CAPES (Proex 590-2014) provides the scholarship to the first author. LRGG and LCAM are Research Fellows of CNPq.

We also want to thank Lívia Botelho de Abreu, Elson Santiago Alvarenga, Antônio Carlos Saraiva da Costa, Antônio Carlos de Azevedo, and Hudson Wallace Pereira de Carvalho for helping during the experiment.

## References

Ahmad, Munir, Ahmad, Mahtab, Usman, A.R.A., Al-Faraj, A.S., Abduljabbar, A.S., Al Wabel, M.I., 2017. Biochar composites with nano zerovalent iron and eggshell powder for nitrate removal from aqueous solution with coexisting chloride ions. Environ. Sci. Pol. Res. 1–15. doi:https://doi.org/10.1007/s11356-017-0125-9.

Al-Ghouti, M.A., Da'ana, D.A., 2020. Guidelines for the use and interpretation of adsorption isotherm models: a review. J. Hazard. Mater. 393, 122383. https://doi.org/10.1016/j.jhazmat.2020.122383.

Amen, R., Bashir, H., Bibi, I., Shaheen, S.M., Niazi, N.K., Shahid, M., Hussain, M.M., Antoniadis, V., Shakoor, M.B., Al-Solaimani, S.G., Wang, H., Bundschuh, J., Rinklebe, J., 2020. A critical review on arsenic removal from water using biochar-based sorbents: the significance of modification and redox reactions. Chem. Eng. J. 396. https://doi.org/10.1016/j.cej.2020.125195.

Asiabi, H., Yamini, Y., Shamsayei, M., 2017. Highly selective and efficient removal of arsenic(V), chromium(VI) and selenium(VI) oxyanions by layered double hydroxide intercalated with zwitterionic glycine. J. Hazard. Mater. 339, 239–247. https://doi.org/10.1016/j.jhazmat.2017.06.042.

Baty, F., Ritz, C., Charles, S., Brutsche, M., Flandrois, J.-P., Delignette-Muller, M.-L., 2015. A toolbox for nonlinear regression in R: the package nlstools. J. Stat. Softw. 66, 1–21.

Bothe, J.V., Brown, P.W., 1999. Arsenic immobilization by calcium arsenate formation. Environ. Sci. Technol. 33, 3806–3811. https://doi.org/10.1021/es980998m.

BRASIL, (2011) no 430, Ministério do Meio Ambiente. Conselho Nacional de Meio Ambiente - Conama. Resolução no 430, de 13 de maio de 2011 [WWW Document].

Bouargane, B., Biyoune, M.G., Mabrouk, A., Bachar, A., Bakiz, B., Ahsaine, H.A., Billah, S.M., Atbir, A., 2020. Experimental investigation of the effects of synthesis parameters on the precipitation of calcium carbonate and portlandite from Moroccan phosphogypsum and pure gypsum using carbonation route. Waste and Biomass Valori. 11, 6953–6965. https://doi.org/10.1007/s12649-019-00923-3.

Bundschuh, J., Armienta, M.A., Morales-Simfors, N., Alam, M.A., López, D.L., Delgado Quezada, V., Dietrich, S., Schneider, J., Tapia, J., Sracek, O., Castillo, E., Marco Parra, L.M., Altamirano Espinoza, M., Guimarães Guilherme, L.R., Sosa, N.N., Niazi, N.K., Tomaszewska, B., Lizama Allende, K., Bieger, K., Alonso, D.L., Brandão, P.F.B., Bhattacharya, P., Litter, M.I., Ahmad, A., 2020. Arsenic in Latin America: new findings on source, mobilization and mobility in human environments in 20 countries based on decadal research 2010–2020. Crit. Rev. Environ. Sci. Technol. 0, 1–139. https://doi.org/10.1080/10643389.2020.1770527.

Bundschuh, J., Bhattacharya, P., Nath, B., Naidu, R., Ng, J., Guilherme, L.R.G., Ma, L.Q., Kim, K.-W., Jean, J.-S., 2013. Arsenic ecotoxicology: the interface between geosphere, hydrosphere and biosphere. J. Hazard. Mater. 262, 883–886. https://doi.org/10.1016/j.jhazmat.2013.08.019.

Bundschuh, J., Litter, M.I., Parvez, F., Román-Ross, G., Nicolli, H.B., Jean, J.-S., Liu, C.-W., López, D., Armienta, M.A., Guilherme, L.R.G., Cuevas, A.G., Cornejo, L., Cumbal, L., Toujaguez, R., 2012. One century of arsenic exposure in Latin America: a review of history and occurrence from 14 countries. Sci. Total Environ. 429, 2–35. https://doi.org/10.1016/j.scitotenv.2011.06.024.

Bundschuh, J., Schneider, J., Alam, M.A., Niazi, N.K., Herath, I., Parvez, F., Tomaszewska, B., Guilherme, L.R.G., Maity, J.P., López, D.L., Cirelli, A.F., Pérez-Carrera, A., Morales- Simfors, N., Alarcón-Herrera,M.T., Baisch, P., Mohan, D.,Mukherjee, A., 2021. Seven potential sources of arsenic pollution in Latin America and their environmental and health impacts. Sci. Total Environ., 146274 https://doi.org/10.1016/j.scitotenv.2021.146274.

Chiban, M., Zerbet, M., Carja, G., Sinan, F., 2012. Application of low-cost adsorbents for arsenic removal: a review. J. Environ. Chem. Ecotoxicol. 4, 91–102. https://doi.org/10.5897/jece11.013.

Costa, E.T.S., Guilherme, L.R.G., Lopes, G., Lima, J.M., Curi, N., 2021. Sorption of cadmium, lead, arsenate, and phosphate on red mud combined with phosphogypsum. Int. J. Environ. Res. 15, 427–444. https://doi.org/10.1007/s41742-021-00319-z.

Cozzolino, D., Chandra, S., Roberts, J., Power, A., Rajapaksha, P., Ball, N., Gordon, R., Chapman, J., 2018. There is gold in themhills: predicting potential acid mine drainage events through the use of chemometrics. Sci. Total Environ. 619–620, 1464–1472. https://doi.org/10.1016/j.scitotenv.2017.11.063.

Cree, D., Rutter, A., 2015. Sustainable bio-inspired limestone eggshell powder for potential industrialized applications. ACS Sustain. Chem. Eng. 3, 941–949. https://doi.org/10.1021/acssuschemeng.5b00035.

Dávila-Jiménez, M.M., Elizalde-González, M.P., García-Díaz, E., González-Perea, M., Guevara-Villa, M.R.G., 2014. Using Akaike information criterion to select the optimal isotherm equation for adsorption from solution. Adsorpt. Sci. Technol. 32, 605–622. https://doi.org/10.1260/0263-6174.32.7.605.

Feizi, M., Jalali, M., 2016. Sorption of aquatic phosphorus onto native and chemically modified plant residues: modeling the isotherm and kinetics of sorption process. Desalin. Water Treat. 57, 3085–3097. https://doi.org/10.1080/19443994.2014.981226.

Hao, L., Liu, M., Wang, N., Li, G., 2018. A critical review on arsenic removal from water using iron-based adsorbents. RSC Adv. 8, 39545–39560. https://doi.org/10.1039/c8ra08512a.

Imran, M., Iqbal, M.M., Iqbal, J., Shah, N.S., Khan, Z.U.H., Murtaza, B., Amjad, M., Ali, S., Rizwan, M., 2021. Synthesis, characterization and application of novel MnO and CuO impregnated biochar composites to sequester arsenic (As) from water: modeling, thermodynamics and reusability. J. Hazard. Mater. 401, 123338. https://doi.org/10.1016/j.jhazmat.2020.123338.

Kalsi, A., Celin, S.M., Bhanot, P., Sahai, S., Sharma, J.G., 2021. A novel egg shell-based bio formulation for remediation of RDX (hexahydro-1,3,5-trinitro-1,3,5-triazine) contaminated soil. J. Hazard. Mater. 401, 123346. https://doi.org/10.1016/j.jhazmat.2020.123346.

Lafuente, B., Downs, R.T., Yang, H., Stone, N., 2015. The power of databases: the RRUFF project. In: Armbruster, T., Danis, R.M. (Eds.), Highlights in Mineralogical Crystallography. W. De Gruyter, Berlin, Germany, pp. 1–30. https://rruff.info/. (Accessed 2 December 2020).

Lazaridis, N.K., Hourzemanoglou, A., Matis, K.A., 2002. Flotation of metal-loaded clay anion exchangers. Part II: the case of arsenates. Chemosphere 47, 319–324. https://doi.org/10.1016/S0045-6535(01)00218-1.

Lee, S.S., Lim, J.E., Abd El-Azeem, S.A.M., Choi, B., Oh, S.E.,Moon, D.H., Ok, Y.S., 2013. Heavy metal immobilization in soil near abandoned mines using eggshell waste and rapeseed residue. Environ. Sci. Pollut. Res. 20, 1719–1726. https://doi.org/10.1007/s11356-012-1104-9.

Lin, L., Qiu,W.,Wang, D., Huang, Q., Song, Z., Chau, H.W., 2017. Arsenic removal in aqueous solution by a novel Fe-Mn modified biochar composite: characterization and mechanism. Ecotoxicol. Environ. Saf. 144, 514–521. https://doi.org/10.1016/j. ecoenv.2017.06.063.

Lin, L., Song, Z., Khan, Z.H., Liu, X., Qiu,W., 2019a. Enhanced As(III) removal from aqueous solution by Fe-Mn-La-impregnated biochar composites. Sci. Total Environ. 686, 1185–1193. https://doi.org/10.1016/j.scitotenv.2019.05.480.

Lin, L., Zhang, G., Liu, X., Khan, Z.H., Qiu,W., Song, Z., 2019b. Synthesis and adsorption of Fe–Mn–La-impregnated biochar composite as an adsorbent for As(III) removal from aqueous solutions. Environ. Pollut. 247, 128–135. https://doi.org/10.1016/j.envpol.2019.01.044.

Litter, M.I., Ingallinella, A.M.,Olmos,V., Savio, M.,Difeo,G., Botto, L., Torres, E.M.F., Taylor, S., Frangie, S., Herkovits, J., Schalamuk, I., González, M.J., Berardozzi, E., García Einschlag, F.S., Bhattacharya, P., Ahmad, A., 2019. Arsenic in Argentina: technologies for arsenic removal from groundwater sources, investment costs and waste management practices. Sci. Total Environ. 690, 778–789. https://doi.org/10.1016/j.scitotenv.2019.06.358.

Liu, B., Kim, K.H., Kumar, V., Kim, S., 2020. A review of functional sorbents for adsorptive removal of arsenic ions in aqueous systems. J. Hazard. Mater. 388, 121815. https://doi.org/10.1016/j.jhazmat.2019.121815.

Lopes, G., Guilherme, L.R.G., Costa, E.T.S., Curi, N., Penha, H.G.V., 2013. Increasing arsenic sorption on red mud by phosphogypsum addition. J. Hazard. Mater. 262, 1196–1203. https://doi.org/10.1016/j.jhazmat.2012.06.051.

Markou, G., Inglezakis, V.J.,Mitrogiannis, D., Efthimiopoulos, I., Psychoyou, M., Koutsovitis, P., Muylaert, K., Baziotis, I., 2016. Sorption mechanism(s) of orthophosphate onto Ca (OH)2 pretreated bentonite. RSC Adv. 6, 22295–22305. https://doi.org/10.1039/c5ra27638a.

Markovski, J.S., Marković, D.D., Dokić, V.R., Mitrić, M., Ristić, M.D., Onjia, A.E., Marinković, A.D., 2014. Arsenate adsorption on waste eggshell modified by goethite, α-MnO2 and goethite/α-MnO2. Chem. Eng. J. 237, 430–442. https://doi.org/10.1016/j.cej.2013.10.031.

Metcalf, Eddy, 2014.Wastewater Engineering: Treatment and Resource Recovery 5th ed. McGraw-Hill Education, New York.

Migaszewski, Z.M., Gałuszka, A., Dołęgowska, S., 2018. Arsenic in the Wiśniówka acid mine drainage area (south-central Poland) – mineralogy, hydrogeochemistry, remediation. Chem. Geol. 493, 491–503. https://doi.org/10.1016/j.chemgeo.2018.06.027.

Montes-Hernandez, G., Concha-Lozano, N., Renard, F., Quirico, E., 2009. Removal of oxyanions from synthetic wastewater via carbonation process of calcium hydroxide: applied and fundamental aspects. J. Hazard. Mater. 166, 788–795. https://doi.org/10.1016/j.jhazmat.2008.11.120.

Moon, D.H., Dermatas, D., Menounou, N., 2004. Arsenic immobilization by calciumarsenic precipitates in lime treated soils. Sci. Total Environ. 330, 171–185. https://doi.org/10.1016/j.scitotenv.2004.03.016.

Myneni, S.C.B., Traina, S.J., Waychunas, G.A., Logan, T.J., 1998. Experimental and theoretical vibrational spectroscopic evaluation of arsenate coordination in aqueous solutions, solids, and at mineral-water interfaces. Geochim. Cosmochim. Acta 62, 3285–3300. https://doi.org/10.1016/S0016-7037(98)00222-1.

Nassar, A.M., Alotaibi, N.F., 2021. Eggshell recycling for fabrication of Pd@CaO, characterization and high-performance solar photocatalytic activity. Environ. Sci. Pollut. Res. 28, 3515–3523. https://doi.org/10.1007/s11356-020-10751-x.

Oliveira, D.A., Benelli, P., Amante, E.R., 2013. A literature review on adding value to solid residues: egg shells. J. Clean. Prod. 46, 42–47. https://doi.org/10.1016/j.jclepro.2012.09.045.

Quina, M.J., Soares, M.A.R., Quinta-Ferreira, R., 2017. Applications of industrial eggshell as a valuable anthropogenic resource. Resour. Conserv. Recycl. 123, 176–186. https://doi.org/10.1016/j.resconrec.2016.09.027.

R Core Team, 2016. R: A Language and Environment for Statistical Computing. R Foundation for Statistical Computing, Vienna, Austria URL https://www.R-project.org/.

Ribeiro, I.C.A., Teodoro, J.C., Guilherme, L.R.G., Melo, L.C.A., 2020. Hydroxyl-eggshell: a novel eggshell byproduct highly effective to recover phosphorus from aqueous solutions. J. Clean. Prod. 274, 123042. https://doi.org/10.1016/j.jclepro.2020.123042.

Rigueto, C.V.T., Piccin, J.S., Dettmer, A., Rosseto,M., Dotto, G.L., Schmitz, A.P.O., Perondi, D., Freitas, T.S.M., Loss, R.A., Geraldi, C.A.Q., 2020. Water hyacinth (Eichhornia crassipes) roots, an amazon natural waste, as an alternative biosorbent to uptake a reactive textile dye from aqueous solutions. Ecol. Eng. 150, 105817. https://doi.org/10.1016/j.ecoleng.2020.105817.

Sankaran, R., Show, P.L., Ooi, C.-W., Ling, T.C., Shu-Jen, C., Chen, S.-Y., Chang, Y.-K., 2020. Feasibility assessment of removal of heavy metals and soluble microbial products from aqueous solutions using eggshell wastes. Clean Technol. Environ. Policy 22, 773–786. https://doi.org/10.1007/s10098-019-01792-z.

Shim, J., Kumar, M., Mukherjee, S., Goswami, R., 2019. Sustainable removal of pernicious arsenic and cadmium by a novel composite of MnO2 impregnated alginate beads: a cost-effective approach for wastewater treatment. J. Environ. Manage. 234, 8–20. https://doi.org/10.1016/j.jenvman.2018.12.084.

SIFRECA, 2020. System of freight information [WWW document]. Mens. Indic. URL https://sifreca.esalq.usp.br/ (accessed 8.15.20).

Simonin, J.-P., 2016. On the comparison of pseudo-first order and pseudo-second order rate laws in the modeling of adsorption kinetics. Chem. Eng. J. 300, 254–263. https://doi.org/10.1016/j.cej.2016.04.079.

Thompson, A., Attwood, D., Gullikson, E., Howells, M., Kim, K.-J., Kirz, J., Kortright, J., Winick, H., Lindau, I., Liu, Y., Pianetta, P., Robinson, A., Scofield, J., Underwood, J., Williams, G., 2009. X-ray Data Booklet. Center for X-ray Optics. Advanced Light Source. Lawrence Berkeley National Laboratory. University of California., Berkeley, California.

Toujaguez, R., Ono, F.B., Martins, V., Cabrera, P.P., Blanco, A.V., Bundschuh, J., Guilherme, L.R.G., 2013. Arsenic bioaccessibility in gold mine tailings of Delita, Cuba. J. Hazard. Mater. 262, 1004–1013. https://doi.org/10.1016/j.jhazmat.2013.01.045.

Tran, H.N., You, S.J., Hosseini-Bandegharaei, A., Chao, H.P., 2017. Mistakes and inconsistencies regarding adsorption of contaminants from aqueous solutions: a critical review. Water Res. 120, 88–116. https://doi.org/10.1016/j.watres.2017.04.014.

Tsai,W.-T., Hsien, K.-J.,Hsu, H.-C., Lin, C.-M., Lin,K.-Y., Chiu, C.-H., 2008. Utilization of ground eggshell waste as an adsorbent for the removal of dyes from aqueous solution. Bioresour. Technol. 99, 1623–1629. https://doi.org/10.1016/j.biortech.2007.04.010.

Verma, L., Siddique, M.A., Singh, J., Bharagava, R.N., 2019. As(III) and As(V) removal by using iron impregnated biosorbents derived from waste biomass of Citrus limmeta (peel and pulp) from the aqueous solution and ground water. J. Environ. Manag. 250, 109452. https://doi.org/10.1016/j.jenvman.2019.109452.

World Health Organization, 2017. Guidelines for Drinking-Water Quality. Guidelines for Drinking-Water Quality: First Addendum to the Fourth Edition. Licence. CC BY-NCSA. 3. IGO, Geneva.

Wu, J., Huang, D., Liu, X., Meng, J., Tang, C., Xu, J., 2018. Remediation of As(III) and Cd (II) co-contamination and its mechanism in aqueous systems by a novel calcium based magnetic biochar. J. Hazard. Mater. 348, 10–19. https://doi.org/10.1016/j.jhazmat.2018.01.011.

Yu, Y., Yu, L., Sun, M., Chen, P., 2016. Facile synthesis of highly active hydrated yttrium oxide towards arsenate adsorption. J. Colloid Interface Sci. 474, 216–222. https://doi.org/10.1016/j.jcis.2016.03.030.

Zhang, Y., Gao,W., Ni,W., Zhang, S., Li, Y.,Wang, K., Huang, X., Fu, P., Hu,W., 2020. Influence of calcium hydroxide addition on arsenic leaching and solidification/ stabilisation behaviour of metallurgical-slag-based green mining fill. J. Hazard. Mater. 390. https://doi.org/10.1016/j.jhazmat.2020.122161.

Zhang, T., Sun, D.D., 2013. Removal of arsenic from water using multifunctional micro-/nano-structured MnO2 spheres and microfiltration. Chem. Eng. J. 225, 271–279. https://doi.org/10.1016/j.cej.2013.04.001.

Zhang, D., Wang, S., Wang, Y., Gomez, M.A., Jia, Y., 2019a. The long-term stability of calcium arsenates: implications for phase transformation and arsenic mobilization. J. Environ. Sci. (China) 84, 29–41. https://doi.org/10.1016/j.jes.2019.04.017.

Zhang, T., Zhao, Y., Kang, S., Li, Y., Zhang, Q., 2019b. Formation of active Fe(OH)3 in situ for enhancing arsenic removal from water by the oxidation of Fe(II)in air with the presence of $CaCO_3$. J. Clean. Prod. 227, 1–9. https://doi.org/10.1016/j.jclepro.2019.04.199.

**Figures**

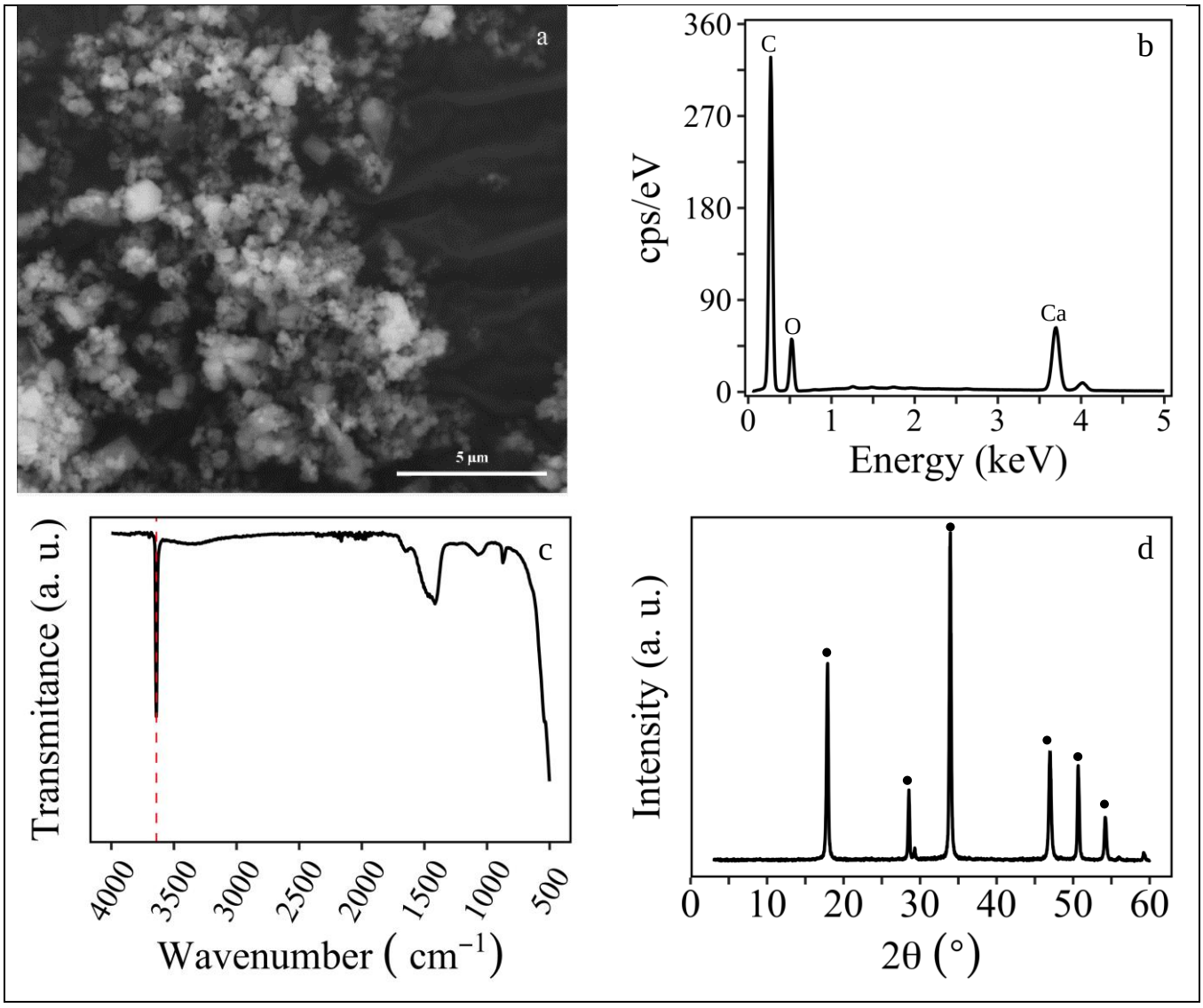
a
5 µm
b
C
O
Ca
cps/eV
Energy (keV)
c
Transmitance (a. u.)
Wavenumber ( cm$^{-1}$)
d
Intensity (a. u.)
2θ (°)

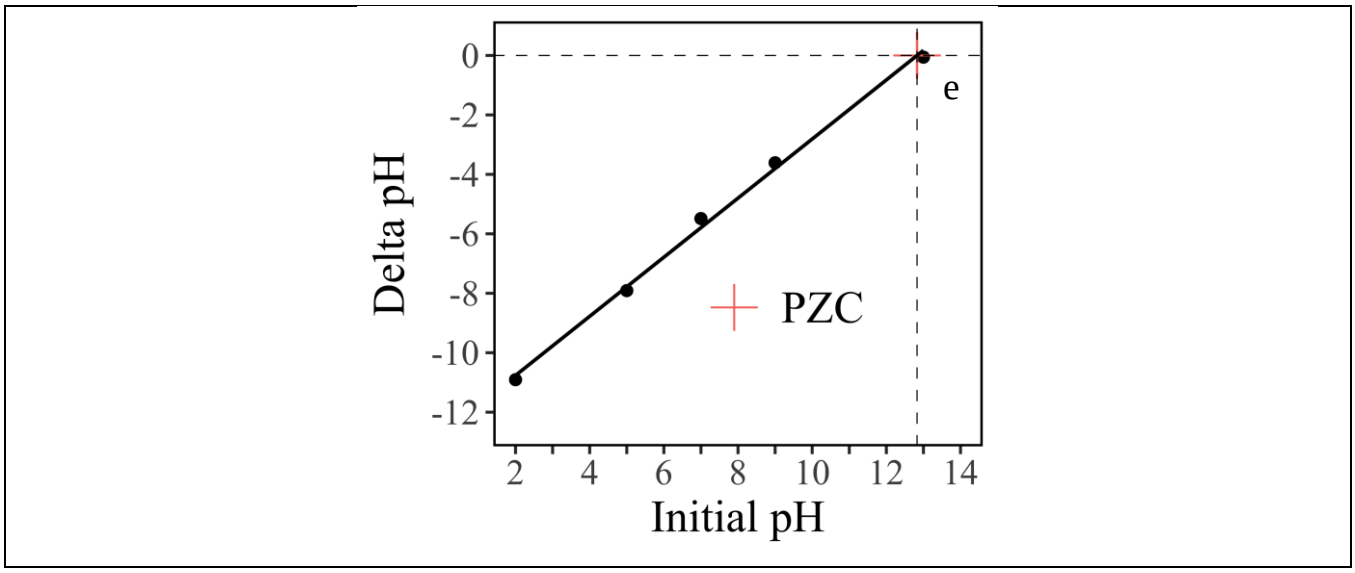

Fig. 1: Selected properties of ES-OH; Scanning electron microscopic image (a), X-Ray fluorescence spectra (b), FTIR (c), X-Ray diffractogram (d); The point of zero charges (e)

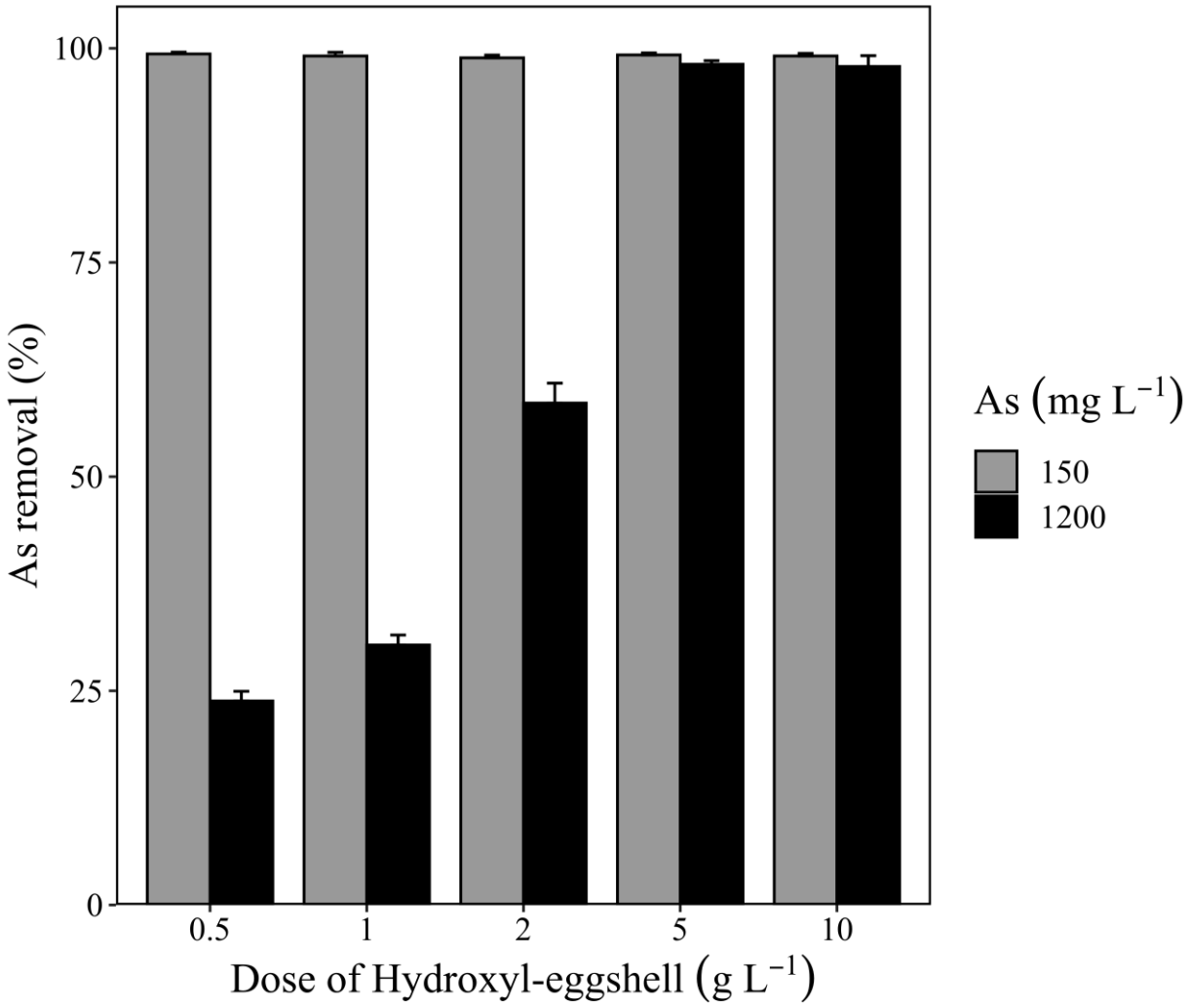


Fig. 2: Effect of ES-OH doses on arsenic removal at two As concentration solutions

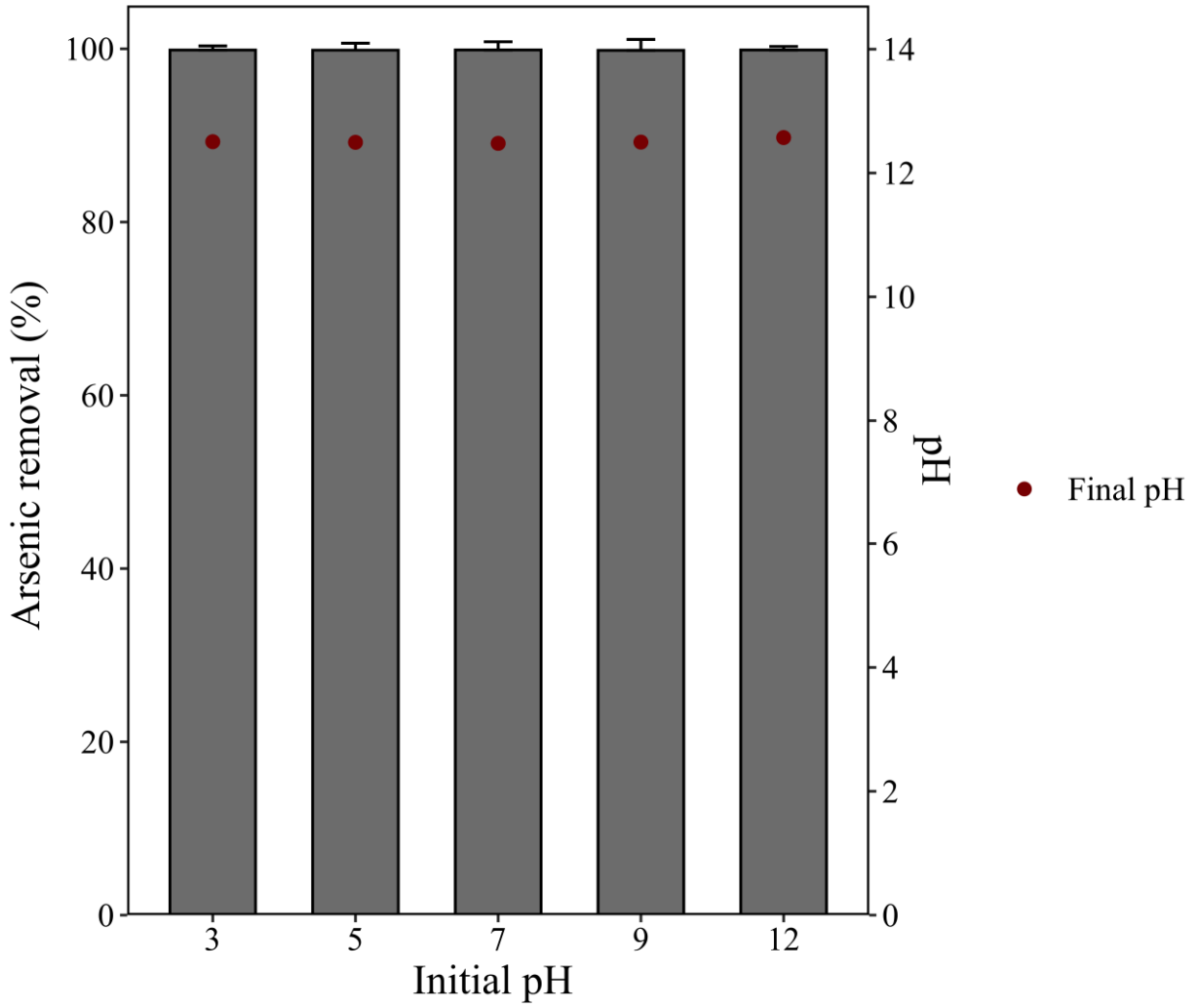


Fig. 3: Effect of initial pH on arsenic removal efficiency by ES-OH. ([As] = 100 mg $L^{-1}$; ES-OH dose = 2.0 g $L^{-1}$)

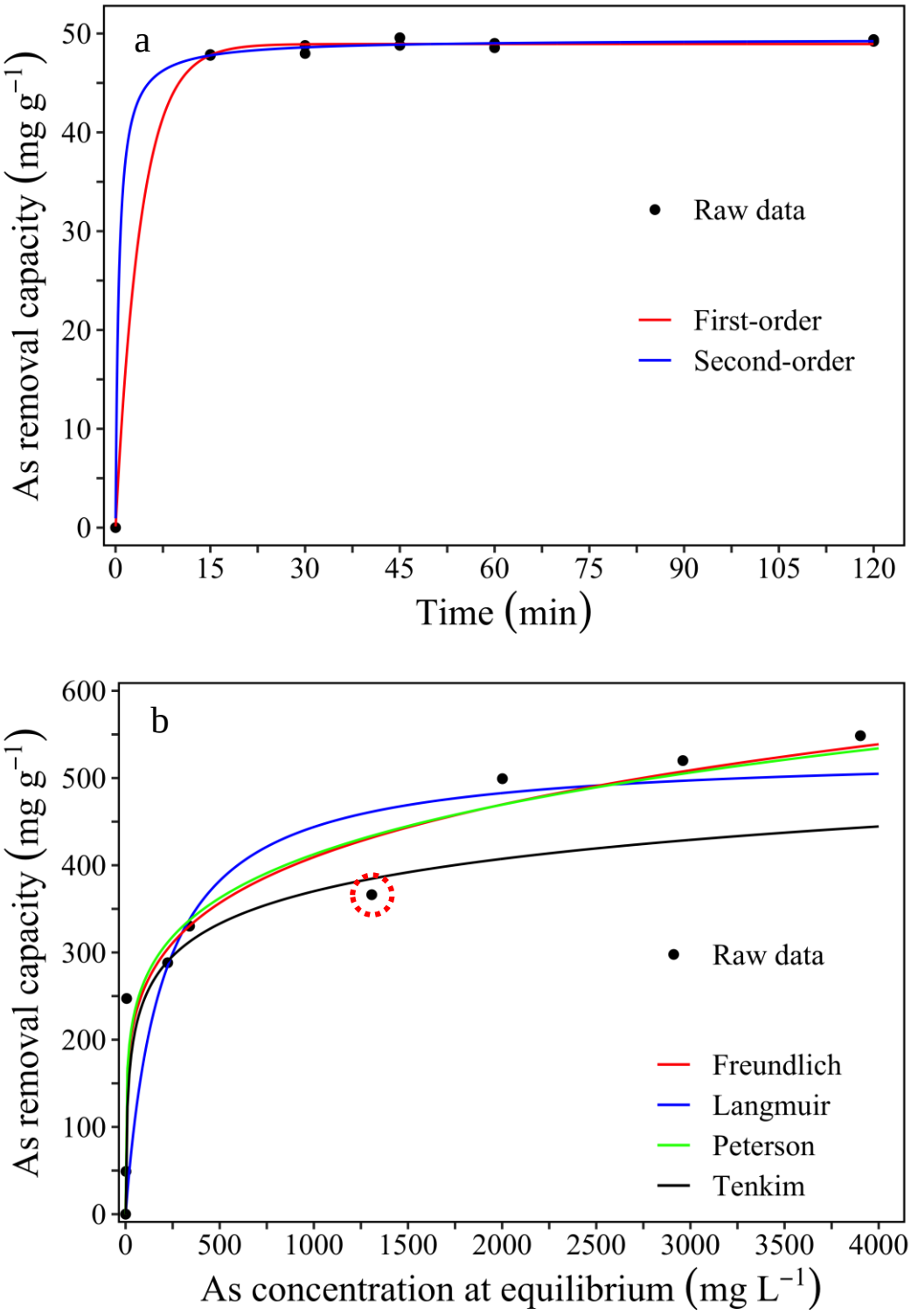


Fig. 4: Kinetics (a) and sorption isotherms (b) of As into ES-OH. ([Initial pH = 7.60, dose = 2 g $L^{-1}$ ES-OH)

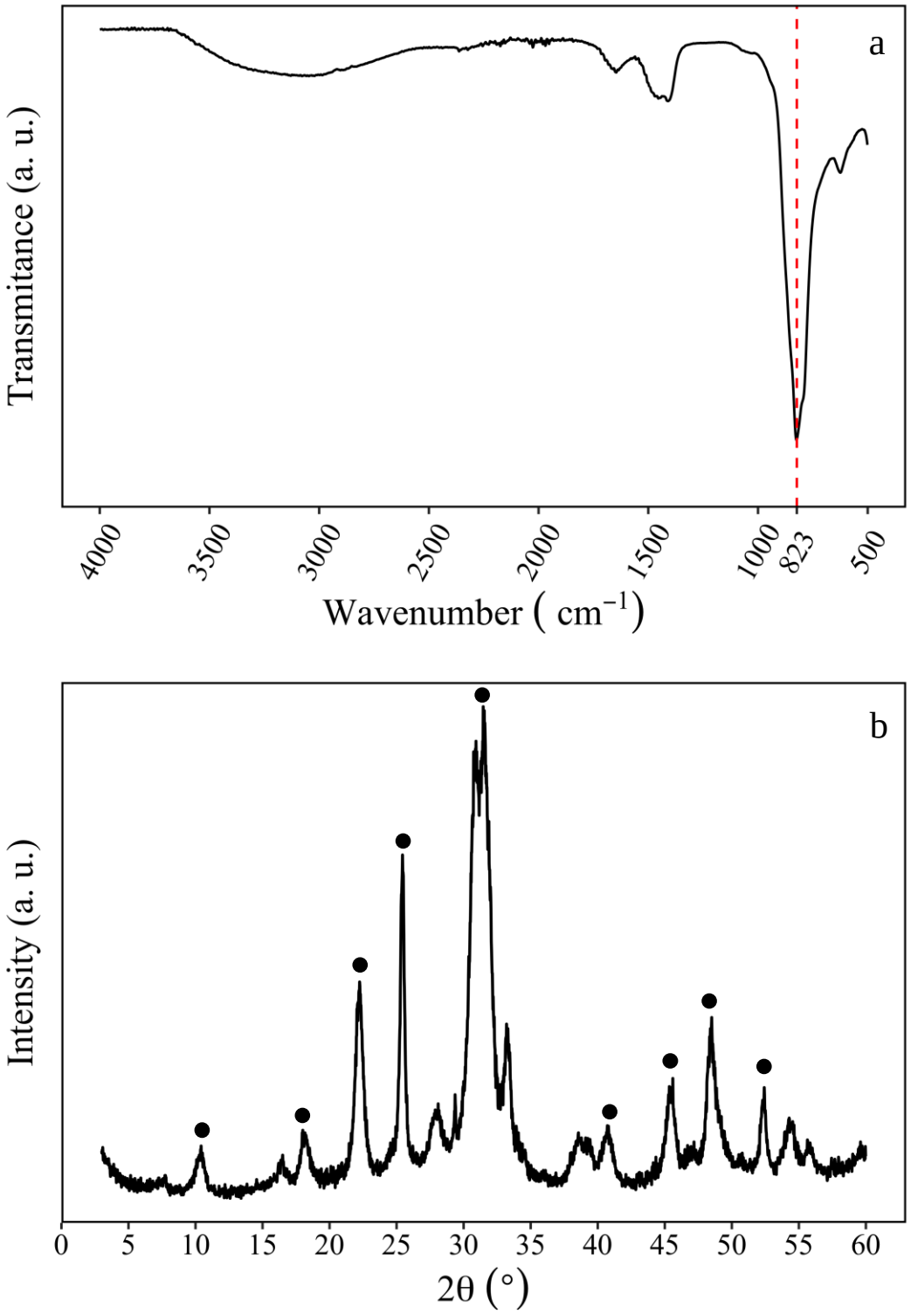


Fig. 5: FTIR spectra(a), and X-ray diffraction patterns (b) of As-loaded hydroxyl eggshell (ES-OH-As).

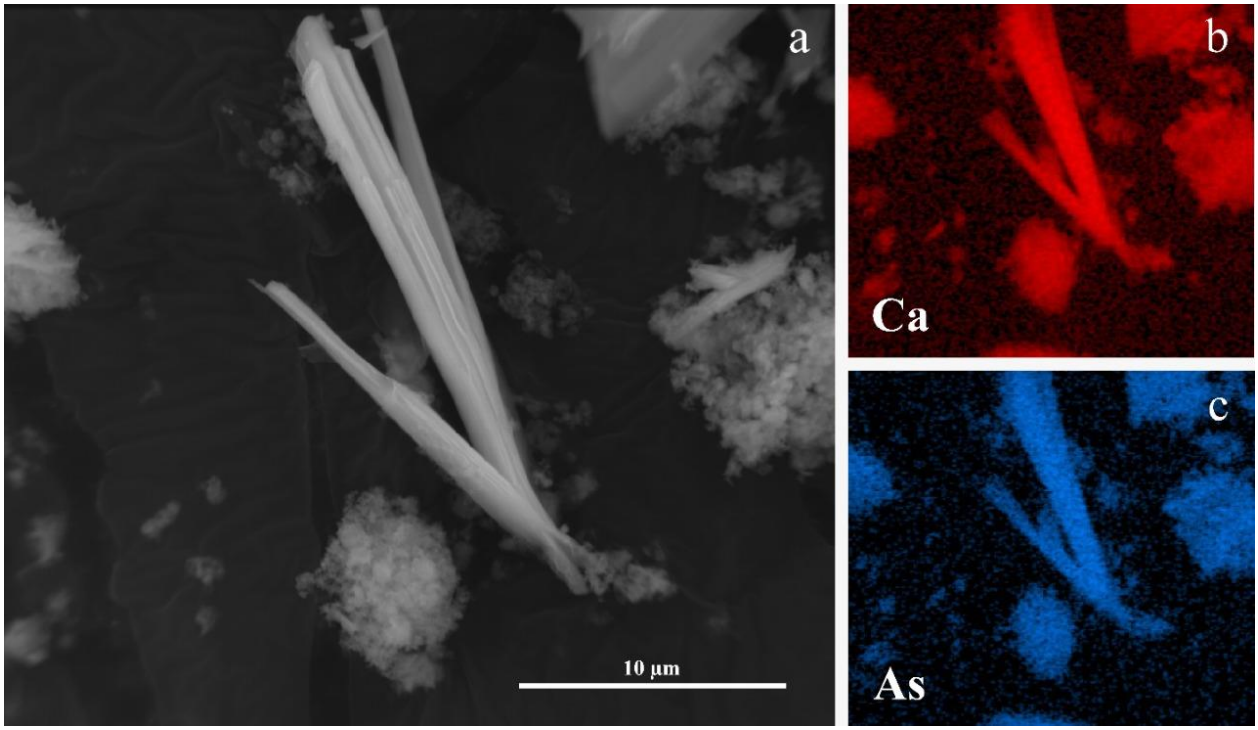


Fig. 6: SEM image of ES-OH-As (a), associated with elemental mapping analysis for calcium (b) and arsenic (c).

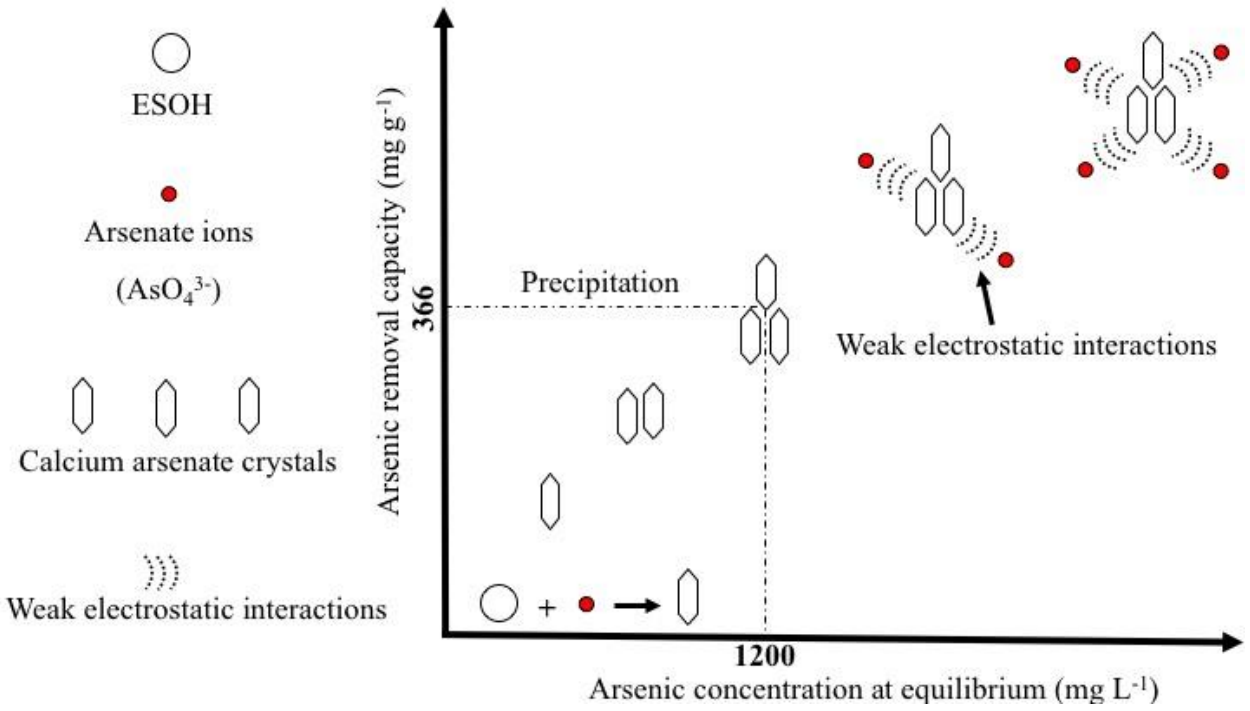


Fig. 7: Proposed arsenic removal mechanism by ES-OH from aqueous solution

Table 5: Kinetics parameters and isotherms models for As removal into ES-OH.

| Model | Parameter 1 | Parameter 2 | Parameter 3 | $R^2$ | AIC |
|---|---|---|---|---|---|
| Pseudo-first-order | $q_e$ = 49.83 mg $g^{-1}$ | $k_1$ = 0.25 $min^{-1}$ | | 0.99 | 16.91 |
| Pseudo-second-order | $q_e$ = 49.43 mg $g^{-1}$ | $k_2$ = 0.039 g $mg^{-1}$ $min^{-1}$ | | 0.99 | 9.74 |
| Langmuir | $q_{max}$ = 529 mg $g^{-1}$ | K = 0.005 L $mg^{-1}$ | | 0.81 | 196.25 |
| Freundlich | $K_F$ = 104.11 mg $g^{-1}$ | n = 5.05 | | 0.92 | 177.12 |
| Temkin | $A_T$ = 2.89 | $b_T$ = 0.046 J $mol^{-1}$ | | 0.90 | 181.84 |
| Redlich-Peterson | $K_R$ = 368.4 g $L^{-1}$ | $a_R$ = 3.21 | g = 0.81 | 0.92 | 179.53 |

$q_e$ = amount of As removed at equilibrium; $k_1$ = pseudo-first order rate constant; $k_2$ = pseudo-second order rate constant; $q_{max}$ = Langmuir maximum removal capacity; $K_f$ and n Freundlich affinity and linearity constants respectively; $K_R$ = Redlich-Peterson isotherm constant (L/g), g = Redlich-Peterson exponent that lies between 0 and 1; $A_T$ and $b_T$ Temkin isotherm constants.

Table 6: As removal capacity of different materials reported in the literature

| Material | q (mg $g^{-1}$) | Reference |
|---|---|---|
| Microstructure $MnO_2$ spheres | 14.5 | (ZHANG; SUN, 2013) |
| Fe-Mn modified biochar | 8.25 | (LIN et al., 2017) |
| Fe-Mn-La impregnated biochar | 15.34 | (Lin et al., 2019b) |
| Water hyacinth (*Eichhornia crassipes*) | 43.28 | (RIGUETO et al., 2020) |
| MnO and CuO impregnated biochar | 12.47 | (IMRAN et al., 2021) |
| $MnO_2$ impregnated alginate beads | 6.59 | (SHIM et al., 2019) |
| Hydrated Yttrium oxide | 480.2 | (Yu et al., 2016) |
| ES-OH | 529 | This study |
| Zwitterionic glycine intercalated layered double hydroxide (Gly-LDH) | 731.6 | (ASIABI; YAMINI; SHAMSAYEI, 2017) |

**Supplementary material**

Table S1. Value of each material needed to prepare ES-OH.

| Material | Market price (US$/kg) | Source (verified on 07-08-2020) |
|---|---|---|
| $Ca(OH)_2$ | 8.99 | https://www.lojanetlab.com.br/reagentes/pa/hidroxido-de-calcio-pa |
| | 5.54 | https://www.metaquimica.com/hidroxido-de-calcio-pa-500g-quimica-moderna-formula-ca-oh-2.html |
| | 7.32 | https://www.biomedh.com.br/007009/hidroxido-de-calcio-pa-500gr.html |

*1 US$ = R$ 5.34 (verified on 07/08/2020);
$Ca(OH)_2$ – purity = 95%

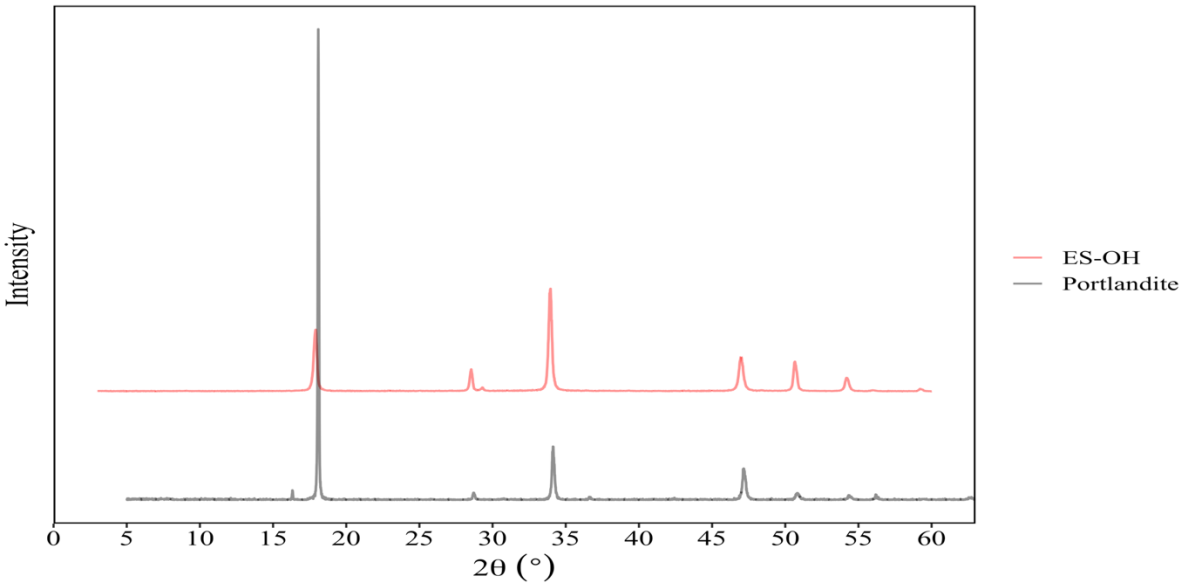


Figure 3: X-ray diffraction patterns of hydroxyl-eggshell (ES-OH) and portlandite. Portlandite spectrum obtained at (LAFUENTE et al., 2016).

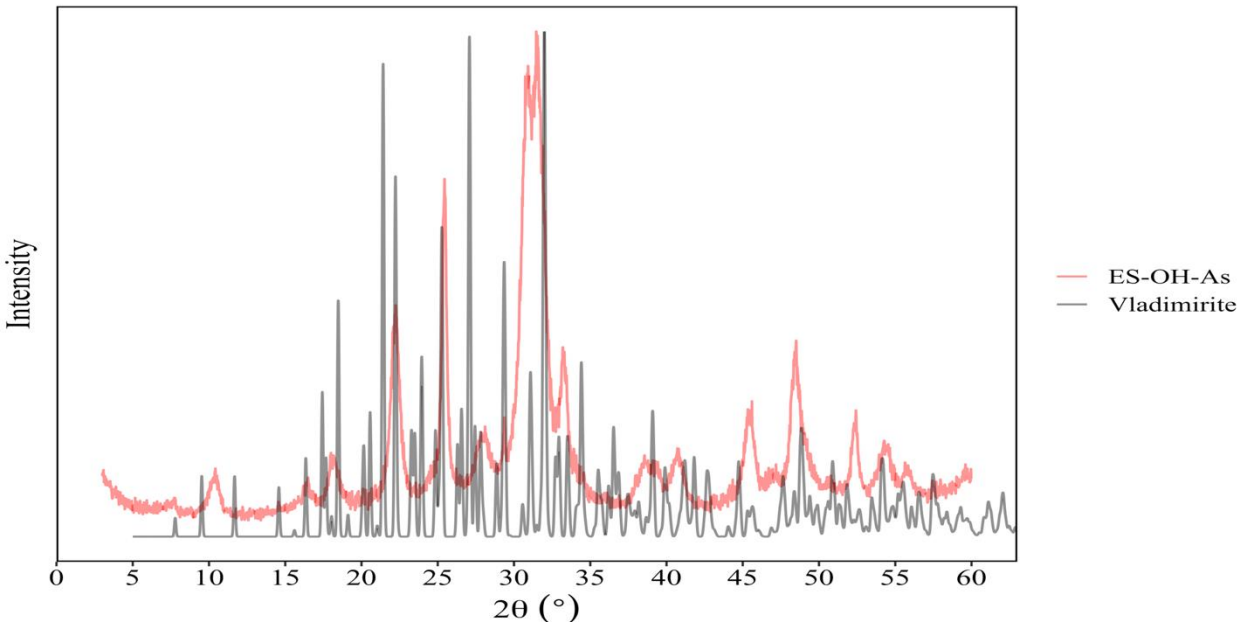


Figure S4: X-ray diffraction patterns of hydroxyl-eggshell loaded with arsenic (ES-OH-As) and vladimirite. Vladimirite spectrum obtained at Lafuente et al. (2016).

Figure S5: Image of a natural vladimirite crystal.
Source: (LAFUENTE et al., 2016).

# Article 3 - A STRAIGHTFORWARD PYROLYSIS METHOD TO CONVERT VACCINE WASTE INTO A NOBLE FERTILIZER

Short communication prepared following the Bioresource Technology guidelines

(to be submitted)

**A straightforward pyrolysis method to convert vaccine waste into a noble fertilizer**

Ivan Célio Andrade Ribeiro[a], Jéssica Cristina Teodoro[a], Marcelo Braga Bueno Guerra[b], Mateus Pimentel Matos[c], Leônidas Carrijo Azevedo Melo[a], Luiz Roberto Guimarães Guilherme[a*]

[a] Department of Soil Science, Federal University of Lavras, Lavras – Minas Gerais, Postal code 37200-900, Brazil

[b] Department of Chemistry, Federal University of Lavras, Lavras – Minas Gerais, Postal code 37200-900, Brazil

[c] Department of Environmental Engineering, Federal University of Lavras, Lavras – Minas Gerais, Postal code 37200-900, Brazil

[*] Corresponding author:
Luiz Roberto Guimarães Guilherme,
Department of Soil Science,
Federal University of Lavras,
Lavras, Minas Gerais, Brazil
Postal code 37200-900.
Phone: +55 35 38291259
E-mail: guilherm@ufla.br

**Abstract**

The influenza virus causes a contagious respiratory illness that infects the nose, throat, and lungs. Hopefully, there is a vaccine that maintains humankind safe from this disease. However, the influenza vaccine production process generates a considerable amount of solid waste, which has to be landfilled into specialized places at a high cost. In this work, we proposed the thermal conversion of vaccine waste into a noble byproduct with the potential to replace commercial phosphorus (P) fertilizer. In summary, the material was incorporated with sawdust and phosphoric acid and pyrolyzed at 500 ºC for two hours. This process generated a biochar with high P content labeled as vaccine waste biochar (VWB). A kinetic study of 40 days was performed to evaluate how the materials release the P over time. Fourier transform infrared spectroscopy (FTIR), scanning electron microscopy with energy dispersive X-ray spectrometry (SEM-EDS), and X-ray diffraction (XRD) were used to characterize the VWB. The kinetics study revealed that TSP released almost all P content at the first day, while VWB released only 2 %. FTIR, SEM-EDS, and XRD confirmed that VWB is a solid that resembles a piece of wood with minerals of calcium phosphate precipitates on its fibers. Finally, a pot experiment confirmed that VWB was as effective as triple superphosphate (TSP) on maize biomass production, proving that VWB is a promising material with great potential to be used in agriculture as an alternative phosphate fertilizer. The findings presented in this work show that thermochemical conversion is a green and sustainable way to treat vaccine waste, and, the same procedure should be evaluated on a large scale.

**Keywords**: Influenza vaccine; Waste valorization; Biochar, Fertilizer

## 1. Introduction

Influenza vaccines were one of the best scientific approaches to maintain humankind protected in the last century. This virus causes acute respiratory illness and affects approximately 10–30% of the human population (Gerdil, 2003). The industries delivered 1.5 billion influenza vaccine doses only in 2019 (Sparrow et al., 2021) to supply the world's demand. Currently, the industries employ embryonated hen's eggs to manufacture this vaccine (Rajaram et al., 2020). In short, the virus sample is inoculated into the egg for replication. After the incubation, a tiny needle extracts the liquid where the virus multiplied, leaving most of the egg in the shell. The remaining material is crushed and dry, forming a yellow powder residue. Due to its hazardous potential contamination, this solid must be correctly discharged in specialized places at a significant price for the companies. However, this solid has nutrients in its chemical composition, which could be used as noble alternative fertilizers. Then, discharging this material, in addition to generating a high cost for companies, a large amount of nutrients is lost and does not return to the environment.

Currently, Brazilian researchers are developing the Butanvac, a novel vaccine against the global outbreak of Coronavirus Disease 2019 (COVID-19). The Butanvac production process is similar to influenza and uses eggs. If the researchers successfully approve this vaccine in combating the coronavirus, a considerable extra amount of waste will be generated. According to Brazilian legislation, solid waste from vaccine industries has to be disposed of in Class 1 landfills due to microbial contamination. These specialized landfills receive only hazardous solids (Brasil, 2005, 2004). The Brazilian legislation also requires that contaminated solid pass for microbial inactivation treatment inside the industries before sending it to landfill. Hence, there are two main expenses: biological inactivation and corrected landfill disposal.

The landfill cost depends on the amount generated and the transportation from the industry to the landfill, which usually are located far away, increasing the cost with specialized transportation of hazardous material. Generally, the correct disposal of biological contaminated wastes range from US$ 1.00 to US$ 6.00 per One of the most prominent vaccine flu industries Brazil uses 300.000 eggs a day to reach the vaccine domestic market demand (Butantan, 2018), generating approximately 1260 tons of the residue per year with a cost of US$ 3.7 mi for the correct disposal at an average price of U$$3,00 per kg of solid waste.

Thus, transforming the hazardous vaccine waste into a sterilized byproduct is needed aiming recycling nutrients and minimize the cost for industries with correct disposal. Pyrolysis technology

is a feasible way to sterilize contaminated materials, since the process occurs from 300 to 900 °C for at least 30 minutes, while recycling the carbon in a stable form and nutrients for reuse as fertilizer. Pyrolysis is the thermal degradation of organic materials in an environment with low oxygen concentration resulting in a byproduct known as biochar (Lehmann and Joseph, 2017; Ye et al., 2019).

There is a vast literature showing the benefits of using biochar as a strategy of improving soil physical and chemical properties such as soil water retention capacity, organic carbon, soil base saturation, nutrient retention, and availability (Barber et al., 2018). Also, applying biochar into soil is one way to store carbon, reducing the atmospheric $CO_2$ concentration (Li et al., 2014; Zhao et al., 2014; Carneiro et al., 2018).

Finally, this work proposes a novel methodology that enables the sterilization of vaccine waste creating a noble alternative fertilizer with nutrient content similar to that found in conventional commercial fertilizers. With the adoption of the proposed methodology, vaccine industries would no longer have expenses with waste disposal in landfills. They would start making a profit from the sale of the fertilizers produced into the novel concept of the circular economy.

## 2. Material and methods

### 2.1 Raw materials

Sawdust (SD) from pine wood was collected in sawmills near the Federal University of Lavras, air-dried at 60 º C, ground through 2.0 mm size, and stocked into sterilized plastic jars. For this study, SD was chosen to produce the biochar because it is formed by carbon compounds, such as lignin and cellulose, and it is easy to obtain in the neighborhood of the vaccine industries.

ENFIL, a waste treatment company from São Paulo, in Brazil, donated a small sample (around 100 g) of vaccine waste. However, this amount was not enough to run the entire study, and the Brazilian legislation does not allow transportation of a considerable amount of hazardous materials to other places than Class I landfill. To avoid contaminating our lab team and agree with the legislation, we made a synthetic vaccine waste. Briefly, 500 fertilized chicken eggs were ground in an industrial blender for 10 min and oven-dried at 60 ºC until constant weight. The dried solid was sieved through a 2.0 mm sieve obtaining a homogenous solid material. This procedure was based on how the vaccine industries generate their waste. The only difference here is the injection step and the withdrawal of the virus. We assumed that the amount of virus injected into the eggs does not change

the total nutrient composition of vaccine waste. Total nutrient content analysis was performed on real and synthetic solid waste to validate that hypothesis, Table 1.

Table 1. Total nutrient content in real and synthetic solid wastes.

| Vaccine waste | N | P | K | Ca | Mg | S | B | Cu | Fe | Mn | Zn |
|---|---|---|---|---|---|---|---|---|---|---|---|
| | ---------- g/kg ---------- | | | | | | ---------- mg/kg ---------- | | | | |
| Real | 50.20 | 5.06 | 11.24 | 196.75 | 1.97 | 6.48 | 4.37 | 3.14 | 170 | 21.47 | 32.26 |
| Synthetic | 48.05 | 5.01 | 12.10 | 198.85 | 2.50 | 7.01 | 4.45 | 3.15 | 160 | 25.45 | 25.0 |

2.2 Biochar production

Sawdust and vaccine waste were immersed in a glass beaker containing 1.0 L phosphorus solution and kept under constant steering. The mass ratio was 1:1:0.15 of sawdust, vaccine waste, and P from phosphoric acid. The solution was prepared with analytical grade phosphoric acid (d = 1.63 g $cm^{-3}$, p = 86%). After 2 h, the suspension was oven-dried at 60 ºC until constant weight. The dried solid was accommodated into a steel cylinder and pyrolyzed in a muffle furnace at 500 °C for 2 h. After slowly cooling, the biochar was ground in a blender and sieved through a 0.25 mm sieve. The final material was labeled as sawdust vaccine waste biochar (SVB). In this small pilot experiment, for each 100 g of vaccine waste used, it was obtained 46.7 $\pm$ 0.4 g of biochar. The optimum proportion, pyrolysis temperature, and duration shown here were reached after intensive laboratory tests. For this reason, the entire procedure has a patent deposit in the National Institute of Industrial Property (INPI), Brazil (Ribeiro et al., 2019)

Considering that 1L of analytical grade $H_3PO_4$ is, on average, $8.69 (Table S2), and the biochar yield reported, the capital cost needed to produce 1 kg of SVB was equal to US$ 3.15. The energy consumption was not considered on the estimation cost because syngas and bio-oil are produced through the pyrolysis processes. Thus, these byproducts' combustion might supply enough energy to keep the system auto-sustainable on a real scale.

2.3 Chemical characterization

Analysis of total elemental composition was assessed in triplicate as recommended by Enders and Lehmann (2012). Briefly, 200.0 ± 5.0 mg of each material was weighed in glass tubes and ashed in a muffle furnace for 8 h at 500 ºC. Subsequently, 5.0 mL $HNO_3$ was added to each tube and heated to 120 ºC on a digestion block to dryness. Samples were cooled to ambient before adding 1.0 mL

$HNO_3$ and 4.0 mL of 30% $H_2O_2$ and then heated again at 120 ºC to incipient dryness. After cooling, concentrated $HNO_3$ and deionized water were added to the tubes to achieve a 5% acid concentration as required for further elemental analysis. The samples were analyzed using inductively coupled plasma optical emission spectrometry (ICP-OES), Model Blue, Germany.

X-ray diffraction (XRD) analyses were carried out to identify the crystalline structure of each material. The diffractograms were recorded using a Rigaku Miniflex II equipment with CuKα radiation and graphite with monochromatic beam, in the range of 20 – 70 2θ degrees and scanning speed of 0.02º / min. Fourier transform infrared (FTIR) spectra were also collected to identify the functional groups in the biochar surface using Digilab Excalibur spectrometer (spectral range 4000-400 $cm^{-1}$ under 4 $cm^{-1}$ resolution with 16 scans). Finally, the surface morphology and the nutrient distribution map of VWB were obtained by scanning electron microscope (LEO EVO 40 XVP – Carl Zeiss) equipped with energy dispersed X-ray spectroscope (Brunker – Quantax EDX).

2.4 P release Kinetics

The kinetic release of P was performed on both biochar and the commercial fertilizer. For that, 0.1 g of each material was mixed, separately, with 40 mL of deionized water into plastic polyethylene centrifuge tubes and agitated in a shaker at 120 rpm at different intervals of time, 0.25, 0.5, 1, 3, 6, 12, 24, 48, 72, 120, and 240 h. After each time, the solution was filtered through 0.45µm filters, and the P was measured in the extract by ICP-OES. The raw data obtained was plotted as the P releases (mg/L) against the time (days). Then, the following models were applied to get the first insights about how P was released from each material (Jalali and Zinli, 2011):

| | | |
|---|---|---|
| Pseudo - first order | $ln(q_e - q_t) = b - k_1 t$ | 1 |
| Pseudo – second order | $\frac{t}{q_t} = \frac{1}{k_2 * q_e^2} + \frac{t}{q_e}$ | 2 |
| Elovich | $q_t = a * t^b$ | 3 |
| Parabolic diffusion | $q_t = R * t^{1/2} + c$ | 4 |

where $q_t$ is the cumulative P released at the time (t), $q_e$ represents the amount of P released at equilibrium; $k_1$, $k_2$, R and α are constants estimate the P released rate; a, b and c are the model's constants.

2.5 Greenhouse experiment

A pot experiment was carried under greenhouse conditions to evaluate the capacity of VWB as a P source compared with one commercial fertilizer. The soil used was an Oxisol collected from a 40-60 cm layer in the Federal University of Lavras campus, Minas Gerais, Brazil. It was air-dried, homogenized through a 2 mm sieve, and physically and chemically analyzed. The results are presented in Table 2. Based on the chemical composition, in 3 kg of soil were placed in plastic bags and mixed with calcium carbonate and magnesium carbonate at a molar ratio Ca/Mg 3:1, aiming to increase the base saturation index up to 70%. The bags were filled with deionized water until 80% of soil water holding capacity and incubated for 30 days. After this time, the soil was air-dried and mixed with 200 mg of P soluble in neutral ammonium citrate from VWB and triple superphosphate (positive control). A negative control treatment, without the addition of P, was also evaluated. The dose of TSP, positive control, is the amount necessary to cultivate plants as recommended by Novais et al. (1991). P sources were mixed to the soil in powder form and the amount added was calculated based on the P soluble in ammonium citrate, shown in Table S2.

Later, the bags with soil were fertilized with 100, 150, 75, 15, 50, 0.5, 1.5, 5.0, 0.1, and 5 mg $kg^{-1}$ of N, K, Ca, Mg, S, B, Cu, Fe, Mo, and Zn, respectively, as recommended by Malavolta (1980) and accommodated in plastic pots. Subsequently, five seeds of maize (*Zea mays*) were sown in each plastic pot containing 3.0 $dm^3$ of the Oxisol and thinned after 7 days to one plant. Maize was grown for 40 days, and the pots received an additional application of N and K fertilizer (100 mg $dm^{-3}$) via fertigation at 15 and 30 days after the seeding. After 45 days, plants were harvested at 10 cm from the soil surface, placed into paper bags, dried at 65 °C for 72h, weighed, and reported as shoot dry mass (SDM). Then, all plant samples were ground into a portable grinder and digested using a nitric-perchloric acid mixture for P content determination. Maize P-uptake was achieved by multiplying P content by shoot dry biomass. Finally, soil samples were collected in each pot to determine pH in water (Teixeira et al., 2017) and soil-available P by anion-exchange resin (Van Raij et al., 1986).

**Table 2**. Physical and chemical properties of the soil under natural conditions used in the greenhouse experiment.

| | |
|---|---|
| pH in $H_2O$ | 4.40 |
| K (mg $kg^{-1}$) | 39.67 |
| P (mg $kg^{-1}$) | 0.36 |

| | |
|---|---|
| $Ca^{2+}$ ($cmol_c$ $kg^{-1}$) | 0.24 |
| $Mg^{2+}$ ($cmol_c$ $kg^{-1}$) | 0.14 |
| O.M. (dag $kg^{-1}$) | 2.49 |
| Zn (mg $kg^{-1}$) | 0.85 |
| Fe (mg $kg^{-1}$) | 58.74 |
| Mn (mg $kg^{-1}$) | 20.73 |
| Cu (mg $kg^{-1}$) | 3.54 |
| B (mg $kg^{-1}$) | 0.08 |
| S (mg $kg^{-1}$) | 11.39 |
| Clay (g $kg^{-1}$) | 670 |

$Ca^{2+}$, $Mg^{2+}$ and $Al^{3+}$: KCl extractor (1mol $L^{-1}$); P, K, Fe, Zn, Mn, and Cu: Mehlich-1extractor; H+Al: SMP extractor; B: Hot water extractor; S: monocalcium phosphate in acetic acid extractor; O.M.: organic matter by $Na_2Cr_2O_7$ 4 mol $L^{-1}$ + $H_2SO_4$ 10 mol $L^{-1}$ oxidation; SB: sum of exchangeable bases; P-rem: remaining phosphorus; T: cation exchange capacity at pH 7; t: effective cation exchange capacity; V: base saturation index; and m%: aluminum saturation index.

### 2.6 Statistical Analysis.

All graphs and statistical analysis were performed using R software version 4.0.3 (Team, 2020). Kinetics of P release was fitted to nonlinear model using nlstools package (Baty et al., 2015). Data from the greenhouse experiment were subjected to analysis of variance (one-way ANOVA, $p < 0.05$), and when the significant difference ($p < 0.05$) was observed, the means were compared the Tukey test ($p < 0.05$) using the emmeans package (Lenth et al., 2018).

## 3. Results and discussion

### 3.1 Total characterization

The main chemical properties of biochar and TSP are summarized in Table 3. The biochar pH was 3.18 units higher than TSP. This result indicates that TSP has 1500-fold more acidity than biochar, considering that pH = - log [H+], where [H+] is the acidity. The TSP acidity results from an industrial chemical process in which the phosphate rock is acidified with pure phosphoric acid

(Novais, 2007). Biochar is usually alkaline due to a decrease in acid functional groups and the formation of alkaline compounds, and the pH value of a particular biochar type depends on the raw material and the pyrolysis temperature (Enders et al., 2012). Also, the presence of eggshells in the vaccine waste have contributed to the high pH, because during the pyrolysis process, the eggshell is converted into calcium oxide, a high alkalinity compound (Torit and Phihusut, 2019).

High pH is a favorable feature for phosphate fertilizers used in acidic soils. These soils show a net positive charge, which strongly attracts the negative ions phosphates present in the solution. Therefore, fertilizers with high pH release negative compounds into the soil solution, avoiding P fixation by the positive soil charge. Consequently, more nutrients will be available to the plants (Novais and Smyth, 1999).

The total content of macro (Mg, Ca, P, S) and micro (B, Cu, Fe, Mn, Zn) nutrients was higher than the values reported for wood biochar in the literature. This indicates that the nutrients from vaccine waste and sulfuric acid were perfectly incorporated into the final biochar. Generally, biochar derived from wood feedstock has low nutrient contents (Domingues et al., 2017).

An outstanding result was observed for the total P content in biochar that reached 60% of the P found in the commercial fertilizer, which suggests that the VWB can be used as a phosphate fertilizer. Concerning potentially hazardous elements, the amount of As, Cd, Pd, Cr, and Hg were lower than TSP, and in accordance with values considered safe by Brazilian legislation, Table 3.

Table 3. Major properties of vaccine waste biochar (BCV), and triple superphosphate (TSP), and potentially hazardous element content permitted by Brazilian legislation.

| | | VWB | TSP | Permitted |
|---|---|---|---|---|
| pH | | 5.95 ± 0.03 | 2.77 ± 0.01 | - |
| K | | 4.13 ± 2.62 | - | - |
| Ca | | 51.04 ± 2.16 | - | - |
| Mg | g $kg^{-1}$ | 1.11 ± 0.07 | - | - |
| S | | 0.09 ± 0.01 | - | - |
| P | | 152.5± 3.6 | 210.8 ± 2.3 | - |
| As | mg $kg^{-1}$ | - | - | 2.0 – 4000.0 |

| | | | |
|---|---|---|---|
| Cd | 0.21 | - | 4.0 – 450.0 |
| Pb | 3.43 | - | 20 .0 – 10,000 |
| Cr | 4.13 | - | 40.0 – 500 |
| Hg | 0.00 | - | 0.05 – 10 |

3.2 Kinetic of P release

In Figure 1 is shown the kinetics of P solubilization in water from biochar and TSP samples over time. Different nonlinear models were used to predict the P released of each material over time, and the model parameters and the AIC are reported in Table 4. The P released by TSP was better predicted by the Elovich equation according to the lower AIC. On the other hand, VWB was better predicted by the pseudo-first-order model equation. As expected, TSP released almost all P content at the first day. Conversely, VWB released only 2 % of P content after the first day and did not reach equilibrium. After 40 days, VWB released around 50% of total P content, as illustrated in Fig. 1.

The formation of less soluble compounds might explain the slow-release during the biochar production process. The eggshells, solid rich in calcium and present in the vaccine waste, might react with the phosphoric acid creating calcium phosphate minerals with low water solubility. Also, during the pyrolysis, some reactions converted the P from phosphoric acid into a less soluble form by incorporating this nutrient into the biochar structure. At high temperatures and oxygen, phosphoric acid reacts with carbon from solid waste, creating a P-O-C bond that is less soluble in water than P bonds of soluble fertilizers (Zhao et al., 2016a).

High total P content and low water-soluble P means that once applied to soil, part of the P is not prompt release, avoiding soil fixation and, consequently, increase P availability, P uptake, and P use efficiency by plants (Novais, 2007).

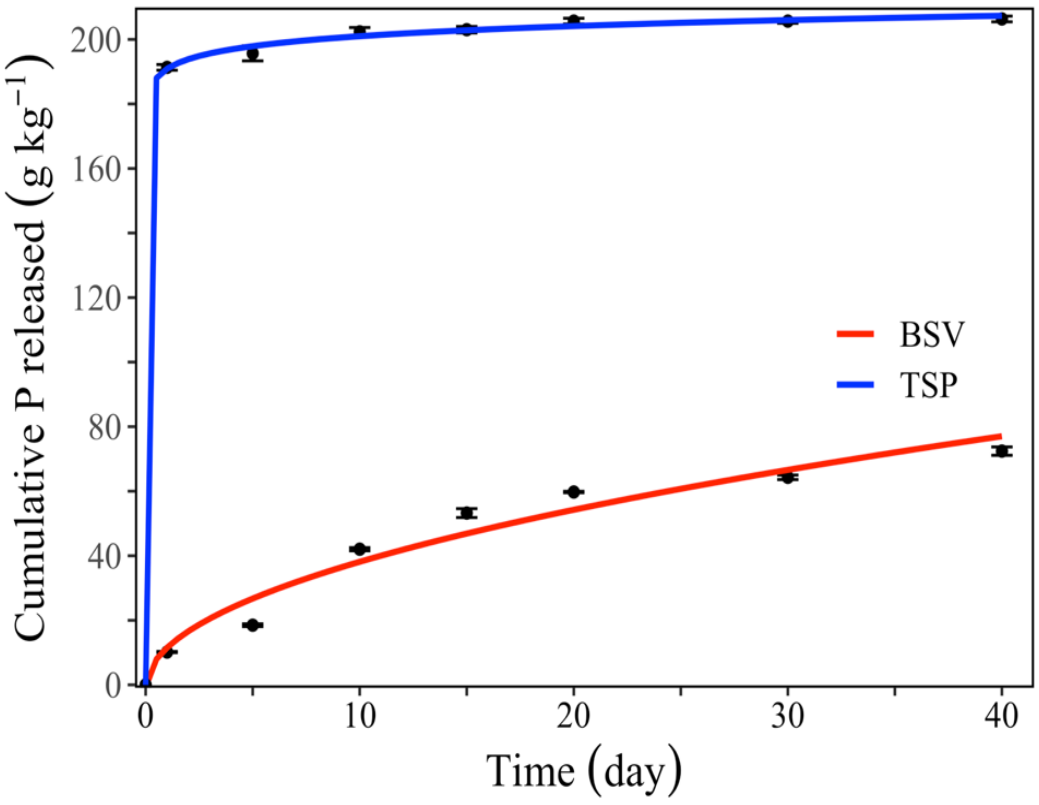


Fig. 6. TSP and biochar kinetics of P release in water.

Table 4. P release kinetics parameters of vaccine waste biochar and triple superphosphate

| Model | Parameter | VWB | TSP |
|---|---|---|---|
| Pseudo-first-order | $q_e$ | 74.59 | 203.11 |
| | $k_1$ | 0.010 | 2.85 |
| | AIC | 46 | 47.3 |
| Pseudo-second-order | qe | 99.61 | 204.52 |
| | $k_2$ | 0.001 | 0.06 |
| | AIC | 47.5 | 43.1 |
| Elovich | α | 0.99 | 3.10 |
| | β | 17.98 | 4.46 |
| | AIC | 51.1 | 28.7 |
| Parabolic Diffusion | A | -0.771 | 102.9 |
| | R | 12.30 | 22.10 |
| | AIC | 53.7 | 91.1 |

$q_e$ = amount of P released at equilibrium; $k_1$ = pseudo-first order rate constant; $k_2$ = pseudo-second order rate constant; $K_R$ = Redlich-Peterson isotherm constant (L/g), g = Redlich-Peterson exponent that lies between 0 and 1; $A_T$ and $b_T$ Temkin isotherm constants. α

## 3.3 Spectroscopies analysis

SEM images of sawdust and the biochar vaccine waste and the EDS spectra from the surface of each material are shown in Fig. 2. It is possible to observe the wood fiber on the sawdust biochar, which is mainly formed by carbon. In the case of VWB, it can be observed a structure that resembles wood fibers with some material deposited on its surface (Fig. 2). The wood fiber comes from the sawdust, while the precipitate formed on its surface comes from the reaction of phosphoric acid with chemical elements of vaccine waste. Elemental mapping analysis revealed that these solids are mainly formed by P, O, and Ca (Fig. 2b, c, and d).

Furthermore, EDS analysis of the specific highlighted point in Fig. 2a reveals that Ca/P was equal to 0.60, which is consistent with the Ca/P ratio of the mineral with was later identified by XRD analysis (Fig. 4).

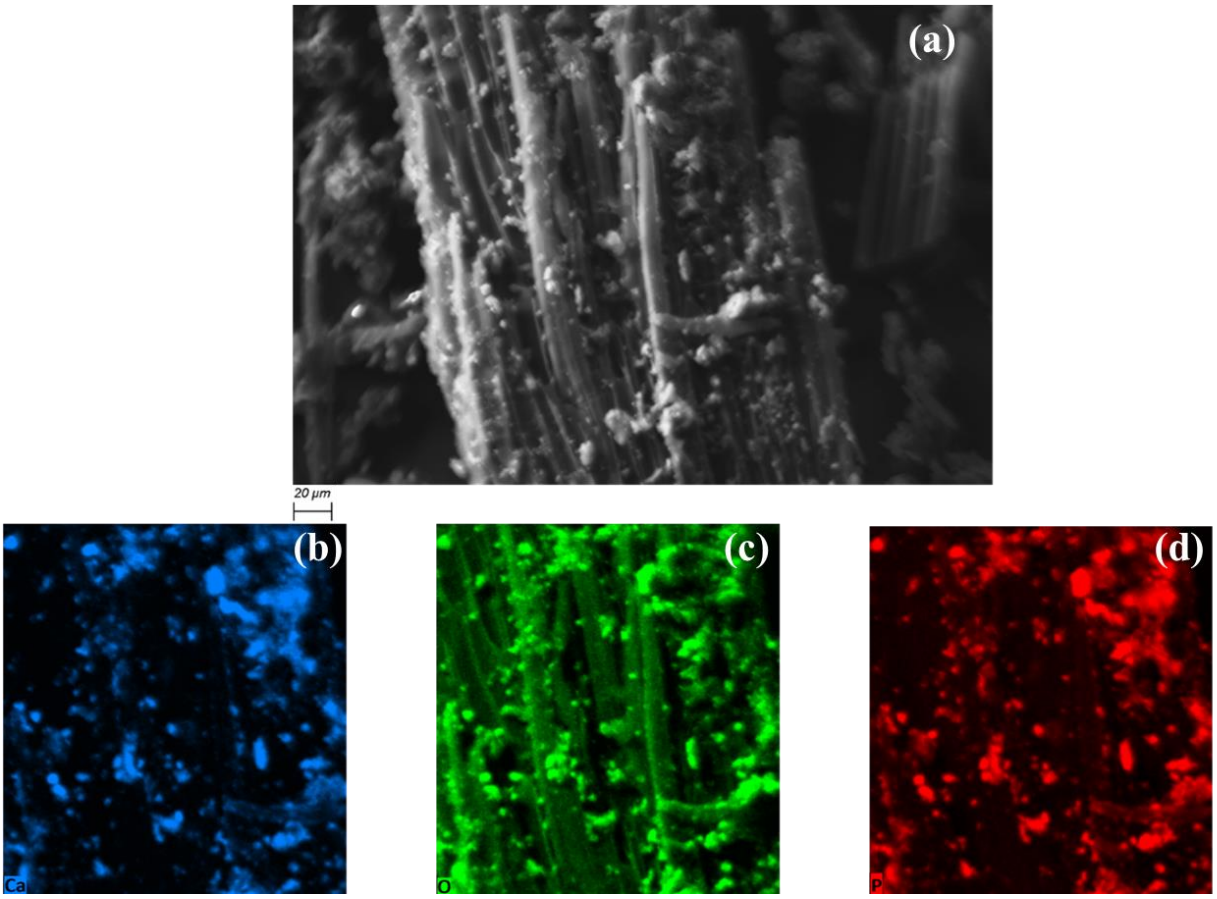

Fig. 7. Scanning electron microscope image (a), and Ca (b), O (c), and P (d) mapping nutrient distribution of sawdust vaccine biochar.

Fig. 3 shows the FTIR spectrum collected on the VWB surface. The wide absorption peak centered around 1600 and 1500cm$^{-1}$ is assigned to the presence C = O, and – C = C antisymmetric stretching of aromatic rings (Zhao et al., 2016a). Most of the peaks observed at wavelengths lower than 1200 cm$^{-1}$ were related to phosphorus groups. The peaks at 1250 and 939 cm$^{-1}$ are assigned to organic phosphates (P = O) and aromatic phosphates (P – O – C) stretching, respectively (Coates, 2004). Identifying such groups suggests that the P from phosphoric acid entered the feedstock structure after the pyrolysis process. After evaluating graphite enriched with phosphorus solution, Oh and Rodriguez (1993), concluded that at elevated temperatures, a complex is formed in which phosphorus species are incorporated into the carbonaceous structure in a unique bonding resulting in a material with more thermal stability. Recently, some authors reported that enrichment of feedstock with phosphoric before the pyrolysis process creates a byproduct with more thermal stability (Carneiro et al., 2018; Zhao et al., 2016b). The peaks at 563 and 472 are related to absorption bonds of $PO_4^{3-}$ groups (Malakauskaite-Petruleviciene et al., 2016). Considering these peaks and the elemental composition of VWB, compounds of calcium phosphates might be precipitated during the feedstock mixture with phosphoric acid or during the pyrolysis process.

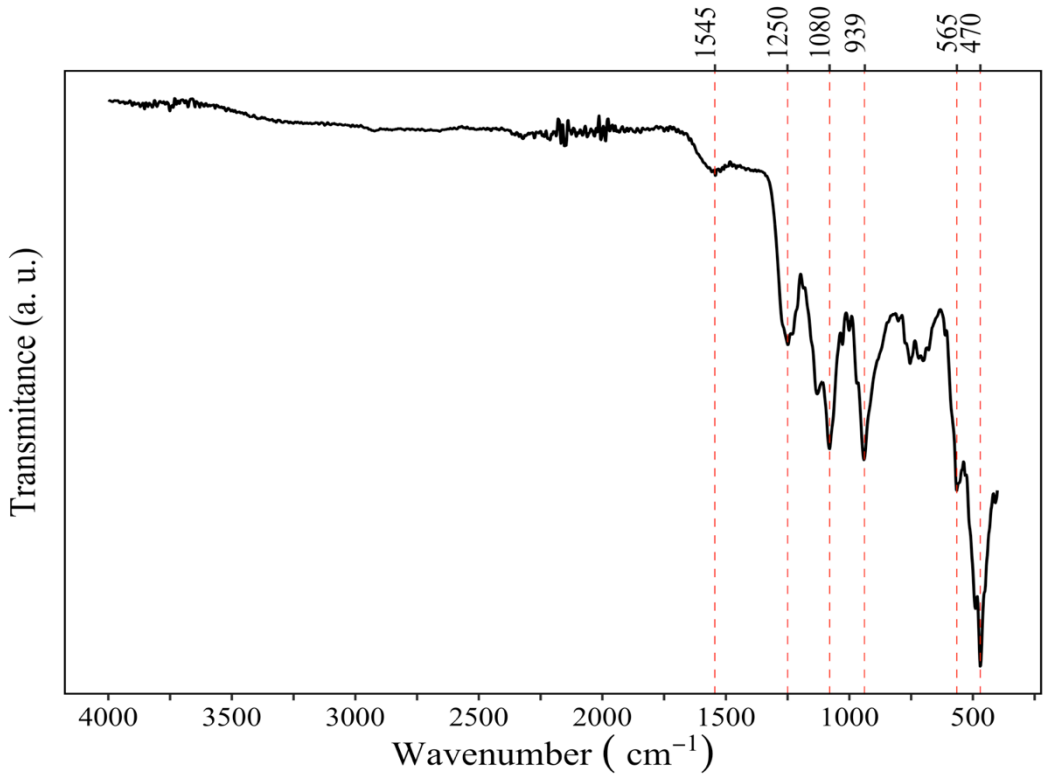


Fig. 8. Furrier Transformed Infrared (FTIR) of biochar vaccine waste (BV.)

Finally, Fig.5 illustrates the X-Ray diffractogram of BVW. The formation of minerals in concentrations below the equipment detection and amorphous compounds explain the noise observed in the diffractogram. The distinct peaks at 25.2, 33.3, and 48.5 were assigned to the presence of calcium-catena-polyphosphate ($CaO_6P_2$), a stable phosphate mineral with broad application in material science (Weil et al., 2007).

After SEM-EDS, FTIR, and XRD analysis, it is possible to conclude that a mixture of sawdust, vaccine waste, and phosphoric acid, at the right proportion, followed by pyrolysis creates a biochar P enriched mainly formed by $CaO_6P_2$.

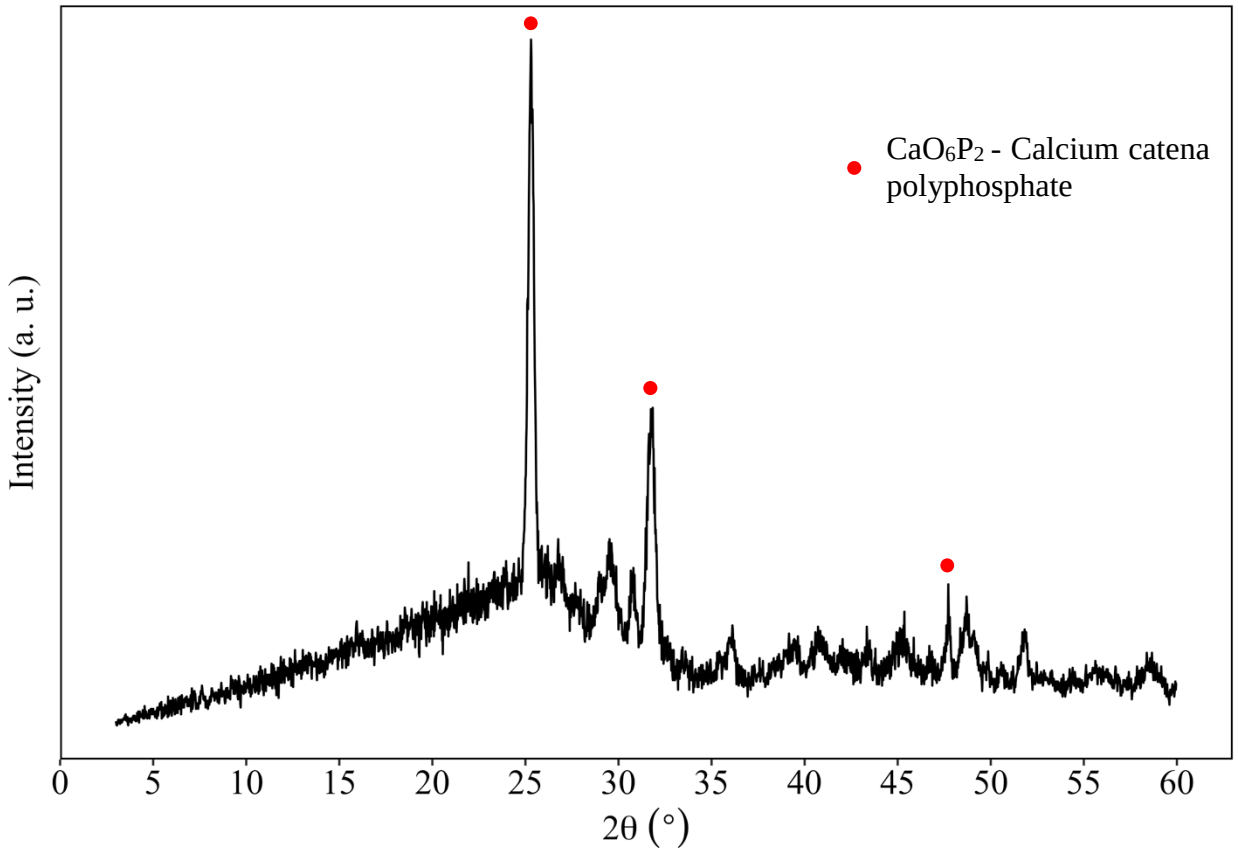


Fig. 9. X-Ray diffractometer (XRD) of biochar vaccine waste (BVW)

3.4 Greenhouse experiment

The parameters measured after 45 days of maize cultivation are summarized in Fig. 5. As expected, an outstanding difference in shoot biomass was observed between treatments that received phosphorus and the control proving that the absence of this nutrient drastically decreases crop development. Concerning the P resin results, the amount was significantly higher in soil treated with either TSP or VWB compared with control (Fig. 5c). The P-resin represents the amount of P available to plants (van Raij et al., 1986). Therefore, either VWB and TSP, besides releasing an ideal amount of P to maize cultivation, also had a considerable amount of this nutrient available in the soil for the next cultivation. The slow-release of VWB in relation to the TSP explains the smaller amount of P available to plant after the cultivation, as reported by Lustosa Filho et al. (2017). When evaluating biochar prepared from poultry litter enriched with phosphoric acid and magnesium, the authors suggested that the maize cultivation time is insufficient for the total P release from this material.

An interesting result was observed in Fig. 5d. Even though the soil had its pH corrected initially, after cultivation, the pH in control was below 5. This result might be explained by adding ammonium nitrate ($NH_4NO_3$) to the soil after 15 and 30 days of cultivation. Once in the soil, $NH_4NO_3$ is hydrolyzed, releasing ions $H^+$, therefore, decreasing the pH value. For each mole of $NH_4^+$, 2 moles of $H^+$ is released, Eq.2. In the cultivated pots, the plants absorbed a fraction of ion ammonium, avoiding acidification by the nitrification process.

| | |
|---|---|
| $NH_{4(aq)}^{+} + 2O_{2(g)} \rightarrow NO_{3(aq)}^{-} + 2H_{(aq)}^{+} + H_2O_{(l)}$ | Eq. 2 |

After all, the pot experiment results proved that VWB successfully increased soil fertility in terms of P availability in high weathered soil. These are the first findings suggesting the use of VWB instead of commercial fertilizer in crop cultivation. Ultimately, it is essential to report that the novel method proposed here was converting hazardous waste into a noble fertilizer to avoid locally environmental issues. The goal here is not to replace any commercial fertilizers because the amount of solid waste generated by vaccine industries is insufficient to supply the amount of fertilizer required by great farms. The economic viability will be discussed further.

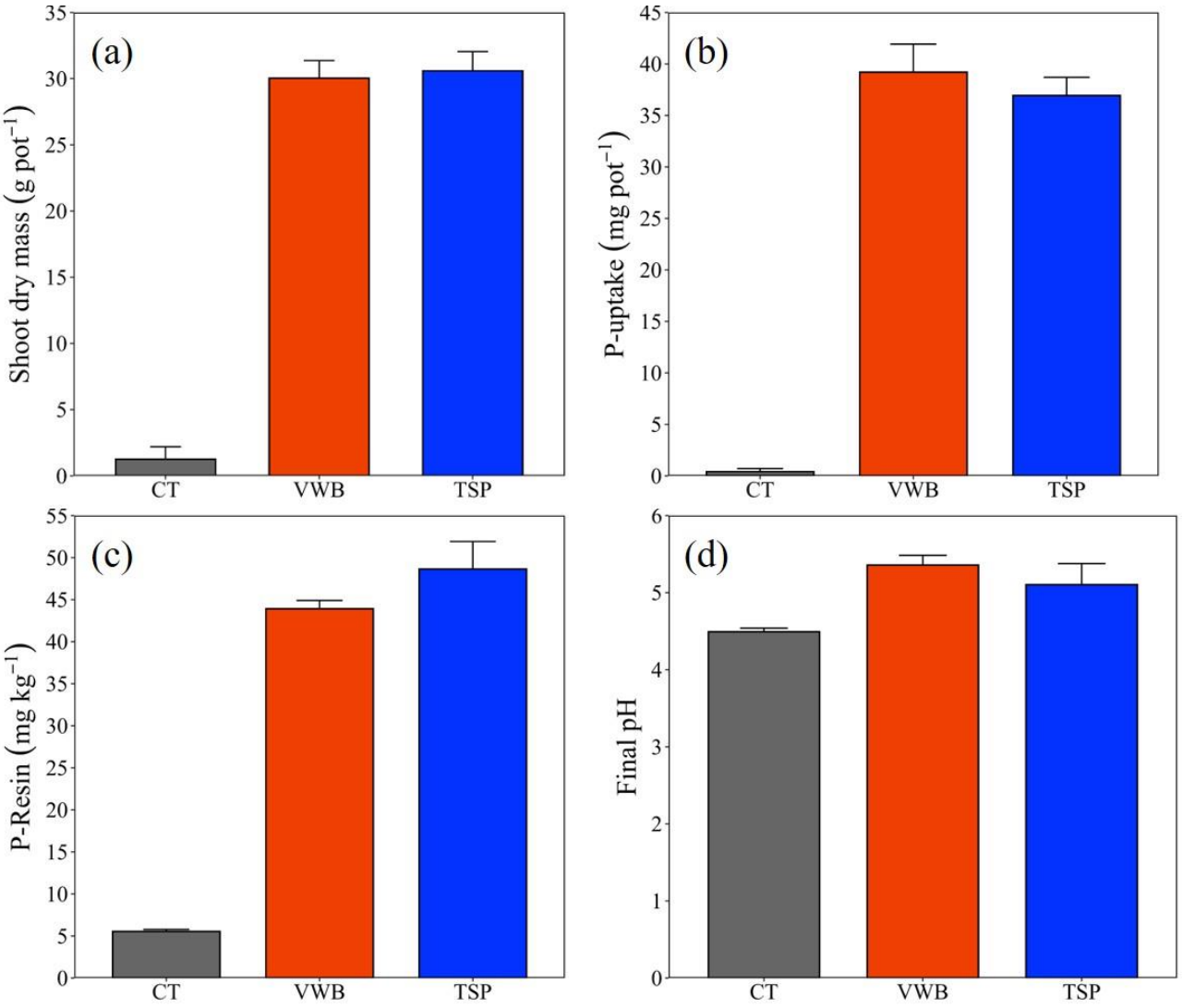


Fig. 5. Shoot dry mass (a), P uptake (b), soil resin P (c), and final pH (d) after maize cultivation. Error bars represent standard error of the mean.

3.5 Economic viability and environmental application

Usually, the decision-makers consider the cost as the main factor in accepting novel technologies. As previously reported, the capital cost necessary to produce one kilogram of VWB was equal to US$3.12, and this value is not competitive in the fertilizer market. However, this cost was based on a pilot project using elemental grade chemicals, and the escalation to a real-scale might considerably decrease the final price. Besides, the capital cost needed for the correct disposal of hazardous waste by the vaccine industries should be considered. Generally, the correct disposal of biological contaminated ranged from US$ 1.00 to US$ 6.00 per kg. Once the process is implemented

on a real scale, there will be no landfill cost, and this saved money can be used in the biochar production process. Also, the biochar could be sold on the local market, creating a novel, economic income for the industry. Implementing this process in the vaccine production plant minimizes the expenses of companies with disposal in landfills, making it possible to obtain a profit from the sale of the byproduct.

It is essential to point out that landfills support a limited amount of solid waste. Therefore, continuing disposing of waste decrease the landfill lifetime, and when it is full, another area has to be prepared to receive more waste. Even after being closed, the full landfill needs to be continuously monitored to avoid environmental contamination.

Maybe it will be difficult to sell fertilizers made with vaccine waste. One alternative to avoid this issue is to use the byproduct as an alternative fertilizer on farms that cultivates crops to feed the chickens that supply eggs to vaccine industries. This procedure will close the loop into a modern circular economy concept.

It is also worth adding that the adoption of the process by the industries is following the concept of economy established by the National Solid Waste Policy in force in the country, which encourages them to reduce, reuse, and recovery solid waste generated in any production process stage.

## 4. Conclusion

This study provides a novel strategy to convert the vaccine waste into a noble fertilizer. Spectroscopies analyses, such as SEM-EDS, FTIR, and XRD, consistently indicate that the VWB is a wood solid surrounded by small plots of calcium phosphate. Also, VWB has excellent potential as an alternative P fertilizer, which could ultimately be commercialized in specialized markets, enabling a new source of income for the vaccine industries and reducing the liability with wastes generated. Future studies should focus on implementing the process on a real scale and evaluating the product in other agricultural cultures. Finally, this study provides a new environmentally friendly process for vaccine waste treatment producing an alternative phosphate fertilizer.

**References**


Barber, S.T., Yin, J., Draper, K., Trabold, T.A., 2018. Closing nutrient cycles with biochar- from filtration to fertilizer. J. Clean. Prod. 197, 1597–1606. https://doi.org/10.1016/j.jclepro.2018.06.136

Baty, F., Ritz, C., Charles, S., Brutsche, M., Flandrois, J.-P., Delignette-Muller, M.-L., 2015. A toolbox for nonlinear regression in R: the package nlstools. J. Stat. Softw. 66, 1–21.

Brasil, 2005. RESOLUÇÃO CONAMA nº 358, de 29 de abril de 2005 [WWW Document]. URL http://www2.mma.gov.br/port/conama/legiabre.cfm?codlegi=462 (accessed 3.23.21).

Brasil, 2004. Resolução Rdc Nº 306, De 7 De Dezembro De 2004 [WWW Document]. Agência Nac. Vigilância Sanitária. URL https://bvsms.saude.gov.br/bvs/saudelegis/anvisa/2004/res0306_07_12_2004.html (accessed 3.23.21).

Carneiro, J.S. da S., Lustosa Filho, J.F., Nardis, B.O., Ribeiro Soares, J., Zinn, Y.L., Melo, L.C.A., 2018. Carbon stability of engineered biochar-based phosphate fertilizers. ACS Sustain. Chem. Eng. acssuschemeng.8b02841. https://doi.org/10.1021/acssuschemeng.8b02841

Coates, J., 2004. Interpretation of Infrared Spectra, A Practical Approach. Encycl. Anal. Chem. 1–23.

Domingues, R.R., Trugilho, P.F., Silva, C.A., De Melo, I.C.N.A., Melo, L.C.A., Magriotis, Z.M., Sánchez-Monedero, M.A., 2017. Properties of biochar derived from wood and high-nutrient biomasses with the aim of agronomic and environmental benefits. PLoS One 12, 1–19. https://doi.org/10.1371/journal.pone.0176884

Enders, A., Hanley, K., Whitman, T., Joseph, S., Lehmann, J., 2012. Characterization of biochars to evaluate recalcitrance and agronomic performance. Bioresour. Technol. 114, 644–653. https://doi.org/10.1016/j.biortech.2012.03.022

Enders, A., Lehmann, J., 2012. Comparison of Wet-Digestion and Dry-Ashing Methods for Total Elemental Analysis of Biochar. Commun. Soil Sci. Plant Anal. 43, 1042–1052. https://doi.org/10.1080/00103624.2012.656167

Gerdil, C., 2003. The annual production cycle for influenza vaccine. Vaccine 21, 1776–1779. https://doi.org/10.1016/S0264-410X(03)00071-9

Jalali, M., Zinli, N.A.M., 2011. Kinetics of phosphorus release from calcareous soils under different land use in Iran. J. Plant Nutr. Soil Sci. 174, 38–46. https://doi.org/10.1002/jpln.200900108

Lehmann, J., Joseph, S., 2017. Biochar for Environmental Management.

Lenth, R., Singmann, H., Love, J., Buerkner, P., Herve, M., 2018. Emmeans: Estimated marginal means, aka least-squares means. R Packag. version 1, 3.

Li, F., Cao, X., Zhao, L., Wang, J., Ding, Z., 2014. Effects of mineral additives on biochar formation: Carbon retention, stability, and properties. Environ. Sci. Technol. 48, 11211–11217. https://doi.org/10.1021/es501885n

London, R.C. of N., 2018. Freedom of Information Follow up Report on Management of Waste in the NHS NHS [WWW Document].

Lustosa Filho, J.F., Penido, E.S., Castro, P.P., Silva, C.A., Melo, L.C.A., 2017. Co-Pyrolysis of Poultry Litter and Phosphate and Magnesium Generates Alternative Slow-Release Fertilizer Suitable for Tropical Soils. ACS Sustain. Chem. Eng. 5, 9043–9052. https://doi.org/10.1021/acssuschemeng.7b01935

Malakauskaite-Petruleviciene, M., Stankeviciute, Z., Niaura, G., Garskaite, E., Beganskiene, A., Kareiva, A., 2016. Characterization of sol-gel processing of calcium phosphate thin films on silicon substrate by FTIR spectroscopy. Vib. Spectrosc. 85, 16–21. https://doi.org/10.1016/j.vibspec.2016.03.023

MAPA, M. da A.P. e A., 2017. Manual De Métodos Analíticos oficiais para fertilizantes e corretivos.

Nogueira, D.N.G., Castilho, V., 2016. Resíduos de serviços de saúde: mapeamento de processo e gestão de custos como estratégias para sustentabilidade em um centro cirúrgico. REGE - Rev. Gestão 23, 362–374. https://doi.org/10.1016/j.rege.2016.09.007

Novais, R.., Neves, J.C.., Barros, N.F., 1991. Ensaio em ambiente controlado. In Métodos de pesquisa em fertilidade do solo, Embrapa-SE. ed. Brasília.

Novais, R.F. et. al., 2007. Fertilidade do solo, 1a ed. Sociedada Brasileira de Ciência do Solo.

Novais, R.F., Smyth, T.J., 1999. Fósforo em solo e planta em condições tropicais. Universidade Federal de Viçosa, Viçosa.

Oh, S.G., Rodriguez, N.M., 1993. In situ electron microscopy studies of the inhibition of graphite oxidation by phosphorus. J. Mater. Res. 8, 2879–2888. https://doi.org/10.1557/JMR.1993.2879

Rajaram, S., Wojcik, R., Moore, C., Ortiz de Lejarazu, R., de Lusignan, S., Montomoli, E., Rossi, A., Pérez-Rubio, A., Trilla, A., Baldo, V., Jandhyala, R., Kassianos, G., 2020. The impact of candidate influenza virus and egg-based manufacture on vaccine effectiveness: Literature review and expert consensus. Vaccine 38, 6047–6056. https://doi.org/10.1016/j.vaccine.2020.06.021

Ribeiro, I.C.A., Teodoro, J.C., Guilherme, L.R.G., Melo, L.C.A., Franco, C.S., Matos, M.P. de, 2019.

Processo de Produção de um Organomineral Fosfatado a Partir de Resíduos da Indústria de Vacinas da Gripe. BR 10 2019 026379 2.

Sparrow, E., Wood, J.G., Chadwick, C., Newall, A.T., Torvaldsen, S., Moen, A., Torelli, G., 2021. Global production capacity of seasonal and pandemic influenza vaccines in 2019. Vaccine 39, 512–520. https://doi.org/10.1016/j.vaccine.2020.12.018

Team, RC, 2020. R development core team [WWW Document]. A Lang. Environ. Stat. Comput. URL https://www.r-project.org/

Teixeira, P.C., Donagemma, G.K., Fontana, A., Teixeira, W.G., 2017. Manual de Métodos de Análise de Solo. Embrapa Solos, Brasília, DF.

Torit, J., Phihusut, D., 2019. Phosphorus removal from wastewater using eggshell ash. Environ. Sci. Pollut. Res. 26, 34101–34109. https://doi.org/10.1007/s11356-018-3305-3

van Raij, B., Quaggio, J.A., da Silva, N.M., 1986. Extraction of phosphorus, potassium, calcium, and magnesium from soils by an ion-exchange resin procedure. Commun. Soil Sci. Plant Anal. 17, 547–566. https://doi.org/10.1080/00103628609367733

Van Raij, B., Quaggio, J.A., Da Silva, N.M., 1986. Extraction of phosphorus, potassium, calcium, and magnesium from soils by an ion-exchange resin procedure. Commun. Soil Sci. Plant Anal. 17, 547–566.

Weil, M., Puchberger, M., Günne, J.S.A. Der, Weber, J., 2007. Synthesis, crystal structure, and characterization (vibrational and solid-state31P MAS NMR spectroscopy) of the high-temperature modification of calcium catena-polyphosphate(V). Chem. Mater. 19, 5067–5073. https://doi.org/10.1021/cm071239i

Ye, Z., Zhang, L., Huang, Q., Tan, Z., 2019. Development of a carbon-based slow release fertilizer treated by bio-oil coating and study on its feedback effect on farmland application. J. Clean. Prod. 239, 118085. https://doi.org/10.1016/j.jclepro.2019.118085

Zhao, L., Cao, X., Zheng, W., Kan, Y., 2014. Phosphorus-assisted biomass thermal conversion: Reducing carbon loss and improving biochar stability. PLoS One 9, 1–15. https://doi.org/10.1371/journal.pone.0115373

Zhao, L., Cao, X., Zheng, W., Scott, J.W., Sharma, B.K., Chen, X., 2016a. Copyrolysis of Biomass with Phosphate Fertilizers to Improve Biochar Carbon Retention, Slow Nutrient Release, and Stabilize Heavy Metals in Soil. ACS Sustain. Chem. Eng. 4, 1630–1636. https://doi.org/10.1021/acssuschemeng.5b01570

Zhao, L., Cao, X., Zheng, W., Scott, J.W., Sharma, B.K., Chen, X., 2016b. Copyrolysis of Biomass

with Phosphate Fertilizers to Improve Biochar Carbon Retention, Slow Nutrient Release, and Stabilize Heavy Metals in Soil. ACS Sustain. Chem. Eng. 4, 1630–1636. https://doi.org/10.1021/acssuschemeng.5b01570

## APPENDIX – PATENTS

Patent 1 - “PROCESSO DE PRODUÇÃO DE HIDRÓXIDO DE CÁLCIO A PARTIR DA CASCA DE OVO”

(Patent published in the National Institute of Industrial Property)

BR102019018675

(21) BR 102019018675-5 A2

**(22) Data do Depósito:** 09/09/2019

**(43) Data da Publicação Nacional:** 23/03/2021

**República Federativa do Brasil**

Ministério da Economia

Instituto Nacional da Propriedade Industrial

---

**(54) Título:** PROCESSO DE PRODUÇÃO DE HIDRÓXIDO DE CÁLCIO A PARTIR DA CASCA DO OVO

**(51) Int. Cl.:** C01F 11/02; C04B 2/02.

(71) **Depositante(es):** UNIVERSIDADE FEDERAL DE LAVRAS; FUNDAÇÃO DE AMPARO À PESQUISA DE MINAS GERAIS.

(72) **Inventor(es):** LEÔNIDAS CARRIJO AZEVEDO MELO; IVAN CÉLIO ANDRADE RIBEIRO; LUIZ ROBERTO GUIMARÃESGUILHERME; JÉSSICA CRISTINA TEODORO.

**(57) Resumo:** PROCESSO DE PRODUÇÃO DE HIDRÓXIDO DE CÁLCIO A PARTIR DA CASCA DO OVO. A presente invenção se caracteriza pela produção de um subproduto, classificado como Hidroxicasca, a partir de cascas de ovos descartadas pelas granjas produtoras de ovos. O material é obtido a partir de uma metodologia simples e de baixo custo que envolve a dissolução das cascas em uma solução de ácido clorídrico, seguida pela precipitação do novo material com uma solução de hidróxido de sódio. A Hidroxicasca apresenta alta capacidade de remoção de fósforo e arsênio de águas residuárias, sendo passível de comercialização para indústrias especializadas nesse setor ou, ainda, de utilização no sistema de tratamento de efluentes da própria granja geradora dos resíduos.

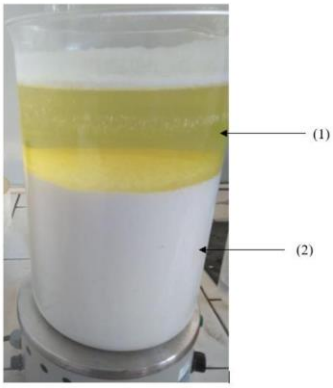
(1)
(2)

# PROCESSO DE PRODUÇÃO DE HIDRÓXIDO DE CÁLCIO A PARTIR DA CASCA DO OVO

## 1. Apresentação do invento ou campo de aplicação

[01] A presente invenção é um processo para produção de um reagente químico a partir de cascas de ovos, classificado como "Hidroxicasca". Esse material se apresenta como uma solução para os problemas envolvidos com a disposição final de resíduos gerados pelas granjas produtoras de ovos. Trata-se de um subproduto que tem potencial para substituição de reagentes químicos comerciais utilizados em sistemas de tratamento de águas residuárias.

[02] A produção da "Hidroxicasca" ocorre a partir de reações químicas simples, utilizando-se reagentes que são facilmente encontrados no mercado e de baixo custo. Basicamente, as cascas de ovos são dissolvidas em uma solução de ácido clorídrico e, em seguida, o novo material é precipitado com uma solução de hidróxido de sódio. O material precipitado, a "Hidroxicasca", pode ser utilizado no sistema de tratamento de efluentes da própria granja de ovos geradora dos resíduos, ou ainda ser comercializado para mercados especializados.

## 2. Estado da técnica

[03] Existem no estado da técnica diversos trabalhos sobre a transformação de cascas de ovos em reagentes químicos com alto valor agregado, tais como: óxido de cálcio (KÖSE, T. E.; KIVANÇ, B. Adsorption of phosphate from aqueous solutions using calcined waste eggshell. **Chemical Engineering Journal**, 2011; TORIT, J.; PHIHUSUT, D. Phosphorus removal from wastewater using eggshell ash. **Environmental Science and Pollution Research**, 2018); bruchita (PANAGIOTOU, E. et al. Turning calcined waste egg shells and wastewater to Brushite: Phosphorus adsorption from aqua media and anaerobic sludge leach water. **Journal of Cleaner Production**, 2018); hidroxiapatita (WU, S.-C. et al. Effects of heat treatment on the synthesis of hydroxyapatite from eggshell powders. **Ceramics International**, 2015); biocarvões (WANG, H. et al. Engineered biochar derived from eggshell-treated biomass for removal of aqueous lead. **Ecological Engineering**, 2017; LIU, X.; SHEN, F.; QI, X. Adsorption recovery of phosphate from aqueous solution by CaO-biochar composites prepared from eggshell and rice straw. **Science of the Total Environment**, 2019).

[04] Além disso, há registro das Patentes CN101648724 e US2014044620 em que os autores descrevem metodologias distintas para a produção de carbonato de cálcio ($CaCO_3$) a partir da casca

de ovo. No entanto, até o momento, não existem no estado da técnica metodologias que sejam simples e de baixo custo para a produção de um material que apresente semelhança com as características químicas da "Hidroxicasca". Trata-se de um material único em literatura nacional e internacional, de alto valor agregado, produzido a partir de cascas de ovos, sem que haja, necessariamente, o uso de mão de obra especializada, reagentes químicos caros e equipamentos sofisticados.

## 3. Problemas do estado da técnica

[05] Com o avanço das técnicas de produção de alimentos, as granjas produtoras de ovos já distribuem, separadamente, as claras das gemas, para seus respectivos consumidores. Esse processo de industrialização proporciona vantagens econômicas com a extensão da vida útil do produto, além de facilidades no transporte e na conservação do alimento. Porém, são geradas, de forma concentrada, quantidades consideráveis de cascas de ovos. Atualmente, no Brasil, parte dessas cascas é doada aos agricultores residentes próximos às granjas produtoras de ovos. Quando não existe essa possibilidade, as cascas são descartadas em aterros sanitários que, além de aumentar os custos de produção das granjas, inviabiliza a recuperação dos nutrientes presentes nas cascas.

[06] A presente invenção tem como objetivo a valorização das cascas descartadas pelas granjas produtoras de ovos. A valorização se dá pela transformação das cascas em um material classificado como "Hidroxicasca". Esse material tem maior valor agregado e apresenta alta capacidade para remoção de fósforo e arsênio de águas residuárias, podendo ser comercializado para indústrias especializadas do setor ou utilizado no próprio empreendimento.

## 4. Objeto da invenção

[07] O processo de produção da "Hidroxicasca" se apresenta como uma solução simples e de baixo custo para a destinação final, recuperação e valorização das cascas de ovos geradas pelas granjas de produção de ovos.

## 5. Descrição da invenção

[08] A metodologia de produção da "Hidroxicasca" é dividida em quatro etapas:

[09] Etapa 1: Adicionar uma amostra de cascas de ovos secas e trituradas a uma solução de ácido clorídrico (HCl) e manter sob agitação, em agitador magnético. O sistema deve ser mantido sob agitação até que todo o carbonato seja convertido em gás carbônico (CO2), água (H2O), e cloreto de cálcio (CaCl2), assim como apresentado na equação 1, abaixo.

$$CaCO_3 + 2HCl \rightarrow CaCl_2 + 2CO_2 + H_2O \qquad 1$$

[10] Etapa 2: Após o sistema entrar em equilíbrio, adicionar uma solução concentrada de hidróxido de sódio (NaOH), até que todo o cloreto de cálcio presente na solução seja convertido em hidróxido de cálcio, como apresentado na equação 2, abaixo.

$$CaCl_2 + 2NaOH \rightarrow Ca(OH)_2 + 2NaCl \qquad 2$$

[11] Etapa 3: A solução deve ser deixada em repouso por 12 horas até ocorrer a sedimentação do precipitado formando um sistema bifásico (1) e (2). O sobrenadante é retirado e o restante do material transferido para cápsulas de evaporação, as quais devem ser mantidas em estufas a 100 °C por 24h.

[12] Etapa 4: Após resfriado, o material deve ser retirado das cápsulas, triturado e homogeneizado em peneira de 0,5 mm. O produto final é classificado como “Hidroxicasca” (3).

[13] O produto final tem diversas possibilidade de aplicações ambientais, notadamente a reciclagem de fósforo a partir de águas residuárias, visando a produção de fertilizante fosfatado. Para efeito de comparação, foi avaliada a capacidade de remoção de fósforo (P) da casca de ovo, do hidróxido produzido partir da casca de ovo e do hidróxido de cálcio padrão de laboratório. Para isso, 5g de cada material foram adicionados em 1L de soluções contendo 500 mg de P. As soluções foram agitadas por 5 min, em agitador magnético, e as suspenções foram deixadas em repouso por 24 horas. Em seguida, foi coletada uma alíquota do sobrenadante, o qual foi filtrado e avaliado quanto a concentração de P pelo método fosfo-molibdílico e medição da absorbância em espectrofotômetro. O efeito da adição de cada material quanto a remoção de P é apresentado na Figura 3.

[14] A hidroxi-casca apresentou eficiência de remoção de P idêntica à do hidróxido de cálcio puro. Tal resultado corrobora com o uso desse novo material em sistemas onde se almeja a recuperação de P de efluentes industriais e agroindustriais. Dessa forma, o material formado apresenta potencial de comercialização em mercados especializados viabilizando uma nova fonte de renda para as indústrias de beneficiamento do ovo. Além da comercialização, o novo hidróxido produzido a partir da casca de ovo pode ser utilizado no próprio sistema de tratamento de efluentes dessas empresas, minimizando gastos e proporcionando um fim ambientalmente amigável para os resíduos gerados. Vale acrescentar que, as empresas estariam de acordo com a Política Nacional de Resíduos Sólido

vigente no país que incentiva a recuperação e reutilização de resíduos sólidos gerados em qualquer etapa do processo de produção.

## 6. Descrição das Figuras/Desenhos/Gráficos

[15] A figura 1 representa o sistema bifásico da etapa 3, composto pelo sobrenadante (1) e o precipitado (2). Já a figura 2 representa o produto final, ou seja, a “hidroxicasca”. Por fim, a figura 3 demonstra uma comparação entre a casca do ovo, hidroxi-casca e o Hidróxido de cálico na eficiência de remoção de fósforo.

## REIVINDICAÇÕES

1. Processo de produção de hidróxido de cálcio a partir da casca do ovo, **caracterizadopor** compreender as seguintes etapas:

a) Adicionar uma amostra de cascas de ovos secas e trituradas a uma solução de ácido clorídrico (HCl) e manter sob agitação, em agitador magnético, o sistema deve ser mantido sob agitação até que todo o carbonato seja convertido em gás carbônico (CO2), água (H2O), e cloreto de cálcio (CaCl2);
b) Após o sistema entrar em equilíbrio, adicionar uma solução concentrada de hidróxido de sódio (NaOH), até que todo o cloreto de cálcio presente na solução seja convertido em hidróxido de cálcio;
c) A solução deve ser deixada em repouso por 12 horas até ocorrer a sedimentação do precipitado formando um sistema bifásico (1) e (2), o sobrenadante é retirado e o restante do material transferido para cápsulas de evaporação, as quais devem ser mantidas em estufas a 100 °C por 24h;
d) Após resfriado, o material deve ser retirado das cápsulas, triturado e homogeneizado em peneira de 0,5 mm.

2. “Hidroxicasca”, obtida pelo processo compreendido na reivindicação 1, **caracterizado por** ter alta capacidade de remoção de fósforo e arsênio de águas residuárias.

3. Uso da “Hidroxicasca”, obtida pelo processo compreendido na reivindicação 1, **caracterizado por** poder ser utilizado no sistema de tratamento de efluentes da própria granja de ovos geradora das cascas

## FIGURAS

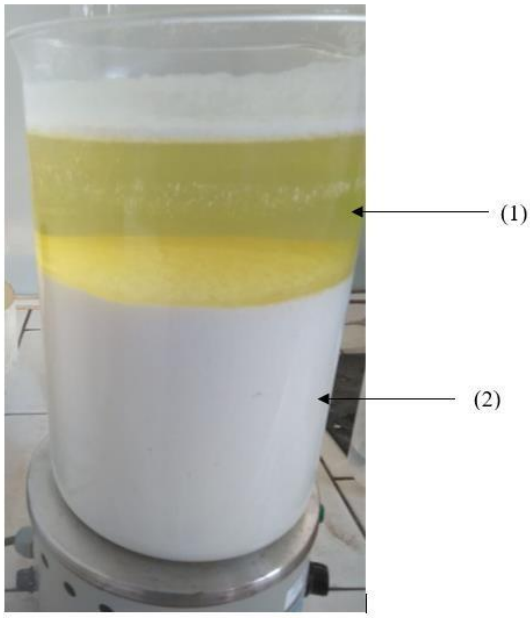


**Figura 1**

**Figura 2**

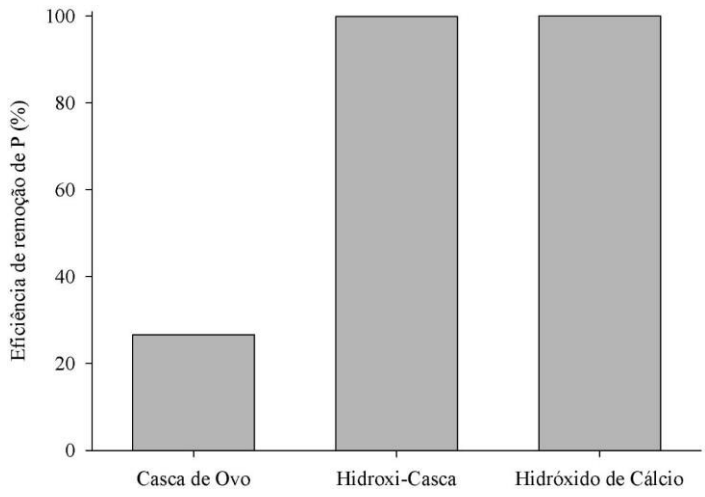
Eficiência de remoção de P (%)
100
80
60
40
20
0
Casca de Ovo
Hidroxi-Casca
Hidróxido de Cálcio

**Figura 3**

## RESUMO

## PROCESSO DE PRODUÇÃO DE HIDRÓXIDO DE CÁLCIO A PARTIR DA CASCA DO OVO

A presente invenção se caracteriza pela produção de um subproduto, classificado como “Hidroxicasca”, a partir de cascas de ovos descartadas pelas granjas produtoras de ovos. O material é obtido a partir de uma metodologia simples e de baixo custo que envolve a dissolução das cascas em uma solução de ácido clorídrico, seguida pela precipitação do novo material com uma solução de hidróxido de sódio. A “Hidroxicasca” apresenta alta capacidade de remoção de fósforo e arsênio de águas residuárias, sendo passível de comercialização para indústrias especializadas nesse setor ou, ainda, de utilização no sistema de tratamento de efluentes da própria granja geradora dos resíduos.

Patent 2 - “PROCESSO DE PRODUÇÃO DE UM ORGANOMINERAL FOSFATADO A PARTIR DE RESÍDUOS DA INDÚSTRIA DE VACINAS”

(Patent published in the National Institute of Industrial Property)

BR 102019026379

**(21) BR 102019026379-2 A2**

**(22) Data do Depósito: 12/12/2019**

**(43) Data da Publicação Nacional: 22/06/2021**

**República Federativa do Brasil**

**Ministério da Economia**

**Instituto Nacional da Propriedade Industrial**

---

**(54) Título:** PROCESSO DE PRODUÇÃO DE UM ORGANOMINERAL FOSFATADO A PARTIR DE RESÍDUOS DA INDÚSTRIA DE VACINAS DA GRIPE

**(51) Int. Cl.:** C05B 17/00; C05F 5/00.

**(52) CPC:** C05B 17/00; C05F 5/002.

**(71) Depositante(es):** UNIVERSIDADE FEDERAL DE LAVRAS; FUNDAÇÃO DE AMPARO À PESQUISA DE MINAS GERAIS.

**(72) Inventor(es):** LEÔNIDAS CARRIJO AZEVEDO MELO; IVAN CÉLIO ANDRADE RIBEIRO; JÉSSICA CRISTINA TEODORO; LUIZ ROBERTO GUIMARÃES GUILHERME; CAMILA SILVA FRANCO; MATEUS PIMENTEL DE MATOS.

**(57) Resumo:** PROCESSO DE PRODUÇÃO DE UM ORGANOMINERAL FOSFATADO A PARTIR DE RESÍDUOS DA INDÚSTRIA DE VACINAS DA GRIPE. A proposta apresenta um processo de produção para o aproveitamento e valorização do resíduo gerado durante a produção de vacinas no Brasil. O material é obtido a partir de uma metodologia de baixo custo que envolve a incorporação do resíduo da indústria de vacinas com serragem de madeira e uma solução ácida rica em fósforo, seguida de pirólise a 500 ºC por duas horas. Essa metodologia viabiliza a esterilização do material e produção de um organomineral fosfatado com capacidade de substituição de fertilizantes convencionais. Com a adoção do processo, as indústrias de produção de vacinas deixariam de ter gastos com a disposição desses resíduos em aterros e passariam a ter lucro com a venda dos fertilizantes produzidos, além de reciclar a matéria orgânica e os nutrientes contidos no resíduo. Dessa forma, o processo em questão permite que as indústrias de vacinas da gripe implementem, de forma inovadora, o conceito de economia circular estabelecido

pela Política Nacional de Resíduos sólidos vigente no Brasil, que incentiva a recuperação, reutilização e valorização de resíduos sólidos gerados em qualquer etapa do processo de produção.

# PROCESSO DE PRODUÇÃO DE UM ORGANOMINERAL FOSFATADO A PARTIR DE RESÍDUOS DA INDÚSTRIA DE VACINAS DA GRIPE

## 1. Apresentação do invento ou campo de aplicação

[01] A proposta apresenta um processo de produção para o aproveitamento e valorização do resíduo gerado durante a produção de vacinas no Brasil. A metodologia viabiliza a esterilização do material e a produção de um organomineral fosfatado com capacidade de substituição de fertilizantes comerciais convencionais. Com a adoção do processo proposto, as indústrias supracitadas deixariam de ter gastos com a disposição dos resíduos em aterros e passariam a ter lucro com a venda dos fertilizantes produzidos. Além disso, o processo em questão se torna uma alternativa para que as indústrias de produção de vacinas implementem o conceito de economia circular, estabelecido pela Política Nacional de Resíduos Sólidos vigente no país, que incentiva a recuperação, reutilização e valorização de resíduos sólidos gerados em qualquer etapa do processo de produção.

## 2. Estado da técnica

[02] Até o momento, não existem no estado da técnica processos de produção de um organomineral fosfatado a partir dos resíduos descartados pela indústria de vacinas da gripe. Como se trata de um material contaminado biologicamente (vírus), ainda não existe processo que promova a sua esterilização completa, gerando um novo material com capacidade de retornar ao ambiente como fertilizante comercial organomineral de eficiência aumentada.

## 3. Problemas do estado da técnica

[03] Atualmente, as indústrias de produção de vacinas utilizam os ovos como meio de cultura durante o processo de produção de vacinas contra a gripe. Em resumo, uma amostra do vírus é inoculada no ovo para que ocorra a sua replicação. Depois do período de incubação, o líquido onde o vírus se multiplicou é extraído, restando ainda a maior parte do ovo com a casca. Esse material é triturado e segue para inativação térmica a 170 °C, formando um resíduo classificado como farinha de ovo (FO).

[04] De acordo com a Resolução do Conselho Nacional do Meio Ambiente - CONAMA n° 358/2005, a FO é classificada como um Resíduo de Serviço de Saúde. Por isso, ela deve ser encaminhada para aterros sanitários controlados a um custo médio de R$3,00 por kg de resíduo aterrado. Cada ovo rende o equivalente a aproximadamente uma dose de um único tipo de vacina da gripe. Considerando que em 2016 foram produzidos cerca de 54 milhões de doses, somente pelo Instituto Butantan de São

Paulo, e levando-se em consideração que a massa seca de cada ovo seja em torno de 20 g, estima-se que foram geradas cerca de 1080 toneladas de FO. Portanto, um gasto em torno de R$ 3.240.000,00, apenas com o aterramento desse material naquele ano.

[05] Por outro lado, os ovos apresentam em sua composição química nutrientes para crescimento desenvolvimento de plantas e animais. A disposição em aterros, além de gerar alto custo para as empresas, inviabiliza o retorno desses nutrientes para o ambiente dentro do conceito moderno de economia circular.

[06] Assim, a metodologia proposta no presente trabalho viabiliza a esterilização da FO e a produção de um organomineral fosfatado com teor de fósforo semelhante ao encontrado em fertilizantes comerciais convencionais. Com a adoção da metodologia proposta, as indústrias de produção de vacinas deixariam de ter gastos com a disposição dos resíduos em aterros e passariam a ter lucro com a venda dos fertilizantes produzidos, gerando emprego e renda e reduzindo ou eliminando passivos ambientais. Além disso, o processo em questão se torna uma alternativa para que tais indústrias adotem o conceito de economia circular estabelecido pela Política Nacional de Resíduos Sólidos vigente no Brasil.

## 4. Objeto da invenção

[07] Processo de produção visando a esterilização, recuperação e valorização do resíduo gerado durante a produção de vacinas da gripe.

## 5. Descrição da invenção

[08] Inicialmente, uma massa de farinha de ovo (1) é misturada à serragem de madeira na proporção de 1:3. A mistura então é adicionada a uma solução ácida com alta concentração de fósforo (P). Em seguida, a suspensão é agitada por um período de 2 h e, posteriormente, seca em estufa a 100 °C por 24 h. Após resfriamento, a amostra é triturada e acondicionada em cilindros metálicos. Os cilindros devem ser fechados, de forma a minimizar a concentração de oxigênio no meio, e conduzidos à pirólise, em forno mufla a 500 °C por 2 h, com posterior resfriamento lento por 24 h. Por fim, o material é homogeneizado em peneira de 0.5mm formando, ao final, o organomineral fosfatado (2).

[09] O esquema completo do processo de produção do organomineral fosfatado é apresentado na figura 3. Vale ressaltar que a permanência do material em ambiente com alta temperatura por um período de tempo relativamente elevado, promove a sua esterilização, eliminando todos os microrganismos presentes no meio.

[10] Os valores de pH e fósforo total ($P_{total}$) foram determinados no organomineral produzido e no Superfosfato Triplo (SFT) para efeito de comparação. Conforme apresentado na Tabela 1, o organomineral formado apresentou cerca de 11,8% de P em sua composição química, o que corresponde a um teor equivalente àqueles encontrados em fertilizantes disponibilizados no mercado agrícola e a 60% do teor encontrado no SFT. Além disso, quando se avalia os valores de pH encontrados, pode-se observar que a acidez do novo material chega a ser mais de 1500 vezes menor do que a do superfosfato triplo. Lembrando que o valor de acidez é encontrado a partir da conversão do pH em concentração de íons hidrogênio, ($pH = - \log [H^+]$).

Tabela 1: Valores de pH e fósforo total ($P_{total}$)

| Fertilizante | pH | Ptotal ($g\ kg^{-1}$) |
|---|---|---|
| Organomineral fosfatado | 5,95 ± 0,03 | 118,0, ± 1,2 |
| Superfosfato triplo | 2,77 ± 0,01 | 208,0 ± 1,5 |

[11] O processo de produção que estamos propondo, portanto, viabiliza a esterilização de um resíduo contaminado biologicamente e possibilita a produção de um organomineral fosfatado que apresenta alto teor de fósforo e menor acidez do que fertilizantes comerciais convencionais. Além disso, o organomineral apresenta em sua composição considerável teor de carbono pirogênico, o qual possui alta estabilidade no ambiente e irá proporcionar uma liberação mais lenta do fósforo. Essas características contribuem para o sequestro de carbono no solo e para o uso mais eficiente de fósforo, principalmente em solos sob cultivo em condições tropicais.

[12] A implementação desse processo na planta de produção de vacinas minimiza os gastos das empresas com a disposição em aterros, sendo possível, ainda, a obtenção de lucro a partir da venda do organomineral produzido. Vale acrescentar também que a adoção desse processo pelas indústrias estaria de acordo com o conceito de economia circular estabelecido pela Política Nacional de Resíduos Sólidos vigente no país, que incentiva a recuperação, reutilização e valorização de resíduos sólidos gerados em qualquer etapa do processo de produção.

**6. Descrição das figuras/desenhos/gráficos**

[13] A figura 1 demonstra a farinha de ovo, a figura 2 demonstra o organomineral fosfatado e a figura 3 demonstra o esquema completo do processo de produção do organomineral fosfatado.

## REIVINDICAÇÕES

1.Processo de produção de um organomineral fosfatado a partir da farinha de ovo gerada pela indústria de vacinas da gripe, **caracterizado por** compreender as seguintes etapas:

a) Misturar uma amostra de farinha de ovo à serragem de madeira, na proporção de 1:3;
b) Adicionar a mistura (1) a uma solução ácida com alta concentração de fósforo (P), mantendo o sistema sob agitação durante 2 horas, seguida por secagem em estufa a 100 ºC por 24h;
c) Após resfriada, a amostra deve ser triturada e acondicionada em cilindros metálicos fechados, sendo estes conduzidos à pirólise, em forno mufla, a 500 °C por 2h;
d) Após resfriamento lento por 24 h, o material deve ser retirado dos cilindros e homogeneizado em peneira de 0,5 mm.

2. Organomineral fosfatado, obtido pelo processo compreendido na reivindicação 1, **caracterizado por** ter 11,8% de fósforo e pH igual a 5,95.

(1)

Figura 1

(2)

Figura 2

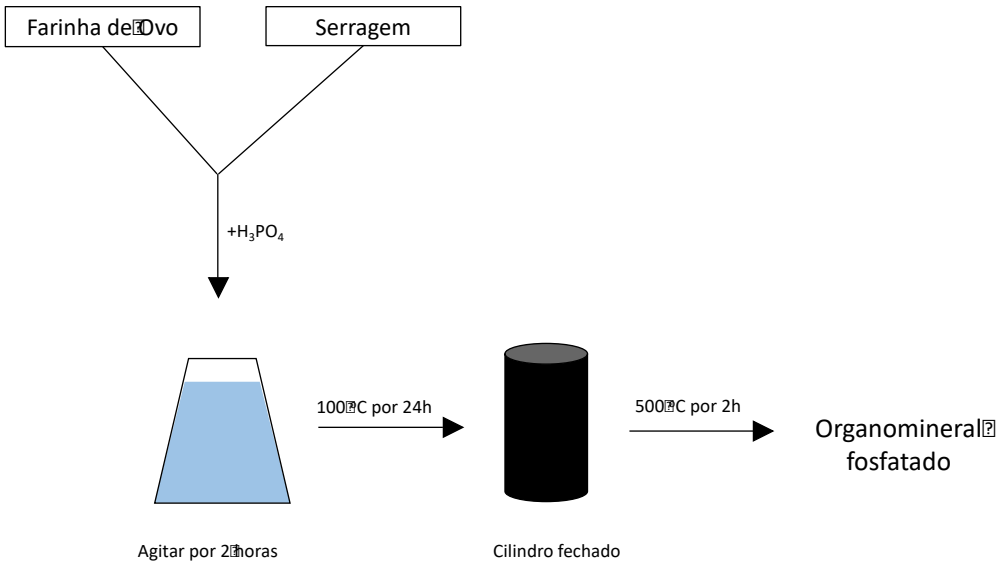


Figura 3

## RESUMO

## PROCESSO DE PRODUÇÃO DE UM ORGANOMINERAL FOSFATADO A PARTIR DE RESÍDUOS DA INDÚSTRIA DE VACINAS DA GRIPE

A proposta apresenta um processo de produção para o aproveitamento e valorização do resíduo gerado durante a produção de vacinas no Brasil. O material é obtido a partir de uma metodologia de baixo custo que envolve a incorporação do resíduo da indústria de vacinas com serragem de madeira e uma solução ácida rica em fósforo, seguida de pirólise a 500 °C por duas horas. Essa metodologia viabiliza a esterilização do material e produção de um organomineral fosfatado com capacidade de substituição de fertilizantes convencionais. Com a adoção do processo, as indústrias de produção de vacinas deixariam de ter gastos com a disposição desses resíduos em aterros e passariam a ter lucro com a venda dos fertilizantes produzidos, além de reciclar a matéria orgânica e os nutrientes contidos no resíduo. Dessa forma, o processo em questão permite que as indústrias de vacinas da gripe implementem, de forma inovadora, o conceito de economia circular estabelecido pela Política Nacional de Resíduos sólidos vigente no Brasil, que incentiva a recuperação, reutilização e valorização de resíduos sólidos gerados em qualquer etapa do processo de produção.

# FINAL REMARKS

The present study proposed the transformation of ES and VW into value-added byproducts. ES was transformed into ES-OH, a promising material for P recovery from an aqueous solution, forming a material with great potential in agriculture as an alternative phosphate fertilizer. ES-OH also has the potential to reduce water As contamination. This work also reported the transformation of VW into biochar fertilizer bases with agronomic potential similar to commercial fertilizers. We tested the processes on laboratory scales, and now they are ready to be implemented on an industrial scale. The implementation of each one of the processes on production plants minimizes companies' expenses with their disposal in landfills, and it is also possible to obtain profit from the sale of value-added byproducts. It is also worth adding that the adoption of the process by industries would be following the concept of economy established by the National Solid Waste Policy in force in Brazil, which encourages the recovery, reuse, and valorization of solid waste generated stage of the production process. Finally, other companies could implement the methods described here as the first attempt to treat their solid wastes locally, avoid environmental contamination, and create a novel income resource.